IMPACT OF WEATHERING ON THE PHYSICAL, MECHANICAL AND HYGRIC PROPERTIES OF NINE MUD PLASTER MIXES APPLIED ON STRAWBALE WALLS

A THESIS SUBMITTED TO
THE GRADUATE SCHOOL OF NATURAL AND APPLIED SCIENCES
OF
MIDDLE EAST TECHNICAL UNIVERSITY

BY

ABDULMELİK ŞAHİN

IN PARTIAL FULFILLMENT OF THE REQUIREMENTS
FOR
THE DEGREE OF MASTER OF SCIENCE
IN
BUILDING SCIENCE IN ARCHITECTURE

SEPTEMBER 2024

Approval of the thesis:

IMPACT OF WEATHERING ON THE PHYSICAL, MECHANICAL AND HYGRIC PROPERTIES OF NINE MUD PLASTER MIXES APPLIED ON STRAWBALE WALLS

submitted by ABDULMELİK ŞAHİN in partial fulfillment of the requirements for the degree of **Master of Science** i**n Building Science in Architecture, Middle East Technical University** by,

Prof. Dr. Naci Emre Altun
Dean, **Graduate School of Natural and Applied Sciences** _____

Assoc. Prof. Dr. Ayşem Berrin Çakmaklı
Head of the Department, **Architecture** _____

Prof. Dr. Soofia Tahira Elias-Ozkan
Supervisor, **Architecture, METU** _____

Examining Committee Members:

Assoc. Prof. Dr. Ayşem Berrin Çakmaklı
Architecture, METU _____

Prof. Dr. Soofia Tahira Elias-Ozkan
Architecture, METU _____

Asst. Prof. Dr. Matthieu Pedergnana
Architecture, Yaşar University _____

Date: 04.09.2024

I hereby declare that all information in this document has been obtained and presented in accordance with academic rules and ethical conduct. I also declare that, as required by these rules and conduct, I have fully cited and referenced all material and results that are not original to this work.

Name Last name : Abdulmelik Şahin

Signature :

ABSTRACT

IMPACT OF WEATHERING ON THE PHYSICAL, MECHANICAL AND HYGRIC PROPERTIES OF NINE MUD PLASTER MIXES APPLIED ON STRAWBALE WALLS

Abdulmelik Şahin
Master of Science, Building Science in Architecture
Supervisor: Prof. Dr. Soofia Tahira Elias-Ozkan

September 2024, 127 pages

Earth-based building materials, such mud, clay, and adobe, provide a number of benefits, such as affordability, sustainability, and visual appeal. Nevertheless, there are a lot of difficulties in using them. Because earth-based materials are prone to erosion, water sensitivity, and cracking, durability is a major concern. Another drawback is their structural strength, which is frequently lower than that of contemporary building materials. The amount of maintenance required can be high, as erosion, water damage, and pest problems necessitate regular repairs. The efficiency of earth-based building can also be impacted by the climate, especially in areas with high humidity or harsh temperatures.

This study aims to investigate the impacts of various factors including the amount of earth, water, fiber, aggregate, and different organic additives under weathering conditions and aims to investigate the physical, mechanical, and hygric properties of samples that are exposed several years to nature with no protection. The assessment focuses on physical properties, mechanical properties, the durability of samples, hygric properties, and hydric properties.

These findings show that the composition of the mud-plaster samples has a substantial impact on their mechanical properties, especially their compressive strength. Samples kept in a laboratory typically have greater compressive strengths than samples left outside. The hygric properties—water absorption, vapor permeability, and drying rate are determined by the mud plaster composition, particularly by the amount of organic additives in the mix. Based on the mix composition and exposure to weathering, differences are seen in cohesiveness and resistance to surface abrasion. Over time, variations in temperature, humidity, and precipitation have a substantial impact on the properties of mud-plaster samples, causing a drop in compressive strength, an increase in water absorption, and a reduction in surface cohesiveness.

Keywords: Physical strength of mud plaster, Durability of mud plaster, Hydric properties of mud plaster, Hygric Properties of mud plaster, Weathering

ÖZ

DIŞ ETKENLERE MARUZ KALMIŞ SAMAN BALYAL DUVARLARINA UYGULANAN DOKUZ ÇAMUR SIVA KARIŞIMININ FİZİKSEL, MEKANİK VE HİGRİ ÖZELLİKLERİ

Abdulmelik Şahin
Yüksek Lisans, Yapı Bilimleri, Mimarlık
Tez Yöneticisi: Prof. Dr. Soofia Tahira Elias-Ozkan

Eylül 2024, 127 sayfa

Çamur, kil ve kerpiç gibi toprak temelli yapı malzemeleri, uygun fiyatlılık, sürdürülebilirlik ve görsel çekicilik gibi bir dizi avantaj sağlar. Bununla birlikte, bunları kullanırken birçok zorluk vardır. Toprak temelli malzemeler erozyona, suya duyarlılığa ve çatlamaya eğilimli olduğundan, dayanıklılık büyük bir endişe kaynağıdır. Bir diğer dezavantajı, sıklıkla çağdaş yapı malzemelerinden daha düşük olan yapısal mukavemetleridir. Erozyon, su hasarı ve haşere sorunları düzenli onarımlar gerektirdiğinden, gereken bakım miktarı yüksek olabilir. Toprak temelli yapının verimliliği, özellikle yüksek nem veya sert sıcaklıkların olduğu bölgelerde iklimden de etkilenebilir.

Bu çalışma, toprak bileşimi, su içeriği, lif türleri, agregalar ve katkı maddeleri dahil olmak üzere çeşitli faktörlerin hava koşullarına maruz kalma koşulları altındaki etkilerini kapsamlı bir şekilde araştırmayı ve hiçbir koruma olmadan doğaya birkaç yıl maruz kalan numunelerin fiziksel, mekanik ve higroskopik özelliklerini araştırmayı amaçlamaktadır. Değerlendirme fiziksel özelliklere, mekanik özelliklere, numunelerin dayanıklılığına, higroskopik özelliklere ve hidroskopik özelliklere odaklanır.

Bu bulgular, çamur sıva örneklerinin bileşiminin mekanik özellikleri, özellikle basınç dayanımları üzerinde önemli bir etkiye sahip olduğunu göstermektedir. Laboratuvarda tutulan örnekler genellikle dışarıda bırakılan örneklerden daha fazla basınç dayanımına sahiptir. Higrik özellikler (su emilimi, buhar geçirgenliği ve kuruma hızı) çamur sıvanın bileşimi, özellikle eklenen organik katkı maddelerinin miktarı tarafından belirlenir. Bileşime ve maruz kalma ayarlarına bağlı olarak, kohezyonda ve yüzey aşınmasına karşı dirençte farklılıklar görülür. Zamanla, sıcaklık, nem ve yağıştaki değişiklikler çamur sıva örneklerinin özellikleri üzerinde önemli bir etkiye sahip olur, basınç dayanımında düşüşe, su emiliminde artışa ve yüzey kohezyonunda azalmaya neden olur.

Anahtar Kelimeler: Çamur sıvasının fiziksel mukavemeti, Çamur sıvasının dayanıklılığı, Çamur sıvasının hidrik özellikleri, Çamur sıvasının hidrik özellikleri, Hava ve çevre koşullarına dayanıklılık

To my mother

ACKNOWLEDGMENTS

I would like to express my deepest gratitude to my supervisor Prof. Dr. Soofia Tahira Elias-Ozkan for her guidance and patience. This research was made possible by her invaluable and innovative contributions. She always believed in me and encouraged me to keep going. I would also like to thank Dr. Matthieu Pedergnana for providing information on the mud-plaster compositions that he had prepared and applied on the experimental strawbale walls and suggestions regarding the compressive strength tests. I also extend my gratitude to Dr. Bilge Alp Güney for his guidance with the experimental setup in the Materials Conservation Laboratory where some of the tests were conducted.

I would like to express my heartfelt appreciation to Gönül, Aslı, Ceren, Pınar, Melek and Elif for their timely support throughout my master's studies. Their assistance meant a great deal to me and facilitated my academic career.

I extend my sincerest gratitude to my mother for imparting to me the significance of education, despite not having had the opportunity to pursue it herself. Her teachings have instilled in me the values of diligence and perseverance, which have been instrumental in my personal and professional growth. I am grateful for her unwavering help and guidance, which have contributed to my success.

This research was supported by the Middle East Technical University (METU) Scientific Research Projects (Bilimsel Araştırma proje-BAP) funding for BAP-02-01-2015-001, BAP-02-01-2015-002 and BAP-02-01-2016-003 and BAP-02-01-2016-003 projects.

TABLE OF CONTENTS

LIST OF TABLES

TABLES

LIST OF FIGURES

FIGURES

LIST OF ABBREVIATIONS

ABBREVIATIONS

Ke	Kerkenes with earth
Sd	River sand (4mm max)
Fb	Fiber (short straw)
Mo	Molasses
Eg	Egg white
Dj	Decomposition juice
Cd	Cow dung

CHAPTER 1

INTRODUCTION

This chapter presents the Argument for the research, the problem definition, the aims and objectives of the study, the research questions that will be answered to reach the objectives and the methodology that will be applied to obtain answers to these questions. At the end of the chapter the section on disposition will highlight the contents of the ensuing chapters of this thesis.

1.1 Argument

The rapid expansion of construction activities, coupled with the prevalent use of materials in contemporary building practices that pose challenges for recycling, has led to a progressive degradation of natural ecosystems and the sustainability of life. Concurrently, heightened attention has been directed towards ensuring occupants' well-being, health, and the energy efficiency of built environments. Earth-based materials, such as mud-plaster, are being revived as viable alternatives to conventional construction materials due to their environmentally benign characteristics and their demonstrated ability to enhance occupants' comfort, health, and energy efficiency.

Clayey earth mortars are not only environmentally friendly plastering materials, but they also have lower embodied energy compared to other plaster types; Hence, their applications on walls, ceilings and roofs may significantly improve occupants' environment.

Additionally, contemporary buildings use construction materials that pose significant recycling challenges. This trend has contributed to the ongoing degradation of natural ecosystems and the disruption of sustainable living conditions.

Earth materials, such as mud-plaster, are often praised for their recyclability; however, they also have certain limitations. Researchers around the world are trying to overcome these limitations, there are many examples, some of them are Faria (2016) and Minke (2012) focus on physical strength, Lerner and Donahue (2003) study mechanical strength, Morel (2012) investigate durability performance, Laborel-Préneron (2018) focuses on hygric properties, and Guiheneuf (2020) focus Hydric properties of materials. All of these researchers and many more, try different methods with different approaches in return they come up with results that improve our understanding and approach

1.2 Aim and Objectives

The principal aim of this study is to investigate the impact of outdoor conditions over time on specific mud plaster samples, in terms of their physical, mechanical, hydric, and hygric properties across different compositions. The aim is also to identify correlations among these properties to acquire a deeper understanding of their interplay.

Hence the main objective of this study is to analyze the nine unique mud-plaster samples that were applied on 3 experimental strawbale walls to test them for their resistance to weathering over a period of five years. The secondary objectives are:

- To determine the key material properties of these samples, including compressive strength, surface strength, water resistance, erosion resistance and resistance to abrasion, capillarity absorption, drying capacity, water vapour permeability.
- To gain an understanding of the relationships between the mechanical, and hygric properties of these earth-based mortars, considering the effects of time and outdoor conditions.
- To understand the impact of time and outdoor conditions on the performance and properties of mud-plaster samples by comparing these results with those

obtained from the initial study on these plaster mixes under laboratory conditions.

1.3 Research Questions

- What are the mechanical properties (compressive strength) of mud-plasters with varying compositions, and does it change under the influence of outdoor conditions?
- What are the hygric properties of mud-plasters and how do they vary with different organic additives?
- How durable are these samples with respect to surface abrasion, and cohesion properties?
- How do outdoor environmental conditions (such as temperature fluctuations, humidity levels, and exposure to precipitation) impact the properties of mud-plaster samples over time?

1.4 Research Methodology

This thesis is a continuation of previous research conducted with funding from the Middle East Technical University (METU) Scientific Research Projects (Bilimsel Araştırma proje-BAP) Projects No. BAP-02-01-2015-001, BAP-02-01-2015-002 and BAP-02-01-2016-003 that have been reported in a PhD dissertation (Pedergnana, 2022) and published papers (Pedergnana & Elias-Ozkan, 2021a, and Pedergnana & Elias-Ozkan, 2021b). In the funded research projects, many earth plaster samples were first produced and tested in the METU Civil Engineering Materials laboratory and comprehensively examined for the multifaceted impacts of earth composition, water content, fiber types, aggregate materials, and additives on the physical, hygric, mechanical, and hydric properties of earth plasters in 2015 and 2016. Then, 9 of the tested plaster mixtures were selected, and applied in panels on three strawbale walls built outside in METU Ankara campus in October 2016. These

walls withstood weather conditions for over 5 years, and were taken down in April 2023, after large plaster samples had been removed from the 9 panels for testing in the laboratory. The retrieved pieces from the experimental strawbale walls were cut up to test them for their physical, mechanical, hydric and hygric properties, as well as their surface resistance to abrasion and water. The materials and methods have been presented in detail in chapter 3.

1.5 Disposition

There are five chapters in the thesis. The introduction, justification for the research topic, problem description, goal, and objectives of the study are all discussed in the first chapter. The second chapter covers an extensive literature review that starts with sustainability through building materials, manufactured and sustainable building materials, and proceeding to Earth as a building material, earth mortars and mud plaster are analyzed with its composition, and its crucial properties. Finally, research on physical, mechanical, hygric and hydric performance is analyzed. The third chapter is about material and method where used materials and methods with the procedure of sampling and conducted laboratory experiments are discussed. In the fourth chapter results are presented and in the final chapter, the results, obtained through this experiment will be compared with the samples that are prepared and analyzed under the laboratory conditions with funding from the METU Scientific Research Projects BAP.

CHAPTER 2

LITERATURE REVIEW

2.1 Sustainability through building materials

Sustainability embodies a state of system stability wherein alterations are limited to maintain stability in the immediate future. For architects, engineers, and stakeholders engaged in constructing new facilities, sustainability holds paramount importance due to the substantial environmental impact of the structures we erect. Built environments serve as our interface with the natural world, providing protection from the elements and fulfilling various human needs, including shelter and status. However, they also consume natural resources and leave ecological footprints in their wake. As the creators and builders of these structures, we possess the capability to enhance their sustainability, ensuring they meet societal demands without compromising the needs of future generations or jeopardizing humanity's ongoing presence on Earth.

Alternatively, Salgado & Marques (2007) proposes that "sustainability" encompasses addressing environmental, social, and economic concerns in every human endeavor, striving to mitigate negative impacts across these domains and fostering a prosperous future for all. According to Salgado & Marques (2007), the initial stage of architectural design involves decision-making meetings where construction techniques and material selections take precedence. Consequently, the materials chosen profoundly to influence the environmental sustainability of a construction project, exerting significant influence on its overall environmental footprint. Thus, the determination of building materials shows a pivotal role in shaping the environmental implications of construction activities at large.

Building materials exert adverse environmental effects throughout their life cycle, spanning from extraction to final disposal. Consequently, it is imperative to manage these materials in a manner that minimizes their environmental impact to the greatest extent possible. Careful selection of appropriate materials is essential, considering various factors such as production distance, thermal and acoustic performance, cost implications, ease of operation and maintenance, among others. This strategic approach facilitates the integration of projects into their respective environments while reducing their overall environmental footprint (Salgado & Marques, 2007).

Hastak (1995) outlines three overarching objectives that serve as a framework for applying sustainability principles in material selection for construction projects. These objectives include minimizing the consumption of matter and energy, ensuring a satisfactory level of human well-being, and mitigating adverse environmental effects to the greatest extent possible.

The first objective, aimed at minimizing the consumption of matter and energy, is rooted in the principles of intergenerational equity and the endeavor to curtail entropy gain. Entropy, both in material and energy forms, naturally increases during consumption processes, rendering them less conducive to future utilization. This depletion renders materials and energy less viable for subsequent generations. Hence, a central tenet of sustainability and the utilization of sustainable materials is to optimize efficiency by utilizing minimal material and energy inputs, effectively achieving more with less. Examples of strategies to reduce consumption include selecting products with minimal packaging or sourcing locally produced items to diminish the energy expended in transportation (Hastak, 1995).

The second objective of sustainable material selection, enhancing human pleasure, is related to doing more with less. Trade-offs between resource consumption and human satisfaction must be made to achieve sustainability in construction. However, the goal of human satisfaction is crucial because, without it, individuals won't agree to take the steps required to alter the way things are in the world. So along with reducing resource use, sustaining human pleasure, and accommodating human preferences is our sustainability goal. Economics also has an impact on the human

pleasure component of sustainability since, in the current paradigm of an economy-driven society, no owner is likely to be satisfied unless their financial interests are protected. Selecting materials that enhance human pleasure can have a variety of goals, such as lowering expenses, ensuring human comfort and safety, and upholding the human spirit (Day, 1990).

Furthermore, the preservation of ecosystems, which are integral to the health of the environment, is paramount for the survival of humanity on Earth. Reducing the detrimental effects that building materials have on the environment is one of the main goals of sustainable material selection. Ensuring the well-being of ecosystems is essential, as they provide raw materials for human activities and play a critical role in maintaining biodiversity, habitat integrity, and mitigating pollution. Consequently, safeguarding ecosystems is imperative for human survival. Sustainable construction materials should possess low environmental impact, achieved through recyclability or reusability, environmentally friendly manufacturing processes, and responsibly sourced raw materials from stable ecosystems (Day, 1990).

When evaluating the sustainability of construction materials, it is critical to take into account the efficient use of resources, the improvement of human welfare, and the general mitigation of negative environmental impacts. These three overarching objectives serve as a global framework for evaluating the sustainability of building materials in design and construction practices.

2.1.1 Manufactured building materials

Building materials encompass a wide range of substances utilized in construction activities. These materials include both naturally occurring elements such as clay, rocks, sand, wood, as well as synthetic products like fired bricks, cement composites, concrete, fabric, glass, metal, and plastics. The manufacturing of these materials constitutes a well-established industry in numerous countries, with their usage typically segmented into specialized trades within the construction sector. Building

materials serve as the fundamental components of habitats and structures, including residential homes.

It's crucial to remember, though, that the building and construction sector uses a lot of energy and raw materials (Ding, 2014). His sector accounts for a substantial portion of global energy and raw material usage, estimated at around 24%. High energy content materials are frequently used in construction, including steel, concrete, aluminum, and glass. Buildings have an environmental impact at every stage of their lifecycle, and the materials they are made of have a significant impact on how sustainable and functional they are overall (Zabalza Bribian et al., 2011).

From the time of their original construction to their operational phase, when they undergo maintenance and updates to ensure continued functionality until the end of their service life, buildings interact with the environment at different stages.

2.1.2 Sustainable building materials

Given that buildings consume significant natural resources and contribute to greenhouse gas emissions through the burning of fossil fuels, their environmental impact is considerable. In the United States, the construction industry ranks third in terms of greenhouse gas emissions (Li & Zhu, 2010). It uses 15% of the world's freshwater resources, produces 25% of the world's waste, depletes 40% of natural resources, and emits 40% to 50% of greenhouse gases. It also makes up 40% of the world's primary energy consumption (Ramesh et al., 2010).

In response to these environmental challenges, there has been a growing focus on sustainable building materials as part of research and development initiatives aimed at achieving sustainable construction practices. This shift represents a proactive step by the construction sector to mitigate its environmental footprint and contribute to environmental preservation. Rather than just lowering the total number of construction activities, more focus should be placed on how the design and selection of sustainable building materials can improve living standards, environmental

compatibility, and user health and comfort in order to further the goal of sustainable construction (Du Plessis, 2007).

Sustainable building materials exhibit characteristics such as natural origin, low maintenance requirements, energy efficiency, enhancement of occupant health and comfort, promotion of productivity, and minimal environmental harm. While some naturally occurring substances like turpentine, radon, and asbestos may seem environmentally friendly due to their natural origin, they can have detrimental effects on both built and natural environments (Franzoni, 2011). Therefore, sustainable building materials are those that are ecologically friendly and environmentally responsible throughout their lifecycle. They are often derived from renewable sources and must demonstrate minimal energy consumption during production. Furthermore, they should not emit toxins or other harmful substances that affect human health or comfort throughout their lifespan (Ding, 2014).

2.2 Weathering Impacts

In contrast to extreme weather events, where infrastructure damage is immediate, weathering and deterioration from natural elements often take months or even years to manifest. Both natural environments and man-made structures are vulnerable to gradual degradation due to processes like wind-driven rain, freeze-thaw cycles, ultraviolet (UV) radiation, and chemical reactions in the presence of water and pollutants. Weathering can lead to erosion, material breakdown, and structural weakening over time. Biological agents, such as fungi or molds, can proliferate on surfaces, while chemical agents in moisture contribute to the corrosion of metals and the deterioration of materials like concrete. Thermal agents, including UV radiation, induce dimensional changes in polymers (e.g., vinyl, sealants), leading to cracks and fissures. Freeze-thaw cycles further accelerate the aging of porous materials like stone, brick, and mortar. Mechanical forces such as wind-driven rain and dust also act as structural loads, enhancing the effects of other weathering agents (Lacasse, 2003).

The degree of deterioration varies depending on several factors, including the material type and its exposure to specific environmental agents. For example, thermal aging in polymers depends on how often the material exceeds certain temperature thresholds, while the degradation of wood may be influenced by the frequency of wetting and drying cycles. Understanding these factors is critical for predicting the longevity of materials and implementing maintenance strategies to prevent premature failure of infrastructure Auld et al. (2007).

2.2.1 The impact of weathering on building materials

Premature deterioration of structural materials is increasingly concerning in many regions due to shifts in both physical and chemical environmental conditions, alongside aging and overused infrastructure. These concerns are heightened by reduced public spending on infrastructure replacement and expansion, as infrastructure that was built in previous decades is now more vulnerable to environmental stressors. Aging infrastructure is susceptible to various climatic hazards, including more frequent freeze-thaw cycles caused by warmer winters, which accelerates the weathering of materials such as concrete, masonry, and pavement (Auld, 1999; Green et al., 2003).

In particular, freeze-thaw cycles contribute to mechanical damage in porous materials like mortars, causing cracks and spalling due to moisture absorption and expansion. Similarly, masonry structures, including clay bricks, are vulnerable to such cycles, especially when moisture within the walls freezes and thaws repeatedly, leading to further degradation (Magnuson et al., 2000). Moreover, chemical reactions, especially in the presence of moisture and pollutants, can cause adverse effects, such as carbonation in concrete, which accelerates surface deterioration (Lstiburek, 2002; Lacasse, 2003).

Without timely adaptation actions, existing infrastructure will face accelerated deterioration under the effects of climate change, such as more frequent intense

rainfall and higher wind speeds, which can exacerbate mechanical and chemical damage. As the environment continues to change, the durability of structures will depend on the resilience of materials, construction practices, and the specific regional climate (IPCC, 2001).

2.2.2 Weather data for Ankara

Ankara experiences significant seasonal temperature variation, in figure 2.1, with hot summers and cold winters. During the summer months (June, July, and August), temperatures can reach highs of 35°C.

The weather data charts given in this section have been taken from Climate Consultant 6.0 software.

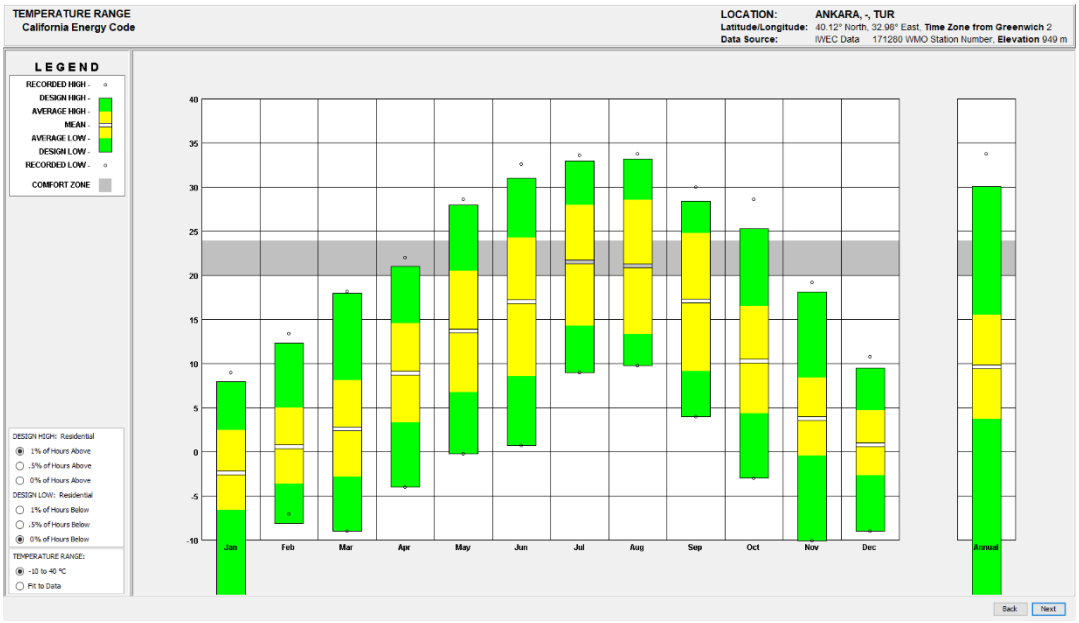

Figure 2-1. Temperature range of Ankara (Source: Climate Consultant 6.0).

In the winter (December, January, and February), lows drop to around -10°C. The average high in July is about 30°C, making it the warmest month, while January sees the lowest average temperatures, close to freezing. In figure 2.1, the comfort zone,

ranging from 18°C to 25°C, is only achieved during short periods in spring (April and May) and autumn (September and October), while the rest of the year falls outside this range. Ankara's climate goes well beyond the comfort zone, particularly in the peak of both seasons.

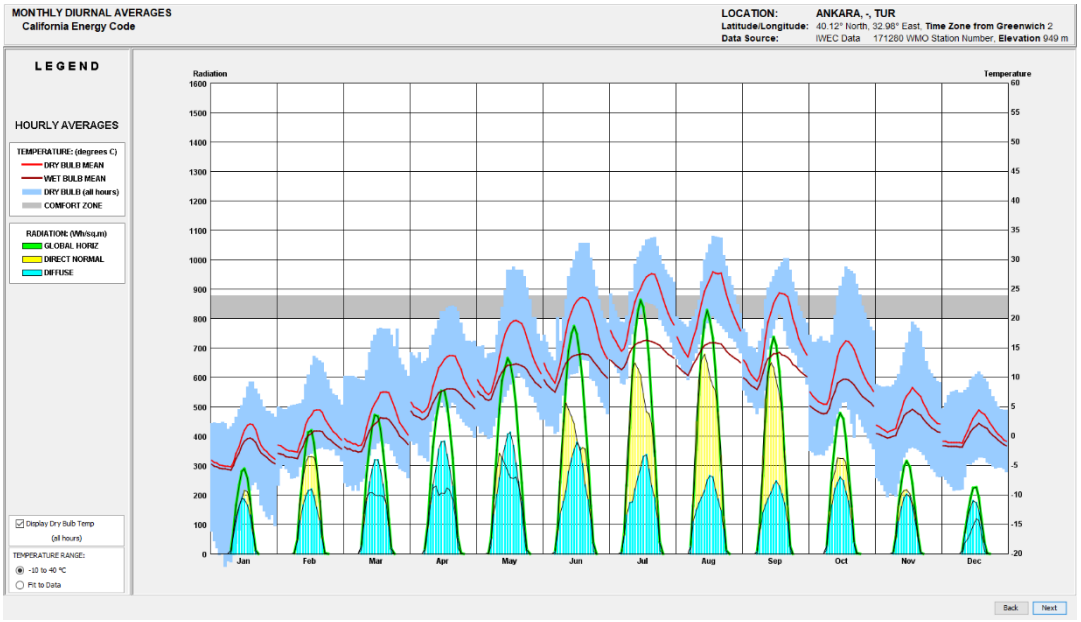

Figure 2-2. Monthly averages of temperature and radiation of Ankara (Source: Climate Consultant 6.0).

As it can be seen from figure 2.2 that, Ankara experiences significant seasonal variations in both temperature and solar radiation, as reflected in the diurnal averages throughout the year. During the winter months (December to February), temperatures remain consistently below 0°C, with dry bulb and wet bulb means indicating cold conditions, while solar radiation is minimal, with global horizontal radiation peaking at less than 200 W/m². In contrast, the summer months (June to August) see a sharp rise in temperature, with dry bulb temperatures reaching 30–35°C and solar radiation levels exceeding 1000 W/m², particularly in July, where direct normal radiation peaks above 1400 W/m². The comfort zone, defined between 18°C and 25°C, is primarily achieved during the transitional months of spring and

autumn, specifically in April, May, September, and October, when temperatures are milder, and radiation is moderate.

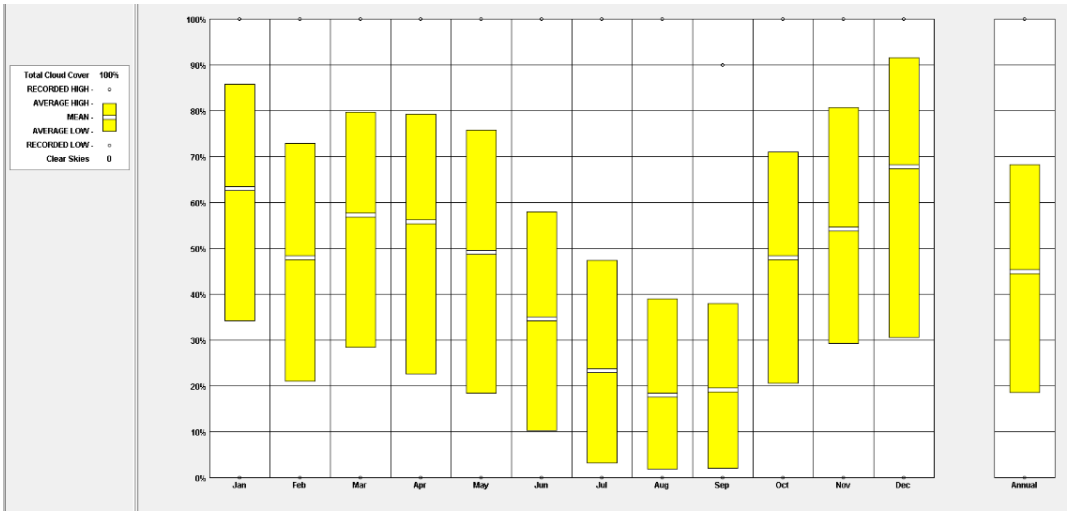

Figure 2-3. Sky cover range of Ankara (Source: Climate Consultant 6.0).

The analysis of sky cover data for Ankara, Turkey, reveals significant seasonal variations in cloud cover throughout the year. From figure 2.3, the highest levels of cloud cover are observed during the winter months, particularly in January, February, and December, where cloud cover ranges from approximately 50% to 90%. These months are characterized by frequent overcast conditions, with mean cloud cover hovering around 70-80%. In contrast, the summer months, especially June, July, and August, exhibit the lowest cloud cover, with values dropping as low as 10-60%, and a mean close to 30%. The transitional months of spring (March to May) and autumn (September to November) show intermediate cloud cover levels, with gradual increases or decreases as the seasons change. Overall, the annual mean cloud cover for Ankara remains around 60%, indicating moderately cloudy conditions throughout the year.

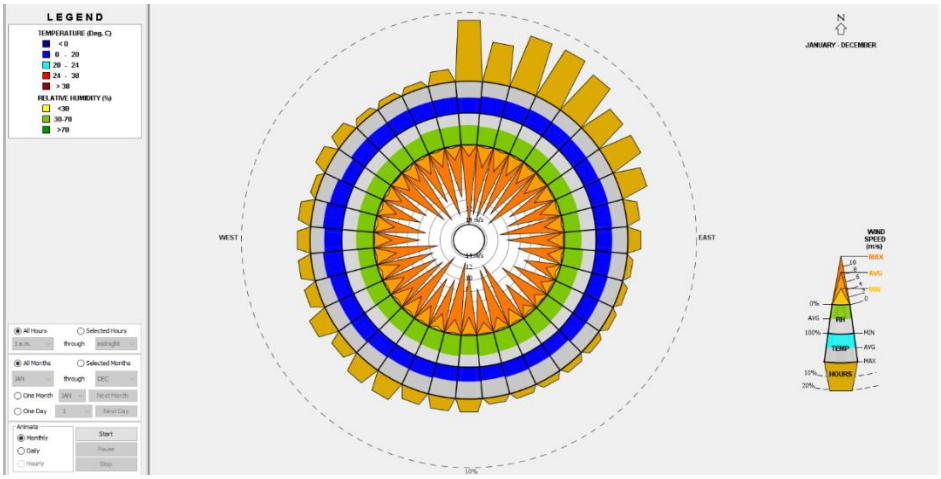

Figure 2-4. Wind Wheel of Ankara (Source: Climate Consultant 6.0).

The wind characteristics and atmospheric conditions of Ankara, Turkey, as illustrated by the wind wheel, reveal important seasonal patterns. Figure 2.4 shows that, wind speeds are generally moderate, ranging from 10 to 15 km/h throughout the year, but winter and early spring can bring stronger gusts of up to 25-30 km/h Throughout the year, Ankara has variations in the direction of the predominant wind. The prevailing wind direction is predominantly from the northwest and west, with average wind speeds ranging from 6 to 12 m/s throughout the year. The highest wind speeds occur during the cooler months, coinciding with lower temperatures, as indicated by the dominance of blue color bands representing temperatures below 20°C. Conversely, during the warmer months, the wind speeds are moderate, with temperatures rising between 20°C and 38°C, as reflected by the green and yellow bands. Relative humidity follows a seasonal trend, with humidity levels ranging from 30-70% during the cooler months and dropping below 30% in the dry summer period. These patterns provide insight into Ankara's semi-arid climate, characterized by windy and relatively humid winters, and dry, warmer summers, which are key factors to consider in local climate and environmental analyses.

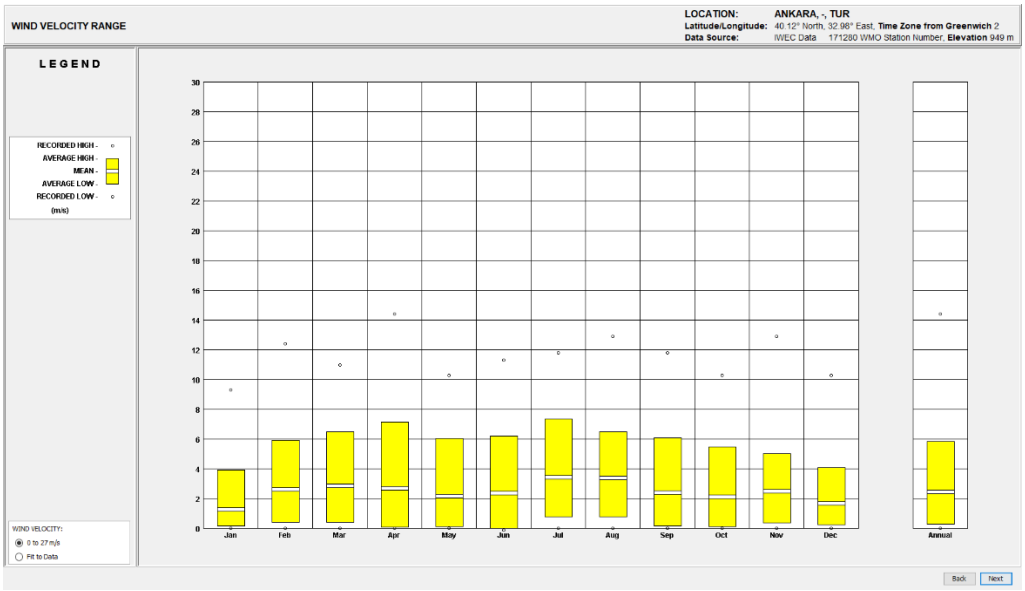

Figure 2-5. Wind velocity range of Ankara (Source: Climate Consultant 6.0).

This image shows a Wind Velocity Range graph for Ankara, Turkey, presenting monthly wind speed data in meters per second (m/s). Figure 2.5 illustrates the recorded high, average high, mean, average low, and recorded low wind speeds for each month, with an additional annual summary on the far right. The data reveals that wind speeds in Ankara remain relatively consistent throughout the year, with some seasonal variation. During the winter months, particularly January and February, the mean wind speed is lower, around 3 to 4 m/s, but gradually increases through the spring months, reaching peaks in April and July where average high wind speeds surpass 6 m/s. The lowest wind speeds are observed in the winter months, while the summer months exhibit slightly higher wind velocities. The recorded high values, shown as dots on the chart, indicate extreme wind speeds, reaching over 14 m/s on rare occasions, particularly in the spring and early autumn months. Annual wind velocity range shows a consistent mean wind speed of about 4-5 m/s, with occasional extreme gusts exceeding 14 m/s throughout the year. These variations in wind speed are indicative of Ankara's temperate climate, with moderate winds year-round and occasional stronger winds, likely linked to seasonal changes and weather patterns.

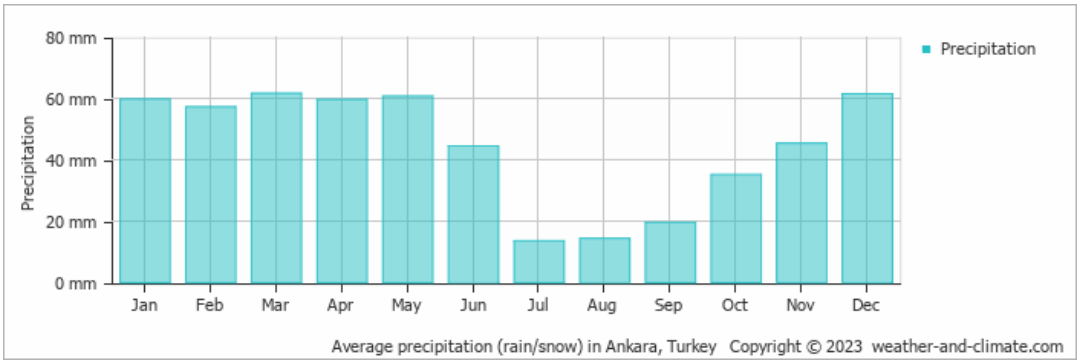

Figure 2-6. Average precipitation (rain/snow) in Ankara (Weather & Climate, n.d.).

Figure 2.6 displays the average monthly precipitation (rain/snow) in Ankara, Turkey. The precipitation levels fluctuate throughout the year, with notable peaks during the winter months. January, February, and December record the highest amounts of precipitation, all around 60-65 mm, suggesting a wet winter season in Ankara. The summer months, particularly July and August, experience the least rainfall, with precipitation levels dropping to around 15-20 mm, indicating a dry period typical of Mediterranean or continental climates. Spring (March to May) and autumn (September to November) show moderate precipitation, with May and November receiving approximately 50-60 mm of rainfall. This pattern reflects Ankara's climate, characterized by hot, dry summers and cold, wet winters. The data underscores the seasonality of precipitation, where transitional months have more rainfall than the dry summer but less than the winter peak.

2.3 Earth as a sustainable building material

Ensuring access to high-quality housing is widely recognized as a fundamental responsibility for promoting the well-being of citizens globally. To fulfill this duty, building materials derived from natural resources are often employed. Among these materials, earth stands out as one of the oldest and most traditional options for constructing walls. Remarkably, approximately 30% of the world's population still

resides in dwellings made of clay-based structures (Jayasinghe & Kamaladasa, 2006).

The foundation of these earthen structures typically consists of a mixture of clay silt or sand combined with varying amounts of water. To enhance the stability of the mixture, additional binders, such as cement, may be incorporated. Furthermore, reinforcement materials like straw are often added to further strengthen the structure (Pacheco-Torgal & Jalali, 2011).

2.3.1 Earth mortars

Since earth mortars are recognized as eco-efficient solutions and can help to improve some important building performance factors linked to occupant health and comfort as well as building sustainability, there is an increasing interest in them on a global scale. With this demand, researchers are making various attempts to understand and improve the properties of this material and make it suitable for use. Attempts that are concentrated on mechanical thermal and hygric properties were examined. Clay-based earth mortars are increasingly recognized worldwide as environmentally efficient options for plastering applications. Notably, in comparison to other types of plasters, they exhibit low embodied energy, contributing to sustainable building practices. Additionally, their use on interior wall surfaces can significantly enhance the health and comfort of occupants (Faria & Aubert, 2016).

Earth mortars typically consist of a blend of sand, clay, and vegetal fibers. Sand provides structural support to the plaster, comprising particles, primarily quartz, ranging in diameter from 0.0625 mm to 2 mm. Clay, a complex mixture of hydrous aluminum silicates, metal oxides, and organic matter, acts as the binding agent in earth mortars. The inclusion of natural fibers in the mixture aids in cohesion and imparts flexibility to the plaster upon drying. This fiber reinforcement mitigates the tendency of clay-based plasters to crack in response to fluctuations in indoor humidity. Moreover, the addition of natural or synthetic additives, such as cellulose, linseed oil, bitumen emulsion, or lime, serves various purposes, including enhancing

physical properties, durability, abrasion resistance, and altering color (Melia et al., 2014).

In traditional raw earth production, local builders often encountered challenges when using clay-rich soils with clay percentages exceeding 40%. To address these challenges and prevent issues such as shrinkage or cracking in walls, builders mixed the clayey soils with sand or natural fibers, such as cereal straw, wood aggregates, or bast fibers. This mixture was then combined with an adequate amount of water to achieve a plastic state suitable for manufacturing raw earth plaster, cob, and wattle and daub constructions (Giada et al., 2019).

The production of earth mortar varies from region to region, but in general, to make earth mortar, combine clay and sand. Optionally, additives can be also used to enhance its properties like fibers, cow dung etc.

2.3.2 Mud plaster

Mud-based architecture originated in Egypt and flourished along the banks of the Nile River. Egyptian Pharaohs employed plaster finishes extensively in their palaces and pyramids, many of which have withstood the test of time and remain remarkably intact to this day. Among the earliest archaeological evidence of plaster use and ancient civilization is the site of Çatalhöyük, dating back to approximately 7500 BC, located in present-day Turkey (Qasab et al., 2020).

Plaster is a viscous mixture that is commonly used for surfacing walls, ceilings, and partitions. It usually consists of lime or gypsum, water, and sand. The mixture solidifies upon drying. Among the earliest construction techniques ever used by humans is plastering. Historical evidence suggests that ancient civilizations applied plaster to their primitive shelters constructed from reeds or saplings, thereby enhancing structural durability and providing improved protection against pests and harsh weather conditions. Over time, mud-based materials were gradually replaced by more durable and aesthetically pleasing alternatives (Qasab et al., 2020). The history of plasterwork dates back over 4,000 years, with early records indicating its

usage in ancient civilizations. In short, adobe has been accompanying our living spaces for a long time and has its strengths and weaknesses in terms of usage.

2.4 The experimental methods utilized for the evaluation of mud plaster

Despite the longevity of earth building as a technique, the field has yet to be the subject of extensive research. Furthermore, the methodologies and experimental designs employed have not been standardized to any significant extent (Jiménez Delgado & Guerrero, 2007). Further study is needed to link the relationship between the different qualities and testing methods (Lima et al., 2020). Researchers often approach this issue based on their individual perspectives and interpretations. This thesis aims to compare the results of the research conducted by Pedergnana. It is important for the results that will be obtained through experiments to be highly like each other for comparisons. The following paragraph will outline the different techniques used to assess these qualities especially (Pedergnana, 2022).

2.4.1 Physical Properties

Methods of analyzing shrinkage and bulk density of the hardened mortars will be examined.

2.4.1.1 Shrinkage

The wall's surface, along with the adjacent wall surface, functions to prevent shrinkage-related size reduction, which could otherwise lead to crack formation. Alcock testing on 4x4x60 cm^3 samples (Avrami, 2008) or 2x2x20 cm^3 samples (Minke, 2012) is advised by the literature on earth building.

Lagouin et al. (2021) conducted a comparison of surface and prism shrinkage; however, the differences in their behaviors are so significant that establishing a precise correlation between them is not feasible. Shrinkage has also been examined

in relation to crack formation on specifically designed samples, as demonstrated by Araya (2019), who utilized specialized software for the analysis—a method previously validated by Rojat et al. (2014) on particularly large samples. According to Faria (2016), factors such as the sample's size, shape, support material, and drying temperature, among others, all influence the extent of shrinkage.

2.4.1.2 Density

Density is typically determined using samples at room temperature that are also utilized in mechanical testing. However, Minke (2012) pointed out that there can be differences in density between the edges of cut samples and unaltered specimens. In the research of Pedergnana (2022), three different specimen types were analyzed for density. These specimens were stored for three weeks under controlled humidity and temperature conditions in a laboratory. To determine their densities, the specimens were precisely weighed, and their dimensions were measured with a Vernier scale. For larger samples, the average of multiple measurements was used to calculate density.

2.4.2 Mechanical Strength

Mechanical testing approaches for earth plasters vary, with some methods concentrating solely on compressive strength, while others assess both compressive and flexural strengths using samples of different sizes and employing various loading protocols.

2.4.2.1 Compressive strength

Compressive strength testing of prismatic or cylindrical samples is guided by standards like ASTM D5731, ASTM C170, ASTM D1633, and EN 1015. Rojat (2014) suggests that sample surfacing is unnecessary, and the orientation of the

sample, including fiber direction, does not significantly affect the results. The challenge in pinpointing the exact failure point in earth plaster arises from the possibility of ductile failure and considerable deformation of the samples (Lerner and Donahue, 2003). Additionally, it has been noted that those formulating mortars for mud bricks often use the brick itself as a test medium (Piattoni, 2011).

2.4.3 Durability

The durability of plaster is influenced by several factors related to the material's long-term preservation. Key concerns include weather resistance, water absorption, abrasion resistance, and erosion resistance, especially since earthen plaster tends to have low resistance to shock and water (Maheri, 2011). Various standardized tests and procedures are used to assess the durability of mud plaster, but these protocols can vary in duration, the amount of water used, and how results are interpreted (Pedergnana, 2022, p. 103). Researchers often use plasters in their experiments, selecting the tests and methods that align best with their objectives. This thesis emphasizes the importance of abrasion resistance, water resistance, and erosion resistance.

2.4.3.1 Water resistance

The stability of the material in water is assessed using two different methods: full submersion and partial immersion. The rate at which the material deteriorates serves as an indicator of its water stability; the faster the material degrades, the less stable it is. In the full submersion test, the stability is evaluated by measuring the loss of material over a set period (Castrillo et al., 2021). The partial immersion test involves either immersing the material in water for a specified duration or submerging half of the material until the water reaches the top (Babe et al., 2020). In this thesis, Pedergnana (2022) employs the submersion test to determine the time required for the material's complete disintegration.

2.4.3.2 Erosion resistance

To determine how rainfall impacts earthen materials, erosion resistance is measured using two main tests: spray and drip.

The spray test involves spraying water at a specific distance and pressure onto the specimen multiple times over a set period, or until the specimen is completely eroded. For instance, some researchers inclined the sample at a 30° angle and used a shower head positioned 50 cm away to wash it for 10 minutes (M. Ouedraogo et al., 2019).

The drip test simulates the effects of rainfall by dripping water onto the samples to evaluate their erosion resistance. Water is dripped during various procedures from different heights, slopes, and time intervals, leading to the standardization of the test in several ways. For example, the Swinburne Accelerated Erosion Test (SAET) involves dripping 500 mL of water for 10 minutes from a height of 1 meter while the specimen is inclined at a 27° angle (Clausell, 2020). In his experiments, Pedergnana (2022) used a drip test where the sample was positioned at a 30° angle and supported to prevent damage while submerged in water. The apparatus was designed with feet that maintained a 40 cm gap between the surface of the tested sample and the container. The container's cap was drilled with a single 40 cm hole, allowing 100 mL of water to be delivered in 30 minutes.

2.4.3.3 Abrasion test

Abrasion tests are intended to assess the durability of materials when subjected to repeated friction. For non-stabilized earth mortar, specific setups with detailed, standardized protocols have been developed. There are two primary standards for abrasion resistance testing: the German and the French standards. The German Standard (DIN18947, 2013) involves using a rotating plastic brush with a 2 kg load. On the other hand, the French Standard employs a method where a metallic brush,

loaded with 3 kg, is pushed and pulled across the material. In this thesis, the French method using the metallic brush is applied.

2.4.4 Surface Properties

The resistance of the mortar's top layer to abrasion and water penetration is known as surface characteristics, and it determines how long the surface will last.

2.4.4.1 Surface abrasion (peeling test)

According to Colas & Bourges (2013), the tape test is the second most used method for assessing surface cohesiveness. This test involves measuring how much plaster adheres to a tape after it has been applied and then removed. However, Faria (2016) notes that this test lacks standardization and relying solely on the quantity of material removed can lead to inaccuracies. To address this, Santos et al. (2018) recommended applying a consistent mass to the tape for a set duration to ensure uniform pressure across all test samples. In his studies, Pedergnana (2022) implemented this method by applying pressure to the tape during the test.

2.4.4.2 Surface water absorption

The first method to measure surface water absorption involves pressing a damp sponge against the plaster with specific pressure and time, then measuring the amount of water absorbed by the plaster's surface layer. Paul and Changali (2020) conducted their tests by placing the sample horizontally on a sample holder, while Colas & Bourges (2013), using a test designed for on-site wall material assessment, positioned the sample vertically when pressing the sponge against it. Pedergnana (2022) conducted his tests using a water-saturated sponge with applied weight for 90 seconds.

2.4.5 Hygric Properties

Hygric properties refer to how mortars manage moisture and water vapor, which is critical for understanding how well a material can absorb moisture from the air and then release it back into the environment. Proper moisture management regulates indoor humidity levels and ensures the mortar's effectiveness in binding wall materials. If a material fails to manage water vapor effectively, it can lead to structural weakening, mold growth, and other issues. Therefore, hygric properties are essential for maintaining the comfort and durability of a building. "Sorption isotherms" are graphs that illustrate how a material's capacity to absorb or release moisture varies under different environmental conditions (Pedergnana 2022).

2.4.5.1 Water vapour permeability

The measurement of water vapor permeability is standardized by various standards such as EN 1015-19, DIN 18947, ISO 12572, ASTM E96, and EN 15803, with sample thickness ranging from 1 to 5 cm depending on the standard. During testing, all parts of the sample except the surface are waterproof, and the sample is placed above water. The test is conducted in an environment with stable humidity and temperature (Laborel-Préneron, 2018). To determine how much moisture passes through the sample, the weight loss due to humidity transfer is measured. This data is then used to calculate the material's water vapor permeability coefficient (Pedergnana, 2022).

2.4.6 Hydric properties

To evaluate the hydric properties of earth mortars, both water absorption and desorption rates, as well as the drying rate, are analyzed. The water absorption assessment considers both the rate at which water is absorbed and the total volume

absorbed. Several standardized methods exist to quantify water absorption and drying capacity (Pedergnana 2022).

2.4.6.1 Water capillarity absorption

Water capillary absorption is commonly assessed through several standardized tests, including EN 1015-18, DIN 2617, and RILEM TC 25-PEM. These tests involve exposing the sample material to water for a set period, determining both the rate of water absorption and the total volume absorbed. The process may involve either direct submersion of the sample in water or maintaining indirect contact with water through a moist medium.

To ensure consistent moisture exposure throughout the test and prevent material loss during measurement, a thin cloth or filter paper (Guiheneuf et al., 2020) is typically attached to the bottom of the sample, which remains in contact with water either directly or indirectly. Additionally, the sides of the sample are often coated with a waterproof material, such as resin or polyethylene film, to maintain the integrity of the sample during the test (Faria, 2016).

The total volume of water absorbed by the sample is heavily influenced by its dimensions, particularly its thickness (Guiheneuf, 2020). This is because capillary forces, which drive the absorption process, continue to draw water into the sample until it reaches the top surface. Once the top surface is reached, the sample becomes saturated as the air within the water dissolves. Therefore, when comparing the water absorption of samples of different sizes, it is essential to consider their dimensions, especially thickness as they have a direct impact on the amount of water the sample can absorb (Pedergnana, 2022).

2.4.6.2 Drying Capacity

The drying behavior is assessed by modifying the procedures from EN 16322, RILEM Test No. II.5, or RILEM TC 25-PEM standards, using the same samples tested for water capillarity absorption. Non-saturated samples serve as a reference to determine the drying behavior (Faria, 2016). Lima et al. (2020) divides the drying capacity assessment into two phases: primary drying, which involves the desorption of water, and secondary drying, which refers to the evaporation of water vapor.

The study found that different types of earth-based mortars absorbed water and dried at different rates. Even though some samples absorbed more water and dried faster, all three mortars reached equilibrium (fully dry) around the same time (10 days). The study didn't find a clear link between water absorption, drying behavior, and the other properties of the mortars, but it suggested that the pore size of the mortars might influence their behavior Lima et al. (2020).

CHAPTER 3

MATERIAL AND METHOD

The mud plaster samples were removed from experimental strawbale walls that had been built on the campus with funding from METU Research Projects (Nos: BAP-02-01-2015-001; BAP-02-01-2015-002 and BAP-02-01-2016-003). As part of these projects many earth plaster mixes had first been tested in laboratory experiments, and then 9 different compositions were selected to be tested in outside conditions on experimental walls. Thus, three strawbale walls were constructed outside the Architecture Faculty Annex building in METU Ankara campus, in October 2016. These walls were divided into 3 vertical panels each for the application of the 9 mixes separately, on the north facing side, while the other 3 sides were protected with plastic sheeting. The plasters were left untouched to test their resilience to Ankara weather conditions, until April 2022. In this study, the plaster samples taken from these strawbale walls are examined in terms of their durability, mechanical strength, hydric properties and hygric properties, and the results are compared with those obtained through the above-mentioned laboratory experiments.

3.1 Materials

All samples had been applied in panels on three strawbale walls built in a row, in 2016 for the METU BAP research projects (Figure 3.1). Samples differed from each other in terms of their compositions, which also look different regarding color, texture and surface cracks. Five and a half years later, in April 2022 the samples that were to be used in the experiments were collected from the walls using a saw, axe and hammer. In Table 3.1 and Table 3.2, the properties of the samples are shown, and in Figure 3.2, how and from where the sampling was taken is shown.

Figure 3-1. Strawbale walls marked A, B and C Panels (ordered left to right).

Figure 3-2. Strawbale wall samples removed from the 9 panels A1(KeSdMo), A2 (KeSdFbEg), A3 (KeSdFbCd), B1 (KeSd), B2 (KeSdFb-1), B3 (KeFb), C1 (KeSdFbDj), C2 (KeFbCd), C3 (KeSdFb-2) (ordered left to right)

3.1.1 Composition of mud plaster samples

Earth mortars were made of a mixture of clayey earth and water, with additional components such as sand, fibers, and additives. The basic combination contained clayey earth, river sand, wheat straw from Sorgun, with short straw lengths ranging from 15 to 30 mm. Additives such as dry cow manure, molasses, egg white and straw decomposition juice were also tested.

A total of nine different mud-plaster mixes had been applied to the three strawbale walls designated as A, B and C to determine their properties under outside weather conditions. Samples were taken from these walls and are marked as A1(KeSdMo), A2 (KeSdFbEg), A3 (KeSdFbCd), B1 (KeSd), B2 (KeSdFb-1), B3 (KeFb), C1 (KeSdFbDj), C2 (KeFbCd) and C3 (KeSdFb-2), where A1 is on the far left and C3 is on the far right (Figure 3.2). The composition of the 9 plasters is given in Table 3-1 and Table 3-2.

The materials used in the samples mixes were earth from Kerkenes (Ke); Sand (Sd), Straw fiber (Fb), Cow dung (Cd), Molasses (Mo), Decomposition juice (DJ), Egg white (Eg). Hence, a mix containing earth, sand, fiber and Egg white is coded as KeSdFbEg. These abbreviated codes are given in the table below.

Table 3.1 Composition with preparation and application data of 9 mud-plaster samples

samples code (Pedergnana 2022)	Panels code	Sample Code (Composition)	earth				aggregate				fibers			
			KerkA (Kerkenes white earth)				river sand (4mm max)				Fb01 (short straw)			
			volume (L)	volume %	weight (g)	%	volume (L)	volume %	weight (g)	%	volume (L)	%	weight (g)	%
Ka610-21101a,b,c	A1	KeSdMo	40	33%	45993	30%	80	67%	108982	70%				
Ka111-32211,a,b,c,d	A2	KeSdFbEg	50	40%	54931	44%	50	40%	70038	56%	25	20%	1193	0.9%
Ka711-102211a,b,c	A3	KeSdFbCd	60	44%	71361	45%	60	44%	85560	54%	15	11%	1126	0.7%
Ka010-2002a,b,c	B1	KeSd	50	36%	58675	31%	90	64%	132849	69%				
Ka011-2211a,b,c	B2	KeSdFb-1	60	40%	70755	45%	60	40%	84175	54%	30	20%	1959	1.2%
Ka001-206	B3	KeFb	80	80%	95665.0	98%					20	20%	1575	1.6%
Ka211-221031a,b,c	C1	KeSdFbDj	50	40%	55245	43%	50	40%	72110	56%	25	20%	1458	1.1%
Ka701-10201a,b,c	C2	KeFbCd	80	80%	90990	98%					20	20%	1440	1.6%
Ka011-2212a,b,c	C3	KeSdFb-2	50	40%	55598	44%	50	40%	68345	54%	25	20%	1515	1.2%

Table 3.2 Composition of mud-plaster samples (amounts and types of additives and water content)

samples code (Pedergnana 2022)	Panels code	sample code (Composition)	additives				Water					bulk density (kg)
			egg white%	decomposition juice%	Molasses	cowdung	volume (L)	weight (g)	% w.t.	% vol.	% (of dry soil)	
Ka610-21101	A1	KeSdMo			9%		20	19410	0.13	0.16	0.42	5.98
Ka111-32211	A2	KeSdFbEg	2%				30	30146	0.24	0.30	0.55	5.65
Ka711-102211	A3	KeSdFbCd				6%	45	46083	0.29		0.29	5.23
Ka010-2002	B1	KeSd					26	26054	0.14	0.19	0.44	6.04
Ka011-2211	B2	KeSdFb-1					46	45552	0.29	0.38	0.64	5.43
Ka001-206	B3	KeFb					33	37458	0.39	0.41	0.39	5.13
Ka211-221031	C1	KeSdFbDj		3%			30	30165	0.24	0.30	0.55	5.66
Ka701-10201	C2	KeFbCd				8%	31	30566	0.25		0.34	4.96
Ka011-2212	C3	KeSdFb-2					25	25041	0.20	0.25	0.45	5.63

3.1.2 Sample sizes used for experiments

Each sample was cut to size according to the dimensions required for each experiment, however, due to the difficulty of cutting the samples, it was very difficult to make a perfect cut, so the samples were cut approximately to the specified dimensions. Thinner samples were used in experiments where the thickness of the samples was not important. The sample sizes used for the different experiments are given below:

- Physical properties test samples are prepared to 4 x 4 x 4 cm^3.
- Mechanical properties test samples are irregular sized samples.
- Durability test samples are prepared to 4 x 4 x 4 cm^3.
- Surface properties test samples are prepared to 4 x 4 x 4 cm^3.
- Water capillary absorption and Drying capacity test samples are prepared to 4 x 4 x 4 cm^3.
- Water vapour permeability test samples are prepared to 4 x 4 x 4 cm^3.

3.2 Laboratory Analysis

Physical properties are examined by shrinkage and density experiments. The mechanical performance of samples was examined by the point load test for vertical and horizontal positions. Surface properties are examined with surface abrasion and surface water absorption tests. The durability of samples was analyzed with water resistance, erosion resistance, and resistance to abrasion tests. The hydric performance of samples was examined by water capillary absorption and drying capacity. The hygric property of water vapor permeability was also examined. Experiments with their detailed procedures are explained under respective subheadings.

3.2.1 Physical Properties

Methods of analyzing shrinkage and density of the mud plasters will be examined.

3.2.1.1 Shrinkage

Shrinkage in terms of width, where the sample's dimensions were measured and compared to the panel size while surface cracks were noted. For calculations the difference between the measured data and scaled photographs were used.

Figure 3-3. (Left) Crack on the surface of panel A1(KeSdMo)(Right), Surface of panel C3(KeSdFb-2).

3.2.1.2 Density

Density of samples was determined by weighing the specimens and calculating their volumes. Sample's weights were measured with precision scales. Calculating volumes was a bit difficult due to samples irregularities, therefore two different methods were used.

The first method was taking measurements with a vernier caliper, where all sides are measured, and the volume of the samples are calculated.

The second method was the Archimedes density measurement method where samples should be sealed from all sides to waterproof them and dipped into a 0.05m-radius beaker filled with water (Figure 3.8). After observing the difference in the height of water level, the volume of samples is calculated by equation 1.

$$V = \pi . r^2.h \quad (1)$$

Figure 3-4. (Left) Samples without any covering (Right) wrapped sample for Archimedes experiment.

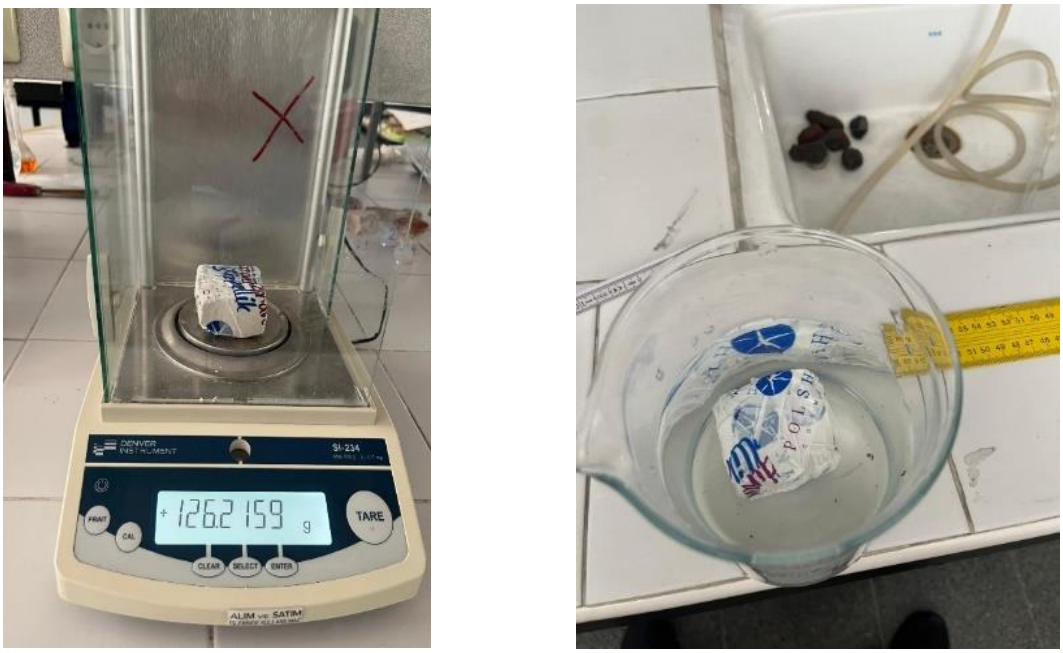

Figure 3-5. (Left) weight with precision scale (Right) calculation of volume with Archimedes method.

3.2.2 Compressive Strength

The mechanical properties of mortars were determined in laboratory conditions; and the Point Load Test was used for calculating compressive strength of the samples.

The compressive strength of samples is analyzed from two perspectives. The first experiment is done to know how samples are durable to the force that comes from outside that are perpendicular to the sample. The second experiment is done to know how strong the samples are to vertical loads. Therefore, samples are tested in two directions, the first experiment is called vertical force test and the second test called horizontal test. All standard procedures are applied for both tests.

First, two support rollers were placed parallel to each other at a specified distance and the loading nose was positioned centrally between the support rollers. After the

first setup sample was placed under the point load on the support rollers such that it was aligned to be centered and aligned properly with the loading nose.

After completing setup, load was gradually started to apply, until the failure happened, with the help of the readings shown in the indicator and area of broken surface the compressive strength of each sample was calculated.

The point load strength index (Is) of the mortar samples was calculated using equation 2.

$$Is = P/De^2 \quad (2)$$

Where,

P : applied load (kN)

De: : equivalent core diameter (mm)

Equivalent core diameter (De) is given by the equation 3 for axial tests.

$$De = \sqrt{4A/\pi} \quad (3)$$

where, A is the minimum cross-sectional area of the test specimen found by multiplying the width of the test specimen with its thickness.

The size-corrected point load strength, Is (50), is calculated from Is, point load strength, index, In his article Brook (1985) suggested the following equation 4;

$$Is\ (50) = F * Is \quad (4)$$

where F, the size-correction factor, which is obtained from De, equivalent core diameter, using the equation 5.

$$F = (De/50)\ \hat{}\ 0.45 \quad (5)$$

To obtain uniaxial compressive strength (U.C.S), it is customary to multiply by IS (50), by the correlation factor ‘k’. It is expressed by the following equation 6.

$$U.C.S = 10.66471 * IS(50) + 22.4739 \quad (6)$$

The values of Is (50) was found by the point load test have been converted into uniaxial compressive strength by the above equation. The results have been given in MPa.

Figure 3-6. (Left) Horizontal sample placement (Right) Vertical sample placement.

3.2.3 Surface properties

Three surface properties of earth plasters were determined by simple tests: surface material adhesion, and surface water absorption.

3.2.3.1 Peeling test

A 4x4 cm2 duct tape first was weighted on precision scale and then it was stuck to the plaster's surface, and it is later removed after 60 seconds. To find the weight of the material adhering to the tape, the weight of the tape that contains materials was

subtracted from the weight of the tape. The test has been modified to apply a 3 kg weight to the tape for 60 seconds rather than using fingers to exert pressure in order to provide more consistent results. Thick foam is positioned between the tape and the weight in order to equally distribute the load caused by the irregularities on the samples' surface.

Figure 3-7. (Left) Sample under the 3kg weight (Right) Adhesive tape with stuck material.

3.2.3.2 Sponge test

A 4x4cm2 sponge was saturated with water and placed in a container whose weight was assessed after placement in order to confirm that the same amount of water was used for each test. The plaster sample was then placed on the sponge with a 3 kg weight on it to ensure uniform pressure and left there for 90 seconds before being removed. The amount of water absorbed was then determined by weighing the difference between the dry and water-saturated samples. After all measurements, the weight difference per m^2 over the 90 seconds is calculated as surface water absorption $g/m^2 \cdot s$.

Figure 3-8. (Left) Sample under the 3kg weight with wet sponge (Right) result of Result of absorption on the test sample.

3.2.4 Durability

Plasters are judged on how long they can withstand rain, water, and abrasion. Tests for water resistance, erosion resistance, and abrasion resistance are conducted to assess this capacity.

3.2.4.1 Water resistance

For each sample are cut to have 4cm thickness with different heights was submerged in 4 cm of water. The amount of time needed to destroy the submerged part was computed.

Figure 3-9. Water resistance test, A1(KeSdMo), A2 (KeSdFbEg), A3 (KeSdFbCd), B1 (KeSd), B2 (KeSdFb-1), B3 (KeFb), C1 (KeSdFbDj), C2 (KeFbCd) and C3 (KeSdFb-2), ordered left to right.

3.2.4.2 Erosion resistance

The sample was set at a 30° angle underneath a 50 mL bottle. For 45 minutes, water dripped from a height of 40 cm. After that, the depth of the hole the drops made was measured with a ruler.

Figure 3-10. (Left) Erosion test setup (Right) 30° sloped sample's base for erosion test.

3.2.4.3 Resistance to abrasion

The abrasion resistance was also calculated on 4x4 cm² samples in compliance with the draft of the French Professional Rules for Earth Plaster (Pedergnana 2022). The plaster was worked in 30 pushes and pulls using a 2.5 cm steel brush that weighed 3 kg. The abrasion resistance is determined by the depth of the grooves made by the metal bristles.

Figure 3-11. French rules test application.

3.2.5 Hydric Properties

The hydric performance of samples was examined by two different experiments which are water capillarity absorption and drying rate.

3.2.5.1 Water capillarity absorption

Using samples measuring 4 by 4 cm², water capillarity absorption was determined using the Minke (2012) and Faria et al. (2015) methods. Samples that had originally been used for the vapour permeability tests were reused in these experiments. Wax had been used to seal the samples' edges to stop water from escaping or entering

during testing. To stop material loss during the capillarity test, the bottom of the samples was protected with filter paper.

The prepared samples were put in a container with a 5 mm deep shallow layer of water. Using a precise scale, samples' original weight was determined. Weighed the samples at regular intervals (30 minutes to 3 hours). After that, Calculated the capillary curve's slope between two given time intervals to find the capillary coefficient.

The square root of the capillary action time, measured in minutes, was shown on the Y-axis of a graph, along with the volume of water absorbed through capillary action, expressed in kg/m², on the X-axis.

The initial capillary coefficient (CC) of the plaster mix was determined by calculating the slope of the plotted line's representative start segment. Hence, CC is given in $kg/m^2 \cdot min^{\cdot 0.5}$.

Figure 3-12. (Left) Water capillary absorption test setup (Right) weighting absorbed water content.

3.2.5.2 Drying capacity

Testing was done on the plaster's drying capacity following studies by Faria et al. (2015) and Lima et al. (2020). After being wetted by the capillarity absorption test, specimens were allowed to dry in the lab setting where the RH ranged between 40 to 50%.

To avoid weakening or cracking, the samples were taken carefully out of the water when the capillarity test finished, being careful not to submerge them completely. As soon as the partially saturated samples were taken out of the water, they were weighed using a precise scale and again at various intervals. Two graphs were made: the first displayed the square root of the recorded sample weight on the X-axis and the time on the Y-axis, together with the recorded sample weight. These graphs were used to calculate the drying behavior. The drying behavior is determined by three different indicators, which show the behavior both throughout the two discrete drying stages and during the whole drying period. The material is dried in the first phase by the primary drying rate (pDR), which is the desorption of liquid vapor; in the second phase, the material is dried by the evaporation of the water content, which is a slower process (Lima 2020). The regulated environment in which samples are placed and the interchange of water and energy with the environment make the temperature and relative humidity (RH) of the drying space crucial. The sDR was determined by plotting the slope of the linear regression of the weight loss against the square root of time, whereas the pDR was determined by the slope of the straight segment of the curve with hours on the x-axis and finally, equation 7 was used to calculate the Drying Index (DI), which measures the amount of time needed to reach full drying, in accordance with Grilo et al. (2014) procedure.

$$DI = \frac{\sum_{i=1}^{i=n}\left[\left(t_i - t_1\right) \times \left(\frac{w_{t_{i-1}} + w_{t_i}}{2}\right)\right]}{w_{max} \times t_f} \quad (7)$$

Where,

DI (-): drying index,

ti (h): test time,

tf (h): total duration of the test,

wti (%): water content in time ti

wmax (%): maximum water content at initial testing time

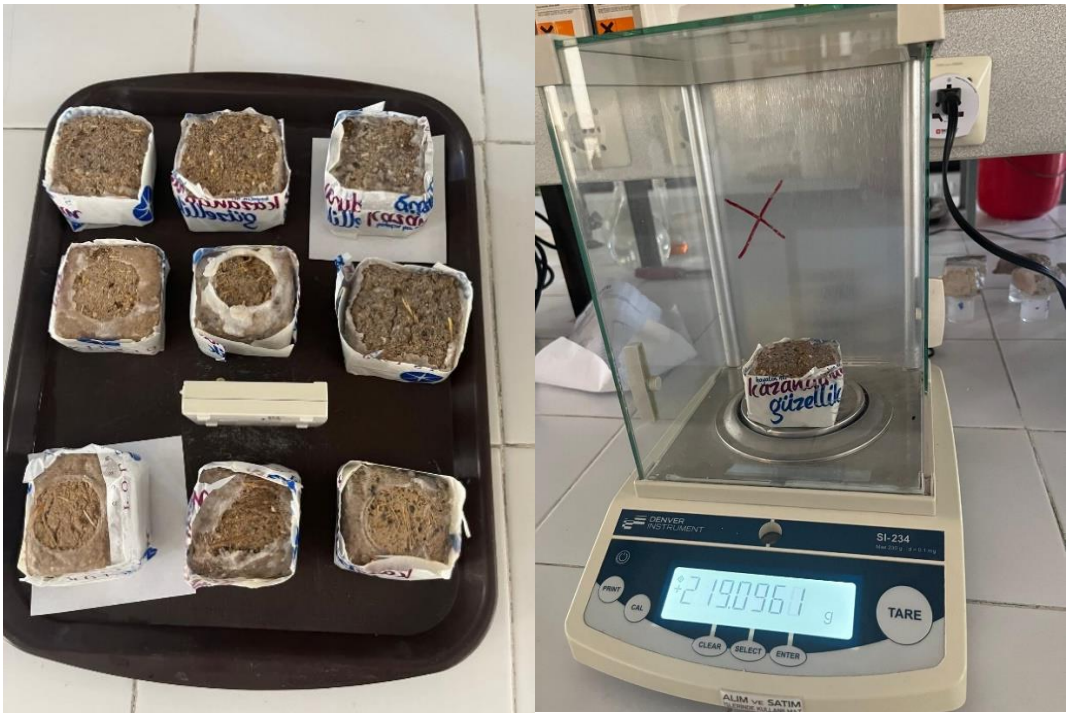

Figure 3-13. (Left) Samples left to dry and weighed periodically to calculate their Drying Index (Right) weighting samples during the drying phase.

3.2.6 Hygric Properties

The hygric properties determined for the nine samples was their water vapour permeability.

3.2.6.1 Water vapour permeability

Water vapor permeability was measured using 4x4 cm^2 square samples with an approximately uniform thickness, in accordance with DIN 18947 methodology of the Wet cup technique. The thicknesses of the samples were measured from three points with a caliper and then the average of these three thickness values were taken as the thickness value for each material. The beakers (2 cm diameter test tube) were filled to leave 2 cm of air space between the sample and the water, then they were covered with the samples. The edges were sealed with melted wax with the help of a brush. Relative humidity, atmospheric pressure and the temperature of the room were recorded. Samples were weighed and the data gathered was used as the initial weight value of the samples. The samples were weighed until weight loss per unit became constant. The samples were checked each day from day to day to up to a week interval. This was done to achieve maximum speed of water discharge through saturation of the material with water and that in the start, the water discharge is slow for the material is not yet saturated with water. All the nine samples were carefully measured and analyzed.

Figure 3-14. Wet cup water vapour permeability test showing samples B1, B2 and B3

Equation (8) has been utilized to calculate the water vapour permeability (δ, kg/ (m s Pa)) (Liuzzi et al., 2018). Equation (9) was used to compute the water vapour diffusion resistance factor (μ, -), in accordance with Cagnon et al. (2014) and Luizzi et al. (2018). Equation (10) and equation (11) was used to compute the equivalent air layer (Sd, m) (Stazi et al., 2015).

$$\delta = \Lambda \times e \quad (8)$$

Where e (m) is the sample thickness and Λ [kg/(m² s Pa)] is the sample permeance determined using EN EN1015-19 (Liuzzi et al., 2018).

$$\Lambda = \frac{1}{\frac{A \times \Delta_p}{flux\ of\ vapor}} \quad (9)$$

Where A (m2) is the cup's opening area, Vapor Pressure Gradient (Pa) is the vapour pressure gradient between the testing environment and the cup, and Vapor Flux (kg/s) is the measured data's slope following a week of weight loss stabilization. ΔP

is expected to be 2537 Pa in an average room with 22.5 °C and 35% relative humidity.

$$\mu = \frac{\delta_{air}}{\delta} \quad (10)$$

Where δair is the air permeability at 22 °C and is taken as 1.96 10−10 kg/(m s Pa)

$$Sd = \mu \times e \quad (11)$$

Where e (m) is the thickness of the sample

CHAPTER 4

RESULTS AND DISCUSSION

4.1 Physical Properties

The results of experiments that are conducted to understand the shrinkage and the density of samples are presented in the table below.

Table 4.1 Physical properties of mud plaster samples

Name of samples	earth (Kerkenes with earth) volume %	river sand (4mm max) volume %	fiber (short straw) volume %	water volume %	egg white volume %	decomposition juice volume %	molasses volume %	cow dung volume %	density-dry (kg/m³)	density-wet (kg/m³)	shrinkage %
A1 (KeSdMo)	33%	67%		13%			9%		2.028	1.684	4.2%
A2 (KeSdFbEg)	40%	40%	20%	24%	2%				1.783	1.535	2.8%
A3 (KeSdFbCd)	44%	44%	11%	29%				11%	1.927	1.474	2.3%
B1 (KeSd)	36%	64%		14%					1.984	1.780	3.2%
B2 (KeSdFb-1)	40%	40%	20%	29%					1.796	1.577	5.1%
B3 (KeFb)	80%		20%	39%					1.778	1.461	8.0%
C1 (KeSdFbDj)	40%	40%	20%	24%		3%			1.637	1.409	3.0%
C2 (KeFbCd)	80%		20%	25%				10%	1.760	1.584	8.3%
C3 (KeSdFb-2)	40%	40%	20%	20%					1.683	1.435	4.7%

4.1.1 Shrinkage

Results of this experiment differ from the previous experiments, because of the sample's size and shape, which is larger than the investigated samples. As pointed out in the literature, Faria (2016) claims that shrinkage is influenced by the sample's size, shape, support material, drying temperature, and other factors.

At first, without any experiments, it is shown in Figure 3.1 that A1 (KeSdMo), B1 (KeSd), and C2 (KeFbCd) have cracks on their surface. The overall shrinkage of samples varies between 2.3% A3 (KeSdFbCd) to 8.3% C2 (KeFbCd).

Different amounts of water have been used in different samples and have an impact on the shrinkage as suggested in the literature. The amount of added water varies from 25% to 24%, while the shrinkage varies from 3% to 8% for these two specific samples C1 (KeSdFbDj and C2 (KeFbCd)).

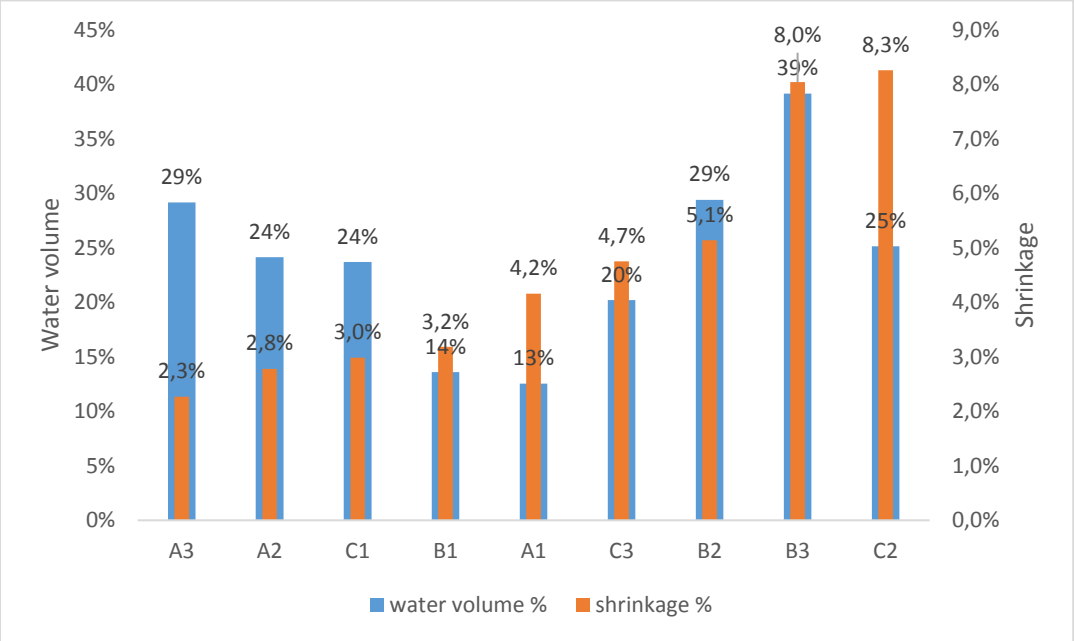

Figure 4-1. Shrinkage of mud-plaster walls with respect to their water volume.

It can be seen in Figure 4.1, there is an increase in shrinkage with an increase in the water percentage. For example, A1 (KeSdMo) and B1 (KeSd) have the one of the

lowest shrinkages with around 13% water content while B3 (KeFb) has the one of the highest shrinkages with 39% water content.

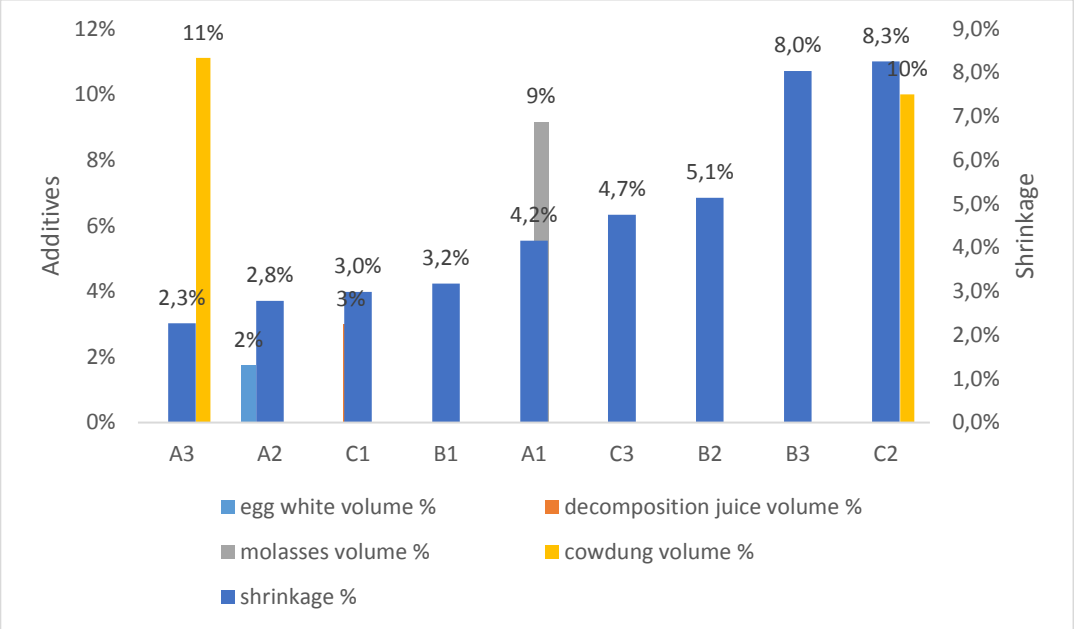

Figure 4-2. Shrinkage of mud-plaster walls with their additive contents.

Figure 4.2 shows that there is a relationship between additives and shrinkage. C2 (KeFbCd) shows the effect of cow dung in their composition while A1 (KeSdMo) shows the effect of molasses, and A2 (KeSdFbEg) shows the effect of egg white on shrinkage. In the absence of molasses B1 (KeSd) performed superior to A1 (KeSdMo). Molasses negatively effects the shrinkage of the sample. On the other hand, the effect of egg white and decomposition juice on the shrinkage is clearly seen on the graph, where A2 (KeSdFbEg) and C1 (KeSdFbDj) performed better than C3 (KeSdFb-2) while their composition slightly similar expect their additive contents.

According to figure 4.3, with the absence of aggregate, samples have a higher shrinkage, like B3 (KeFb) and C2 (KeFbCd), where both do not contain any aggregate while having higher shrinkage.

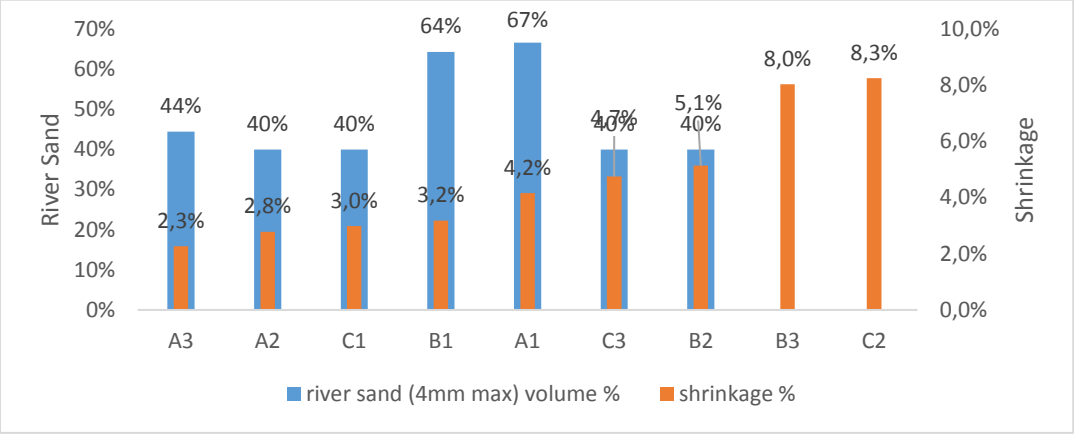

Figure 4-3. Shrinkage of mud-plaster wall samples with their sand content.

A2 (KeSdFbEg), B2 (KeSdFb-1), C3 (KeSdFb-2), C1 (KeSdFbDj), C2 (KeFbCd) and C3 (KeSdFb-2) have the same percentage of fiber, however, all have different shrinkages, while the highest is C2 (KeFbCd) and B3 (KeFb) lowest shrinkage is A2 (KeSdFbEg) and C1 (KeSdFbDj). The reason could be the content of egg white and decomposition juice content of A2 (KeSdFbEg) and C1 (KeSdFbDj). Figure 4.3 shows that the samples that have around %40 aggregate tend to have lower shrinkage, however, in another case, the shrinkage of samples gets affected negatively.

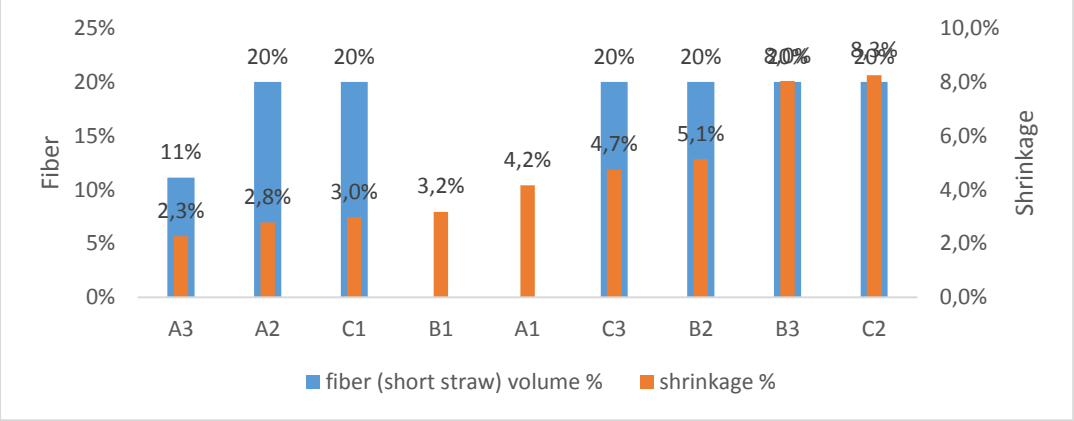

Figure 4-4. Shrinkage of mud-plaster wall samples with their short straw content.

As it can be seen from figure 3.1 that, there is a relationship between surface cracking and fiber content where A1 (KeSdMo), B1 (KeSd), and C2 (KeFbCd) have surface cracking, while A1 (KeSdMo) and B1 (KeSd) do not contain any fiber. On the other hand, C2 (KeFbCd) has the highest shrinkage while containing fiber and cow-dung. Therefore, fiber does not prevent samples from having higher shrinkage alone.

4.1.2 Density

Two experiments are done for calculation density for each sample. The first experiment is dry-density, and the second experiment is Archimedes-density.

For the dry-density experiment where samples were cut with a saw, and their volumes were calculated by ruler; densities vary between 1637 kg/m³ C1 (KeSdFbDj) and 2028 kg/m³ A1 (KeSdMo).

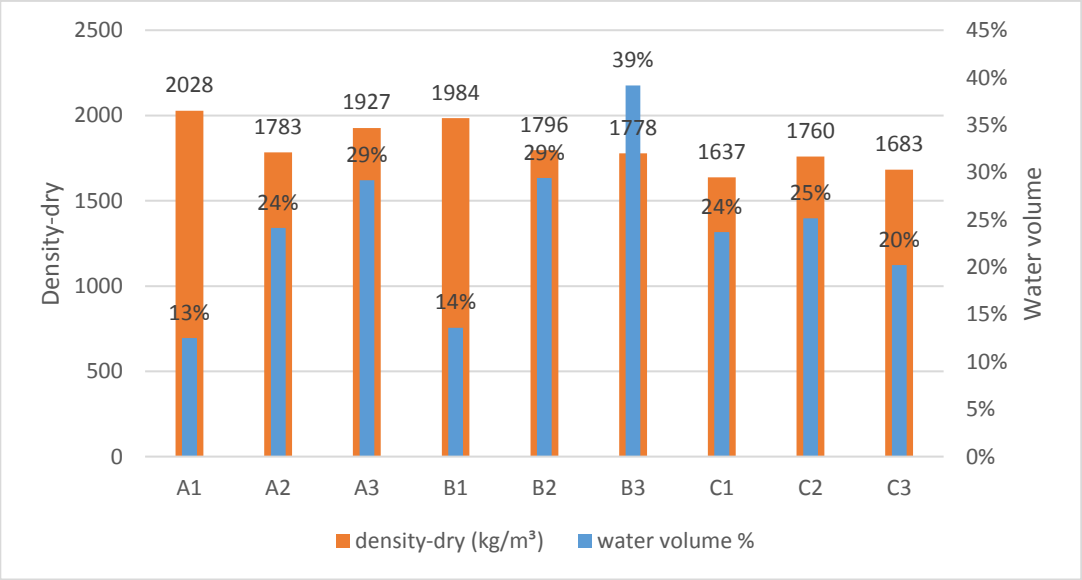

Figure 4-5. Dry-density of mud-plaster samples with water content.

For the second experiment, where Archimedes' principle is used to reduce the margin of error due to the irregular cross-sections of the samples cut roughly with a

saw; density vary between 1409 kg/m³ C1 (KeSdFbDj) and 1780 kg/m³ A1 (KeSdMo).

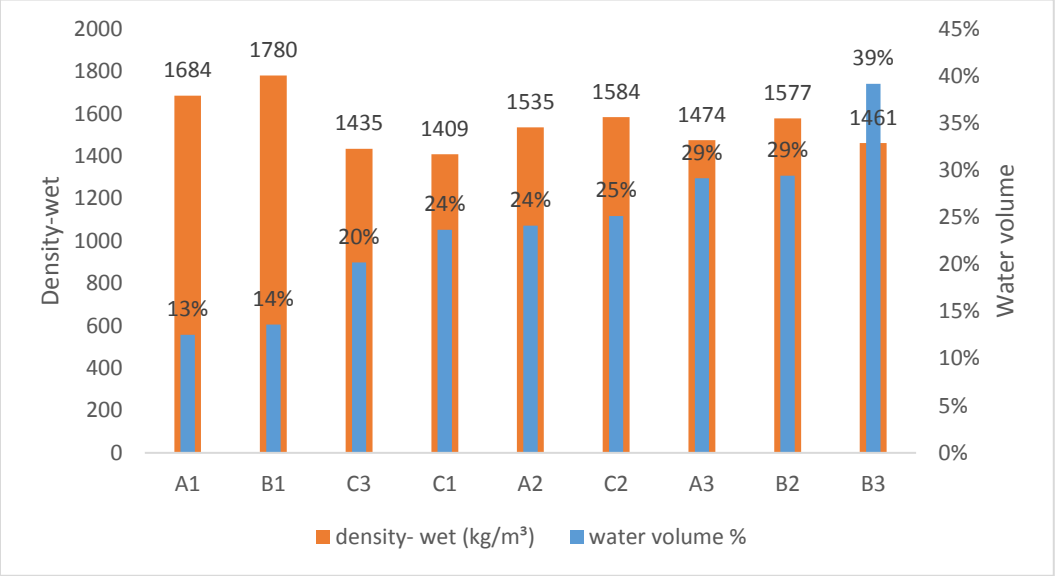

Figure 4-6. Density-wet of mud-plaster samples with water content.

The amount of water added to the mixtures matters. Over-wetting can lead to a weak, porous structure, while under-wetting can result in poor workability and inadequate bonding. To get the maximum density and strength after curing, the right amount of water must be present. These findings indicate that it is best to compare specimens of the same size and water content when comparing the different sample mixes. There is a clear relationship in Figure 4.6, with the increase in water content, the density of samples decreases. B1 (KeSd) and A1 (KeSdMo) support this trend while they both have the lowest water content; they also have the highest density.

Aggregate has an effect on density, as it can clearly see in Figure 4.7 where A1 (KeSdMo) and B1 (KeSd) have the highest density with 65% of aggregate content, they have high density, on the other hand, C2 (KeFbCd) and B3 (KeFb) that has no aggregate content has one of the lowest densities. A3 (KeSdFbCd), B2 (KeSdFb-1),

C1 (KeSdFbDj), and C3 (KeSdFb-2), have 40% aggregate content, while having lower density than A1 (KeSdMo) and B1 (KeSd).

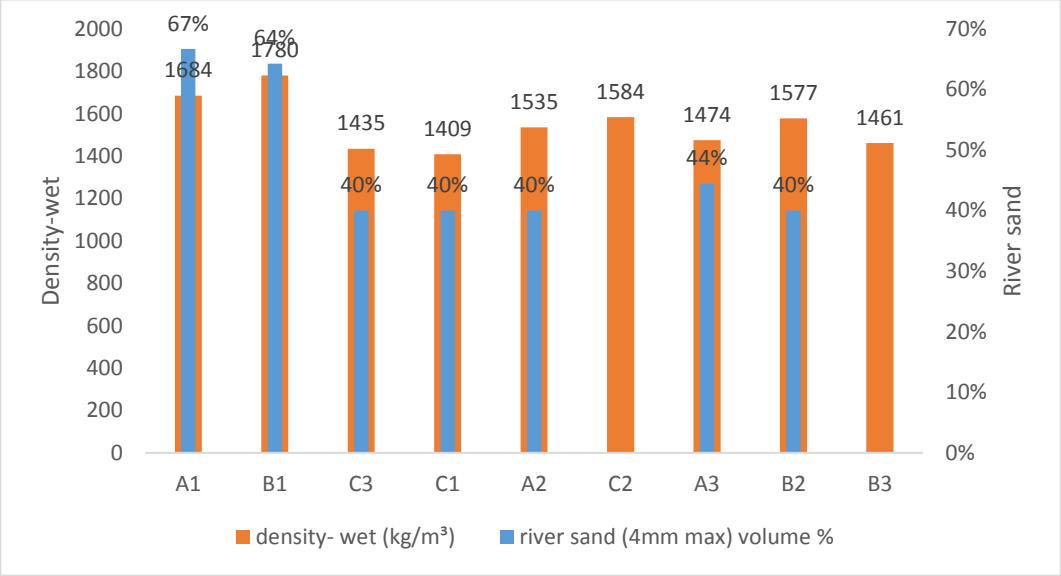

Figure 4-7. Density-wet of mud-plaster wall samples with aggregate content.

Aggregate content has a small effect on density difference where A1 (KeSdMo) and B1 (KeSd) have a close density with similar aggregate content, however, when all the samples are compared more the aggregate content the samples have higher density.

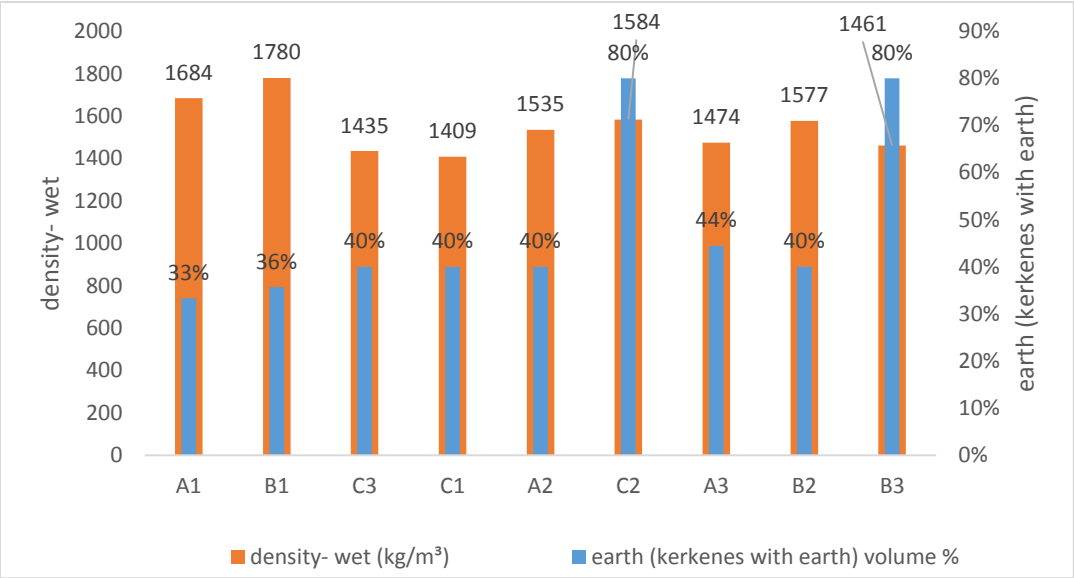

Figure 4-8. Density-wet of mud-plaster wall samples with earth content.

Earth content does not appear to have any effect on density as A1 (KeSdMo) and B1 (KeSd) have the highest density with 33 % earth, on the other hand, B3 (KeFb) and C2 (KeFbCd) have 80% earth and have lower density.

4.2 Mechanical Properties

The horizontal and vertical compressive strength of earth mortars are presented in the following two sections. Each specimen is analyzed three times to get more reliable results, however, due to the difficulty of regularizing plaster, irregularly sized samples were used in this test. Force is applied in a perpendicular direction to the ground plane, where due to the existing side sections irregularities and possible inner cracks (caused by breaking samples off the walls) the average compressive strength of samples is expected a bit lower. The average results of the test are presented in Table 4.2

Table 4.2 Mechanical properties of mud plaster samples.

Name of samples	earth (Kerkenes with earth) volume %	river sand (4mm max) volume %	fiber (short straw) volume %	water volume %	egg white volume %	decomposition juice volume %	molasses volume %	cow dung volume %	vertical compressive strength (Mpa)	horizontal compressive strength (Mpa)
A1 (KeSdMo)	33%	67%		13%			9%		3.6	3.2
A2 (KeSdFbEg)	40%	40%	20%	24%	2%				1.3	0.8
A3 (KeSdFbCd)	44%	44%	11%	29%				11%	1.4	0.5
B1 (KeSd)	36%	64%		14%					1.3	1.1
B2 (KeSdFb-1)	40%	40%	20%	29%					2.1	1.2
B3 (KeFb)	80%		20%	39%					2.6	2.5
C1 (KeSdFbDj)	40%	40%	20%	24%		3%			0.9	1.1
C2 (KeFbCd)	80%		20%	25%				10%	0.8	1.0
C3 (KeSdFb-2)	40%	40%	20%	20%					0.4	0.5

4.2.1 Vertical Compressive Strength

In general, the results are very dynamic to each other, where samples are exposed to external conditions through the years and their strength decreases. Therefore, making comparisons between the samples is crucial to understand where, samples analyzed in terms of their composition.

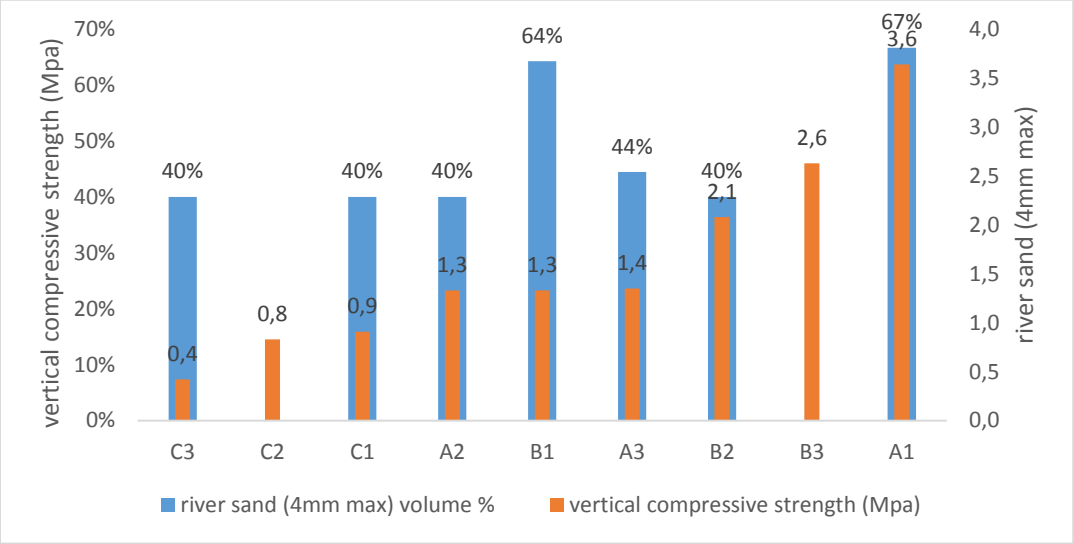

Figure 4-9. Vertical compressive strength relationship with aggregate content.

For the test average compressive strength varies between 3.6 MPa A1 (KeSdMo) and 0.4 MPa C3 (KeSdFb-2). Samples approximately gave similar results. Among all the samples A1 (KeSdMo) has 3.6 Mpa and B3 (KeFb) 2.6 Mpa differ from all others in terms of consistent results to having a higher compressive strength.

A1 (KeSdMo) contains %66 aggregate, %33 earth, and molasses (no fiber), B3 (KeFb) contains %20 short fiber with %80 earth. While A1 (KeSdMo) has a high compressive strength thanks to its aggregate content with molasses, B3 (KeFb) has a higher strength thanks to its high clay content of earth.

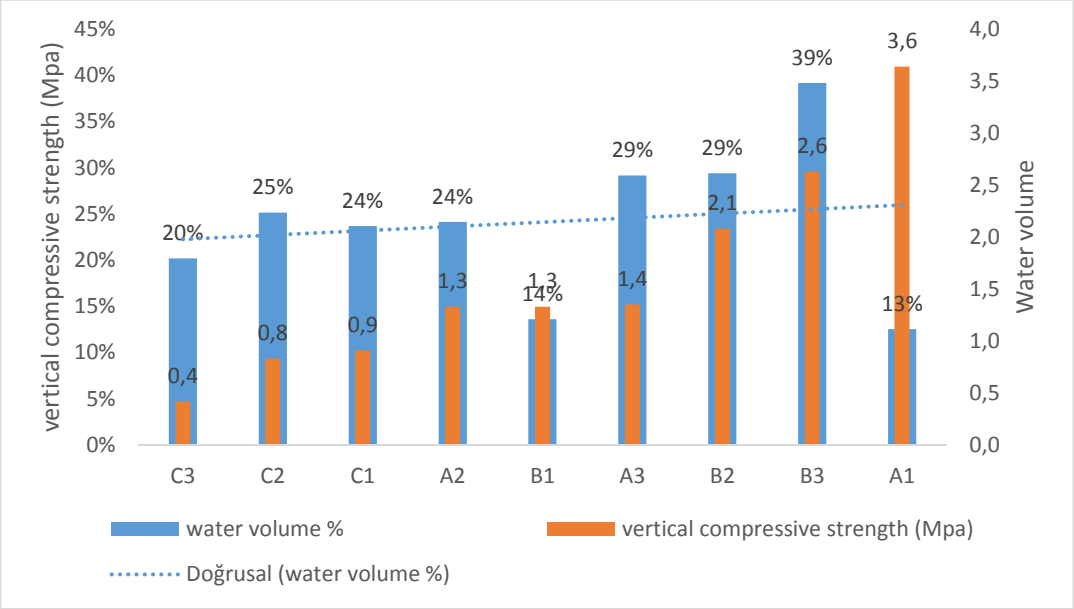

Figure 4-10. Vertical compressive strength with water content percentage

Sample A1 (KeSdMo) has the smallest volume of water while having the highest strength. On the other hand, when B2 (KeSdFb-1) and C3 (KeSdFb-2) compared where B2 (KeSdFb-1) has higher water volume has higher compressive strength.

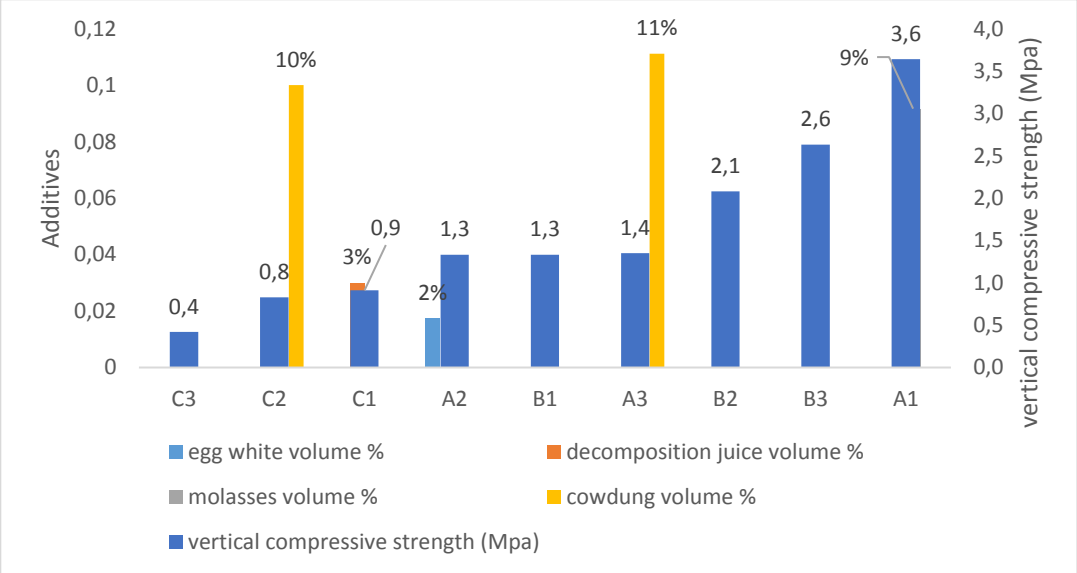

Figure 4-11. Vertical compressive strength with additive content

Additives also play a vital role in the strength of samples, where A1 (KeSdMo) with molasses performs the best. Such stabilizers increase the binding qualities of the clay, which increases compressive strength. However, as analyzed before, molasses has a negative effect on samples shrinkage.

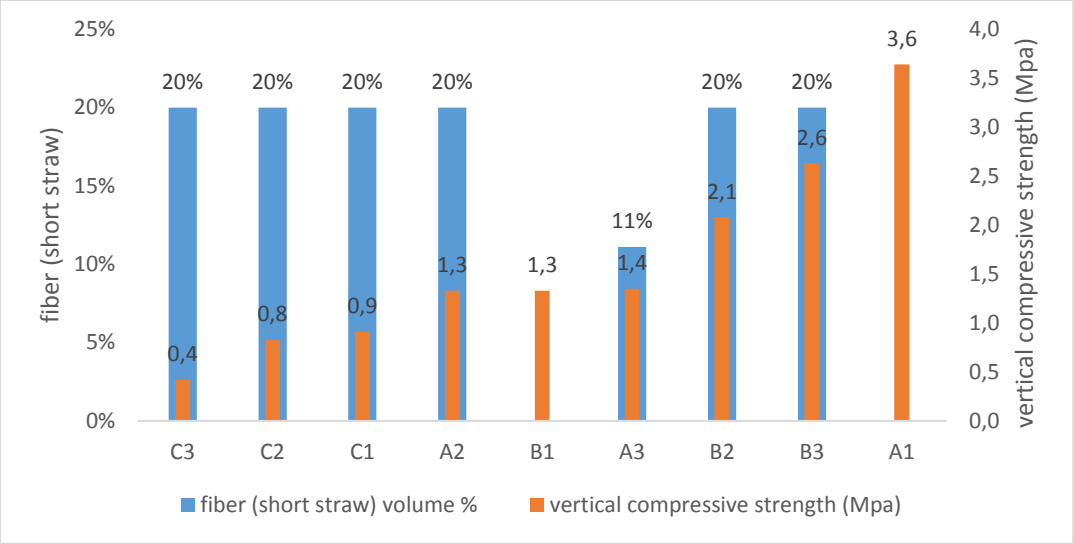

Figure 4-12. The effect of short straw on vertical compression.

When A2 (KeSdFbEg), A3 (KeSdFbCd), B1 (KeSd), B2 (KeSdFb-1), C1 (KeSdFbDj), C2 (KeFbCd), and C3 (KeSdFb-2) are compared, all have similar strengths, while B1 (KeSd) has no fiber content, in addition to this B2 (KeSdFb-1) has lower fiber content while slightly higher strength than some samples. This opposes that a significant increase in the amount of sand and fiber may boost the strength (Piattoni, 2011).

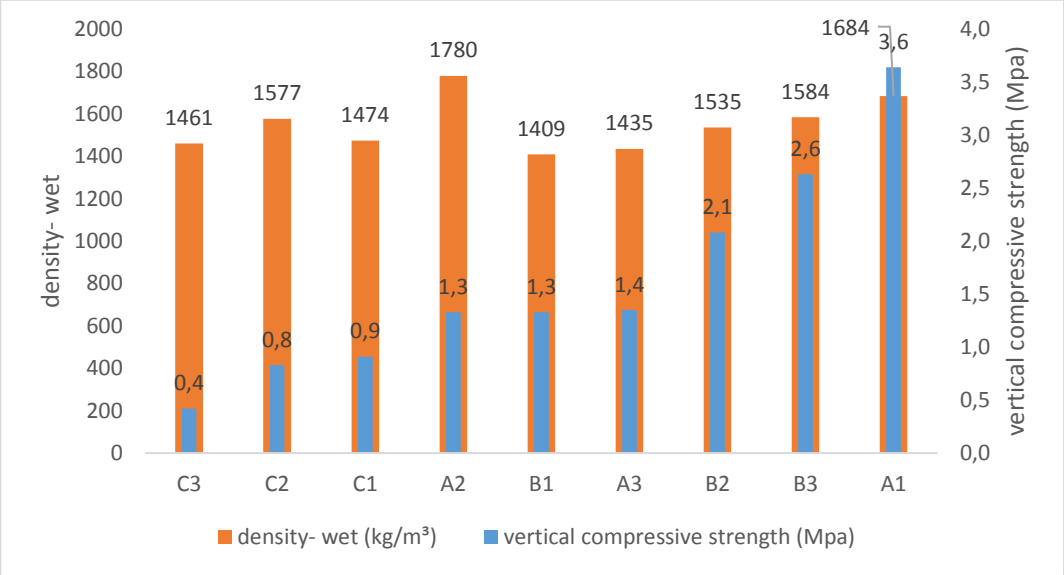

Figure 4-13. Relationship of density and compressive strength.

A1 (KeSdMo) has high density and high strength and B1 (KeSd) is one of the densest samples, while having one of the lowest strengths because it lacks the bonding of fiber in the plaster.

4.2.2 Horizontal Compressive Strength

Average compressive strength samples vary between 3.2 MPa A1 (KeSdMo) and 0.5 MPa C3 (KeSdFb-2). Among all the samples A1 (KeSdMo) and B3 (KeFb) differ from all others in terms of consistent results to being higher compressive strength capacity, where B3 (KeFb) has around 2.5 Mpa and A1 (KeSdMo) has 3.2 Mpa.

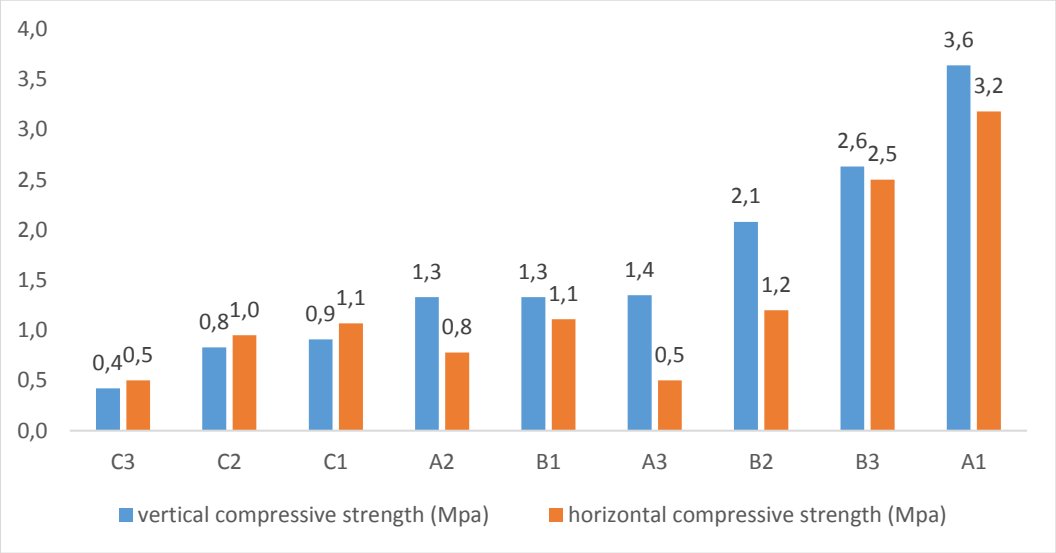

Figure 4-14. Comparison of Horizontal and Vertical compressive strengths.

The horizontal and vertical compressive strength tests were performed in the same way, as can be seen in Figure 4.14. Moreover A2 (KeSdFbEg), B1 (KeSd), B2 (KeSdFb-1), and C2 (KeFbCd) have shown the same horizontal compressive strength of 1 Mpa, which is also close to their individual vertical compressive strengths.

In general, horizontal strength results are lower than the vertical strength, which could be expected to be lower due to the defects and cracks on the surfaces and inside of the samples, however, all the results came out very close to each other, which can be related to the homogeneous composition of samples.

4.3 Surface Properties

The surface properties of earth mortars have been determined on each sample. The results are summarized in Table 4.3 below.

Table 4.3 Surface properties of mud plaster samples.

Name of samples	earth (Kerkenes with earth) volume %	river sand (4mm max) volume %	fiber (short straw) volume %	water volume %	egg white volume %	decomposition juice volume %	molasses volume %	cow dung volume %	amount of material left on the tape (g/m²)	surface water absorption (g/m²·s)
A1 (KeSdMo)	33%	67%		13%			9%		0.59	0.11
A2 (KeSdFbEg)	40%	40%	20%	24%	2%				0.36	0.39
A3 (KeSdFbCd)	44%	44%	11%	29%				11%	0.71	0.28
B1 (KeSd)	36%	64%		14%					0.45	0.26
B2 (KeSdFb-1)	40%	40%	20%	29%					0.16	0.37
B3 (KeFb)	80%		20%	39%					0.06	0.60
C1 (KeSdFbDj)	40%	40%	20%	24%		3%			0.67	0.42
C2 (KeFbCd)	80%		20%	25%				10%	0.56	0.36
C3 (KeSdFb-2)	40%	40%	20%	20%					0.28	0.38

4.3.1 Surface adhesion (peeling test)

The data from the peeling test point to a large variation between the samples regarding material loss, varying from A3 (KeSdFbCd) which is 0.71g/m² to B3 (KeFb) 0.06 g/m².

The material loss is directly related to the surface cohesion, where B3 (KeFb) performed the best test among all the samples, this could be the result of its composition, where it does not contain any aggregate.

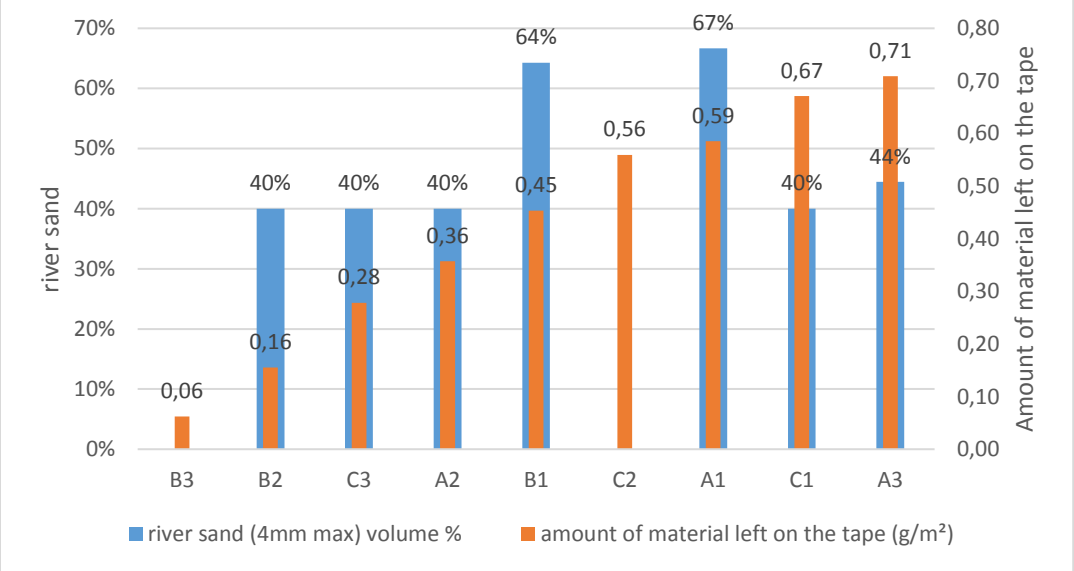

Figure 4-15. Aggregate content with amount of material left on the tape.

A2 (KeSdFbEg), A3 (KeSdFbCd), B3 (KeFb), C1 (KeSdFbDj), C2 (KeFbCd), and C3 (KeSdFb-2), all have different surface cohesion although they all have the same fiber content, so there is no clear relationship between fiber content and surface adhesion.

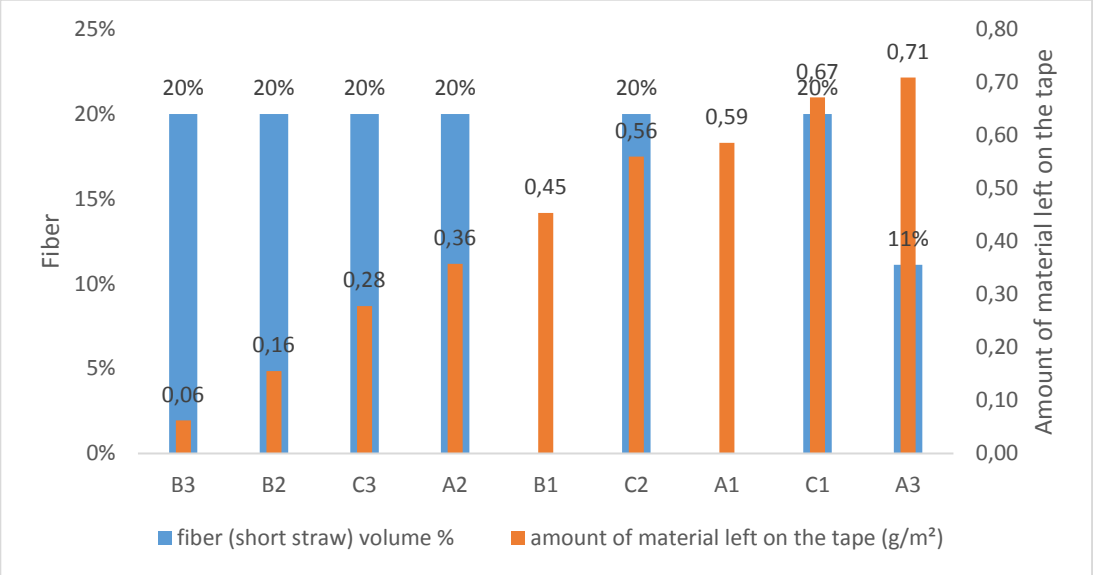

Figure 4-16. Fiber content with amount of material left on the tape.

B3 (KeFb) plaster mix contained nearly 40% water, while having the highest surface cohesion, therefore when the graph is analyzed there is a trend line that shows, that with the increase of water %, there is an increase in surface cohesion, which helps the surface of materials much stronger.

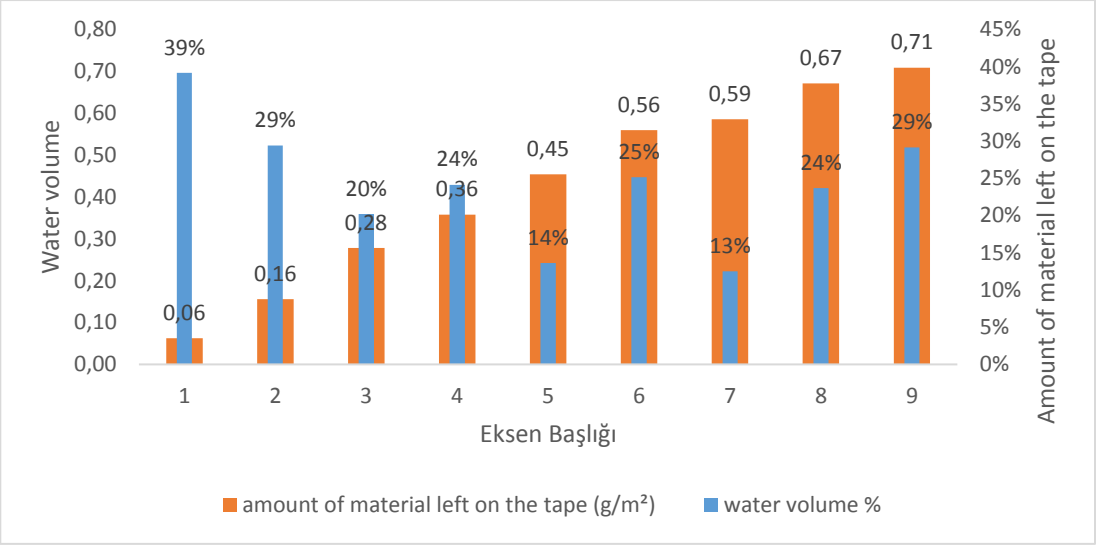

Figure 4-17. Water content with amount of material left on the tape.

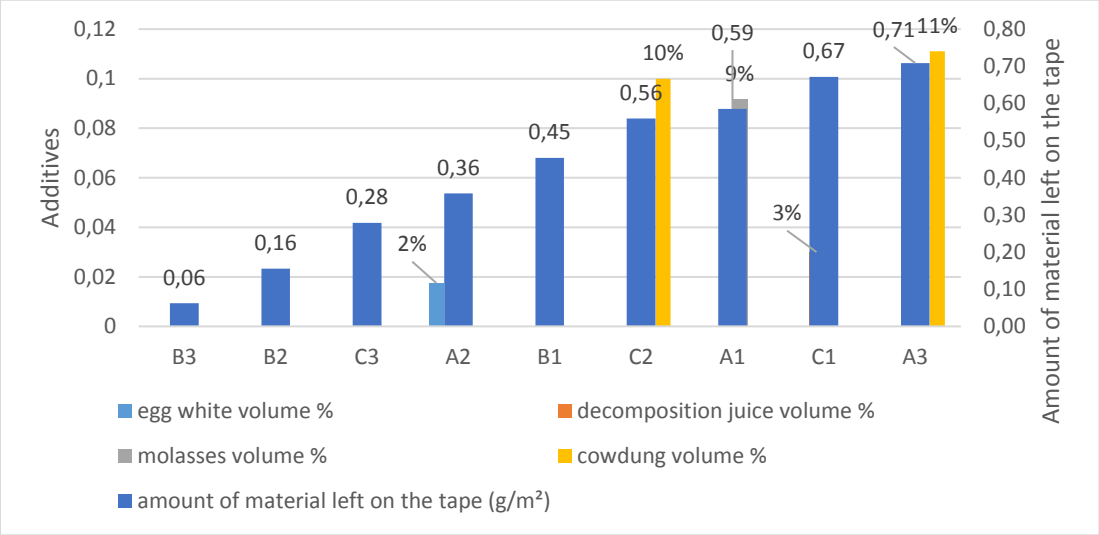

Figure 4-18. Additive content with amount of material left on the tape.

A1 (KeSdMo), A3 (KeSdFbCd), B2 (KeSdFb-1), C1 (KeSdFbDj), and C3 (KeSdFb-2), all have different additives which have no effect on surface cohesion.

In addition to the previously mentioned factors, it is possible that the weight difference is the consequence of the small number of specimens analyzed and the likelihood that some particles are noticeably heavier than others, especially if the specimen has a higher proportion of sand than the fiber.

4.3.2 Surface water absorption

The amount of water absorbed during the surface water absorption for samples submitted to the absorption test that, comprised of between B3 (KeFb) 0.6 g/m²·s and A1 (KeSdMo) 0.1 g/m²·s for an exposition to water for 90 seconds.

A1 (KeSdMo) has the same composition expect molasses that performed as one of the best. Due to the water-absorbing properties of fibers, it was expected that the increase in fiber ratio would also affect the water absorption rate, A1 (KeSdMo), B1 (KeSd), and B2 (KeSdFb-1) support this claim, whereas B2 (KeSdFb-1) has fiber

content, and it has also lower absorbed water than other samples that contain higher fiber content.

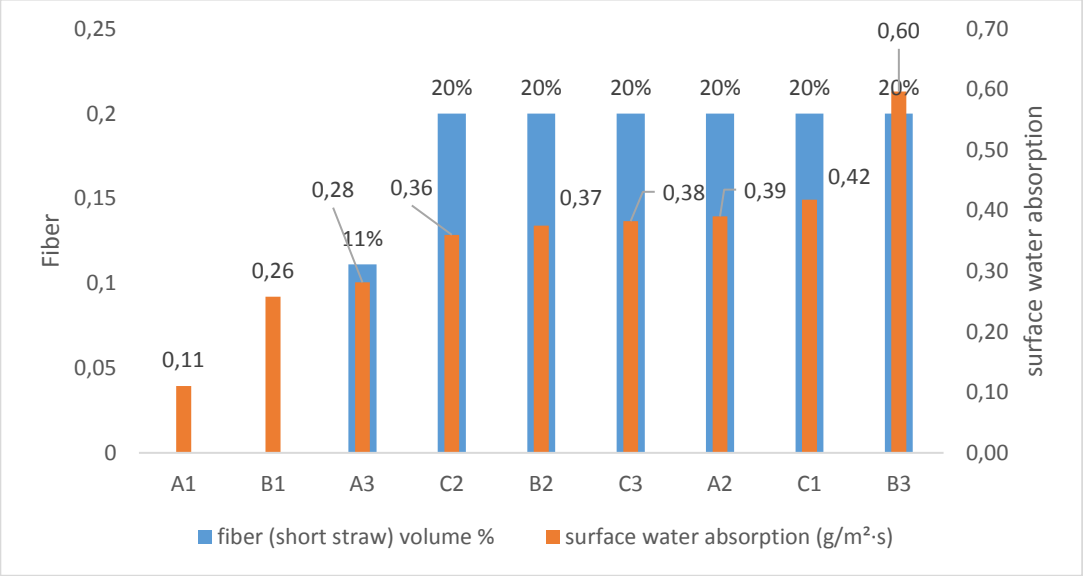

Figure 4-19. Fiber content with absorbed water.

In the experiment, B3 (KeFb) 0.6 g/m²·s show slightly higher water absorption than A1 (KeSdMo) 0.1 g/m²·s. Between both samples, their earth content is slightly different from each other where A1 (KeSdMo) has 33% of earth and C2 (KeFbCd) has 80% of earth. Figure 4.20 illustrates that the more the earth content, the sample absorbs more water.

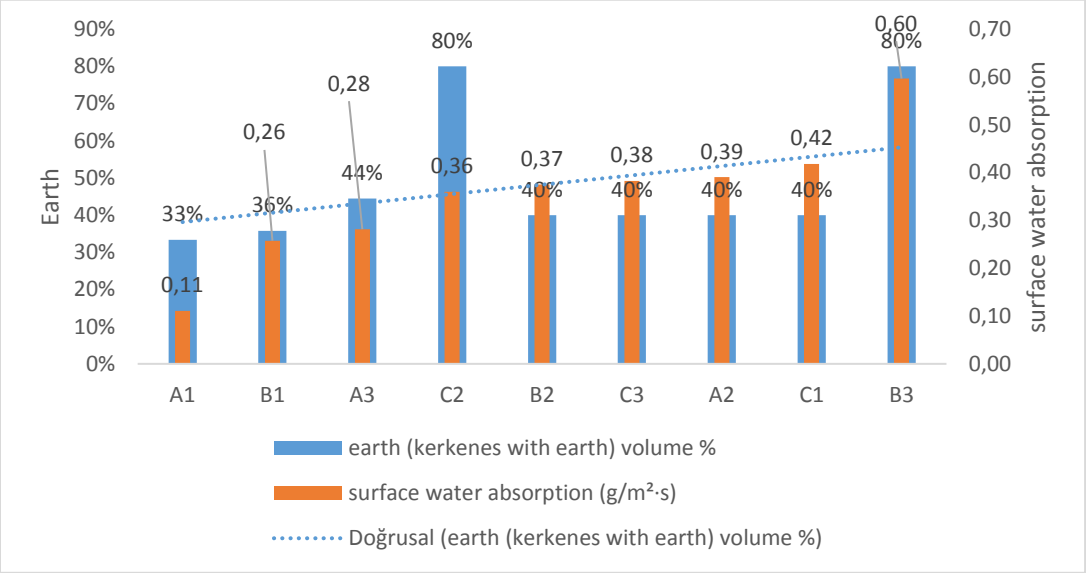

Figure 4-20. Earth content with absorbed water.

Additives also play a critical role in water absorption, especially molasses performed superior to the other additives, which saved A1 (KeSdMo) from failure and made it one of the best-performing samples for the experiment.

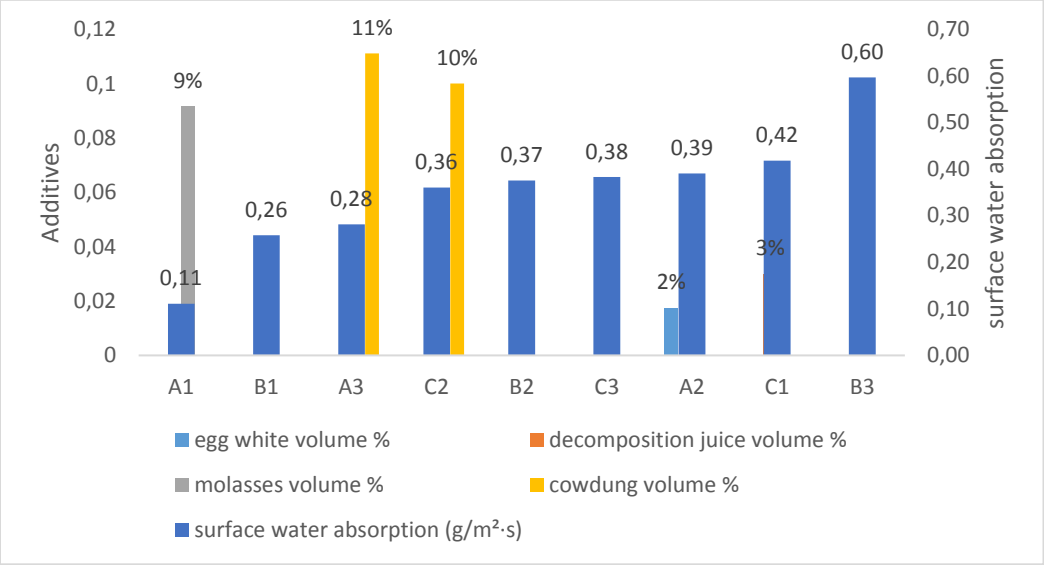

Figure 4-21. Additive content with absorbed water.

On the other hand, while cow dung has a positive effect on surface water absorption, decomposition juice and egg white did not make any changes.

4.4 Durability

The durability properties of earth mortars have been determined on each sample. The results are summarized in Table 4.3 below.

Table 4.4 Durability of mud plaster samples.

Name of samples	earth (Kerkenes with earth) volume %	river sand (4mm max) volume %	fiber (short straw) volume %	water volume %	egg white volume %	decomposition juice volume %	molasses volume %	cow dung volume %	water resistance (min)	depth of the hole (cm)	resistance to abrasion (Frech Rules) amount of trace(mm)
A1 (KeSdMo)	33 %	67%		13%			9%		180	0.7	0.5
A2 (KeSdFbEg)	40 %	40%	20%	24%	2%				25	1.0	3.0
A3 (KeSdFbCd)	44 %	44%	11%	29%				11%	120	0.5	4.0
B1 (KeSd)	36 %	64%		14%					10	-	5.0
B2 (KeSdFb-1)	40 %	40%	20%	29%					25	0.8	5.0
B3 (KeFb)	80 %		20%	39%					15	1.5	1.0
C1 (KeSdFbDj)	40 %	40%	20%	24%		3%			110	0.7	16.0
C2 (KeFbCd)	80 %		20%	25%				10%	35	1.0	15.0
C3 (KeSdFb-2)	40 %	40%	20%	20%					15	Fail	1.0

4.4.1 Water resistance

The resistance to immersion in water varies from 10 minutes for B1 (KeSd) to 180+ minutes for A1 (KeSdMo) (until the end of the test). The samples A2 (KeSdFbEg), B1 (KeSd), B2 (KeSdFb-1), B3 (KeFb), C2 (KeFbCd), and C3 (KeSdFb-2) which seem to have meager water resistance, do show that an increasing number of fibers increases the water resistance. However, during the experiment, according to the observation, fibers held the sample compact during the process.

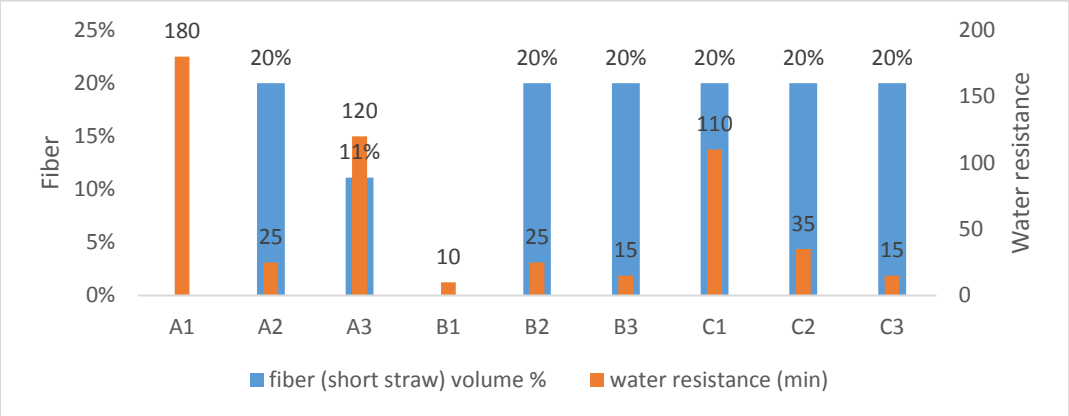

Figure 4-22. Water resistance with fiber content.

On the other hand, additives' effect on samples' water resistance is clearly seen in Figure 4.23, where A1 (KeSdMo) and C1 (KeSdFbDj) performed the best, containing decomposition juice and molasses. However, not every additive performed well like A3 (KeSdFbCd) and C2 (KeFbCd) containing cow dung performed differently while A3 (KeSdFbCd) performed superior to the C2 (KeFbCd) thanks to its base composition.

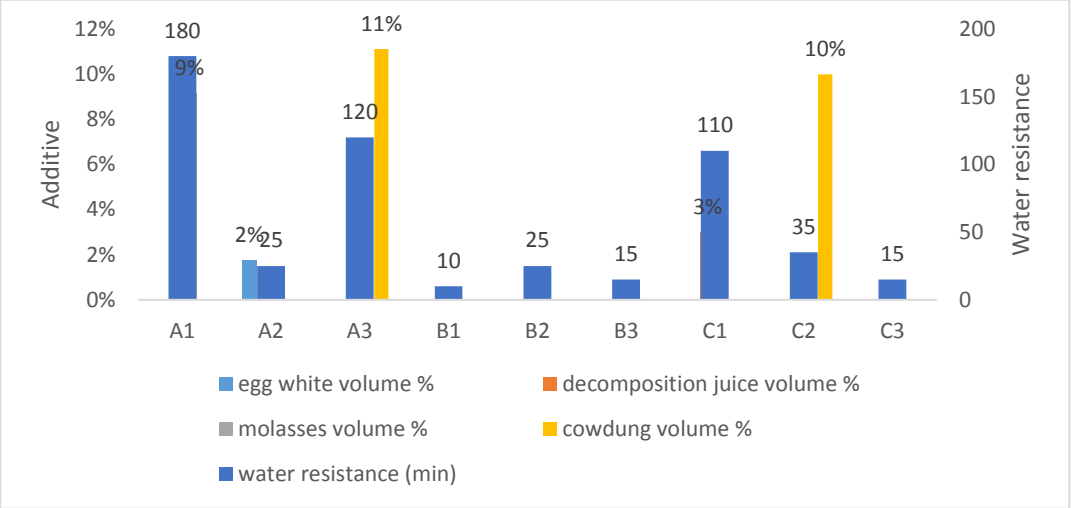

Figure 4-23. Water resistance with additive content.

Overall, most of the samples have failed during the process, only samples that contain appropriate additive content have a durability against immersion in water.

4.4.2 Erosion resistance

The erosion of earth mortars is given Table 4.3 as the depth of the hole made by the dripping of water. The depth varies between 5mm C1 (KeSdFbDj) and 15 mm B3 (KeFb). Despite most values being comprised of between 5.0 mm and 15mm, B1 (KeSd) and C3 (KeSdFb-2) failed during the experiment, where B1 (KeSd) failed within the first 20 minutes and C3 (KeSdFb-2) failed after 40 minutes.

In the article, Lerner & Donahue (2003) and Pedergnana (2022) found that fiber content reduces erosion and B1 (KeSd) failed first during the experiment, because of not having any fiber therefore, it supports their findings of previous experiments.

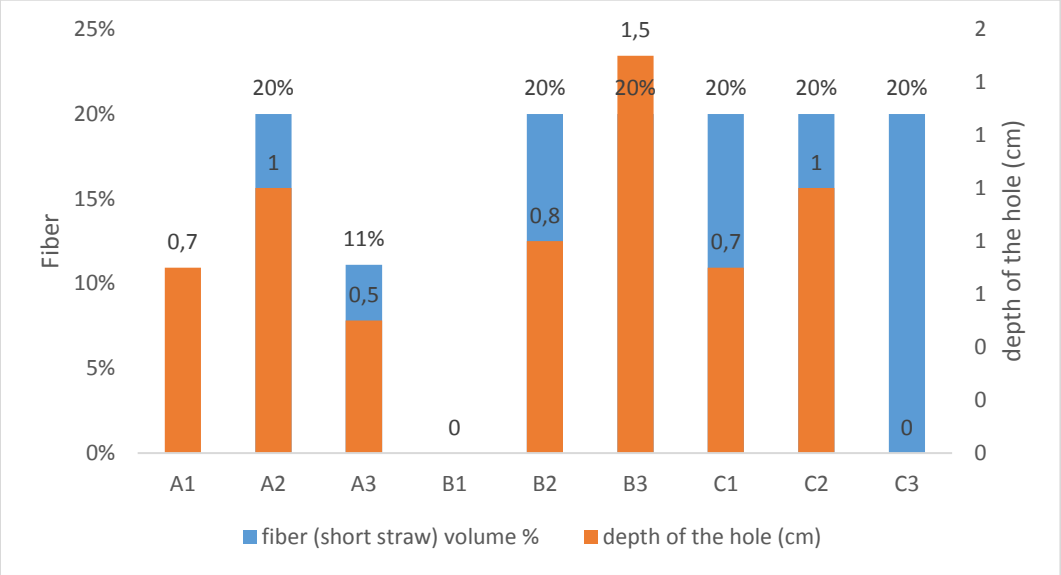

Figure 4-24. Fiber content of samples with depth of hole.

On the other hand, A1 (KeSdMo) performed better where its depth is around 5mm while not having any fiber in it. Therefore, it can be said that the depth of water is not only related to fiber content but also additives, that is molasses in this case.

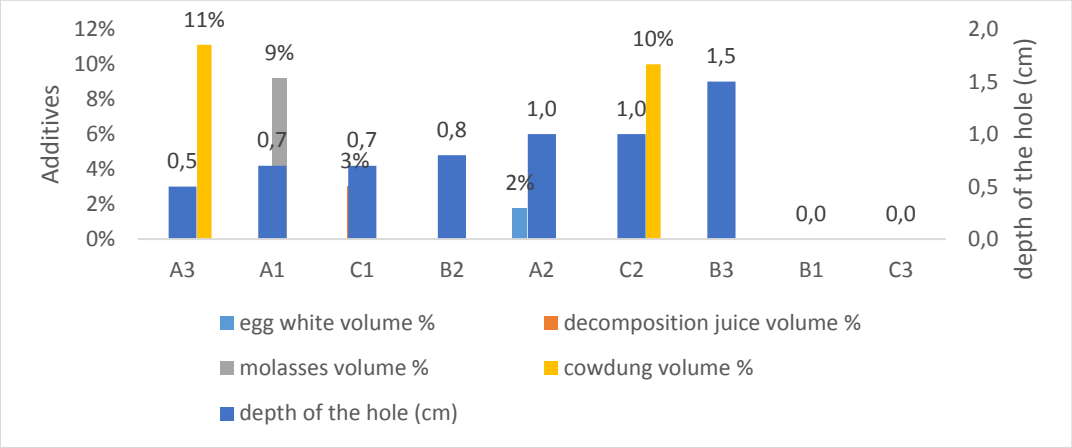

Figure 4-25. Additive content of samples with depth of hole.

A2 (KeSdFbEg) and A3 (KeSdFbCd) are made with the same composition except A3 (KeSdFbCd) has decomposition juice and A2 (KeSdFbEg) has cow dung, thanks to the decomposition juice A3 (KeSdFbCd) performed better performance than A2 (KeSdFbEg).

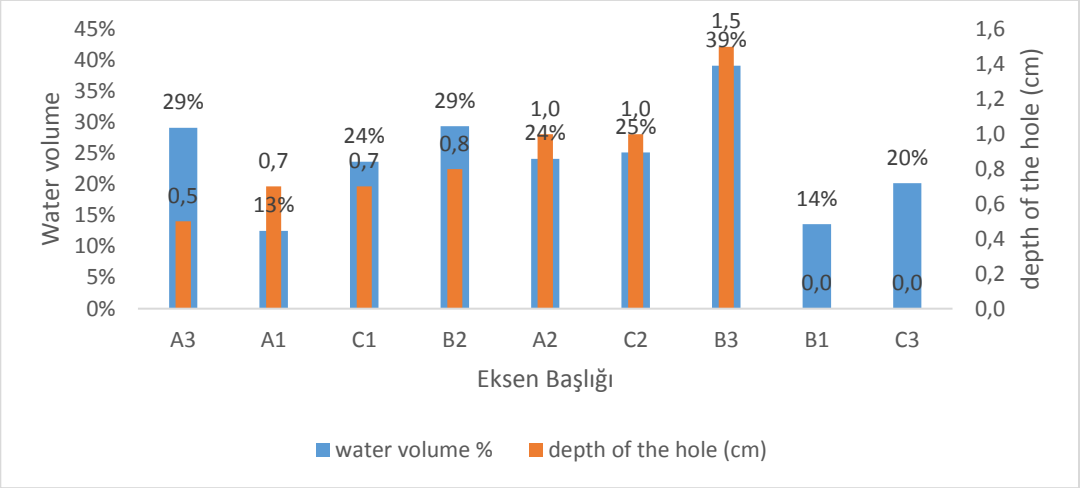

Figure 4-26. Water with depth of hole.

4.4.3 Resistance to abrasion (French Rules)

The abrasion resistance of the mortar was tested according to the amount of groove depth, and the average depth of the grooves made by the brushes varied from 0.5 mm to 16 mm. According to French Professional regulations, a grove should not be deeper than 2 mm. This test is based on the French Standard XP P13-901 for compressed earth bricks.

Samples A1 (KeSdMo), B3 (KeFb), and C3 (KeSdFb-2), are suitable for French Professional regulations, whereas A2 (KeSdFbEg) and A3 (KeSdFbCd) are too weak that they have a 16mm trace. In his dissertation Pedergnana (2022) claims that samples with added sand decrease the abrasion resistance, and the more the addition of sand, the lesser the resistance. However, A1 (KeSdMo) opposes this claim, which

has a huge amount of sand with molasses, while it is very durable to abrasion. On the other hand, B3 (KeFb) supports his claim, that contains no aggregate.

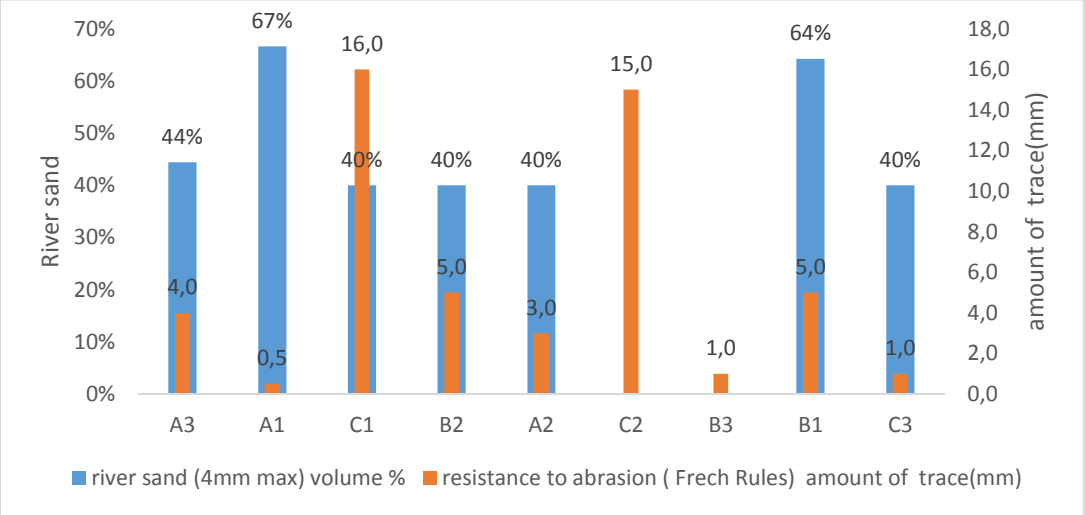

Figure 4-27. Relationship between trace and aggregate

B3 (KeFb) and C2 (KeFbCd), which have %80 earth content show a very high abrasion resistance, where B3 (KeFb) performed best, aggregate content shows a relationship with its strength.

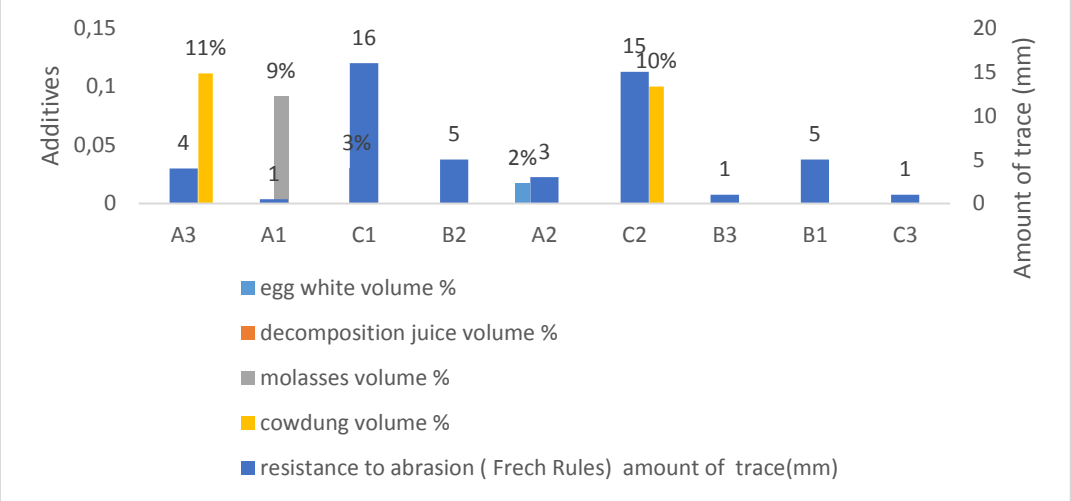

Figure 4-28. Relationship between trace and additive

Using additives can dramatically increase the abrasion resistance, while A1 (KeSdMo) which has molasses in its composition has a 0.7mm hole, B1 (KeSd) has no additives, and it dramatically failed during the process. However, other additives that are used through samples do not show any crucial effect. Therefore, it can be said that using a suitable additive has a huge effect on the samples' abrasion resistance.

4.5 Hydric Properties

The hydric properties of earth mortars have been determined on each sample. The results are summarized in Table 4.5 below

Table 4.5 Hydric properties of mud plaster samples.

Name of samples	earth (Kerkenes with earth) volume %	river sand (4mm max) volume %	fiber (short straw) volume %	water volume %	egg white volume %	decomposition juice volume %	molasses volume %	cow dung volume %	water capillarity absorption(14h)	drying rate (48h)	drying index
A1 (KeSdMo)	33%	67%		13%			9%		0.57	0.20	0.97
A2 (KeSdFbEg)	40%	40%	20%	24%	2%				1.21	0.28	0.92
A3 (KeSdFbCd)	44%	44%	11%	29%				11%	1.09	0.20	0.91
B1 (KeSd)	36%	64%		14%					1.11	0.09	0.90
B2 (KeSdFb-1)	40%	40%	20%	29%					0.79	0.19	0.91
B3 (KeFb)	80%		20%	39%					1.22	0.39	0.90
C1 (KeSdFbDj)	40%	40%	20%	24%		3%			0.87	0.20	0.90
C2 (KeFbCd)	80%		20%	25%				10%	0.86	0.20	0.91
C3 (KeSdFb-2)	40%	40%	20%	20%					1.64	0.40	0.92

4.5.1 Water capillarity absorption

The capillary coefficient water vapor permeability is presented in Table 4.5. According to the results. the lowest CC is calculated for mortar A1 (KeSdMo) and the highest for mortar C3 (KeSdFb-2). Water capillary absorption values found in this work are different from the ones found for similar mortars by Lima & Faria (2017) who found values 4 times lower which is probably due to the experimental setup (Faria et al. 2016). and like the Pedergnana (2022).

Just like Lima & Faria (2017). It is difficult to relate to the amount of sand used. It is shown from Figure 4.29 that the higher the aggregate amount. the lower the CC with samples like A1 (KeSdMo). however. B1 (KeSd) does not show any relation to this claim.

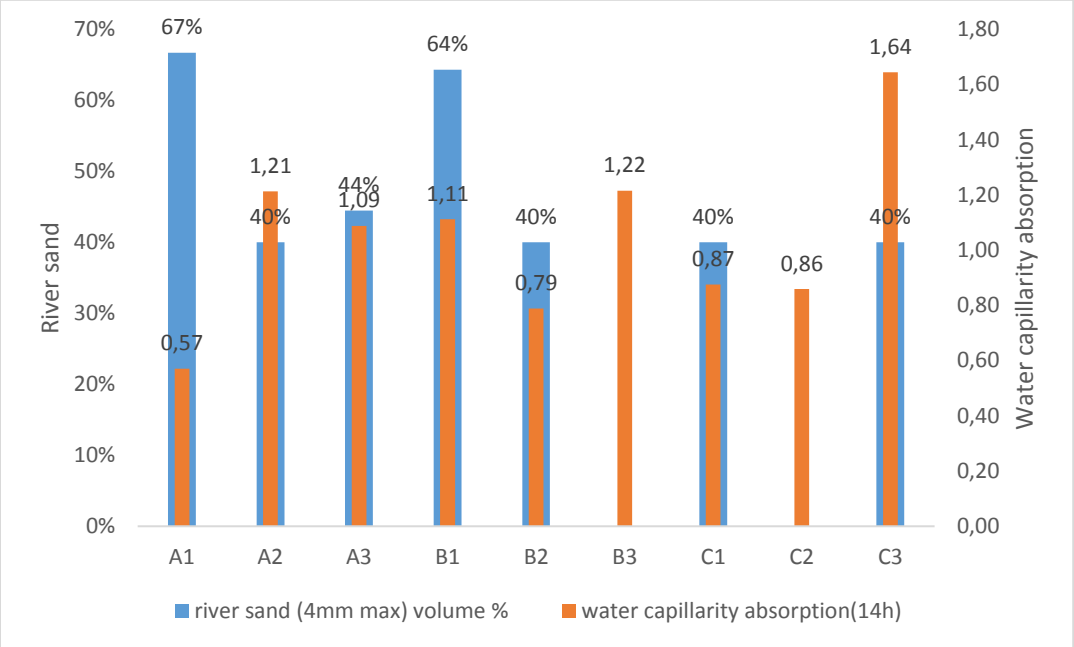

Figure 4-29. Water capillarity absorption with aggregate

Also. earth content shows no relation with CC. Figure 4.30 shows 4 different samples with the same percentage of earth showing slightly different CC. only C1

(KeSdFbDj). and C2 (KeFbCd) are close to each other where the only difference is the decomposition juice and aggregate that C1 (KeSdFbDj) contains and cow dung content that C2 (KeFbCd) has. Therefore, seem to have an effect on CC of samples.

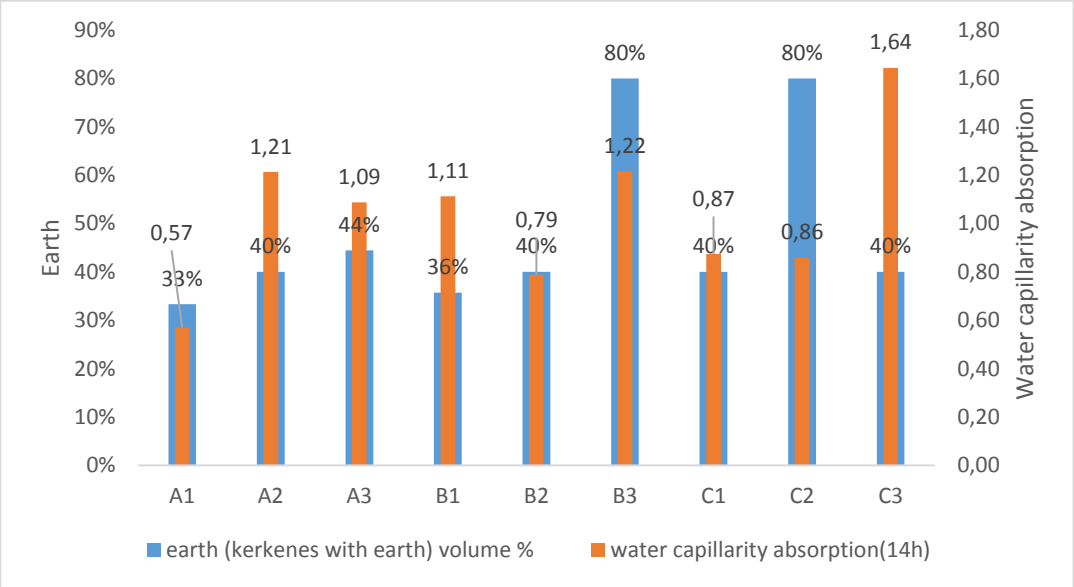

Figure 4-30. Water capillarity absorption with Earth

Pedergnana (2022) claims that a high amount of clay prevents fast absorption but at the same time mortars with a high amount of clay can store a higher amount of water than sandy ones. Moreover, the type of sand seems more important than the amount of sand to modify the absorption rate. In this experiment. samples have the same earth. only their volume changes through samples. According to this claim. the more the earth's content. the sample's CC will be lower. However. when B2 (KeSdFb-1) and C2 (KeFbCd) are compared. where C2 (KeFbCd) has 40% higher earth content. has a lower CC. This result may occur because of the cow dung content that C2 (KeFbCd) has.

Water capillarity has a relationship with the water volume of samples. that are used in the preparation phase. used water creates pores when they dry. and with the help of these pores. water can pass through easily. according to this. more water means

more capillary absorption. As we can see from Figure 4.31. B3 (KeFb) has 40% water while A1 (KeSdMo) has 12% water. A1 (KeSdMo) shows less CC (0.57) than B3 (KeFb) (1.22). It is also clear that C3 (KeSdFb-2) has 20% water while it has the highest CC.

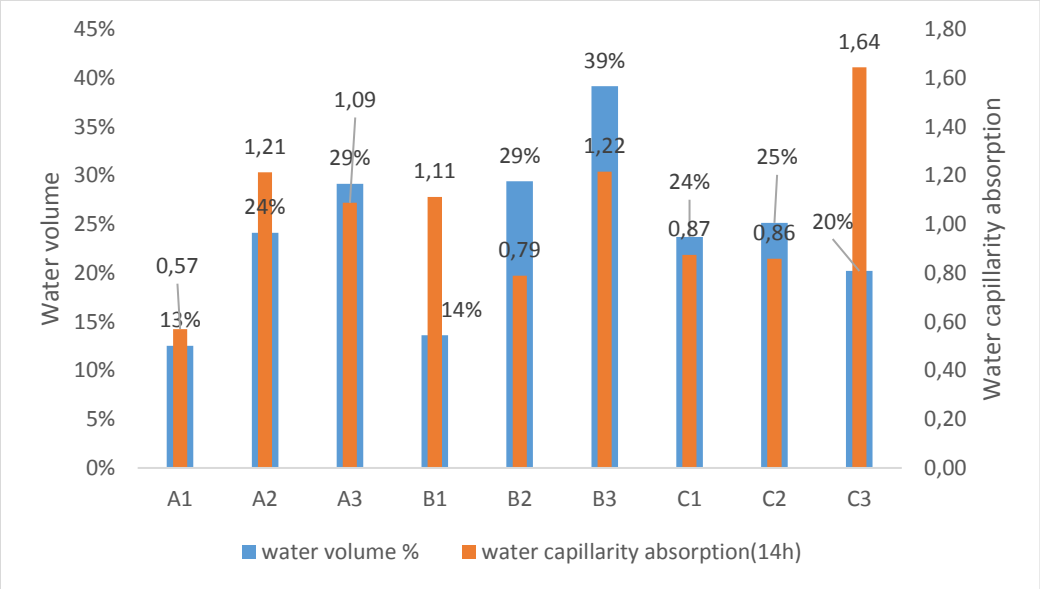

Figure 4-31. Water capillarity absorption with Earth with water.

The amount of absorbed water through time is different for each sample. as it can be seen from Figure 3.32 that C3 (KeSdFb-2) has the highest water lost speed in Time ($min^{0.5}$) and A1 (KeSdMo) is the slowest one. Each sample makes a peak at the beginning of the experiment. but after 30 minutes. it shows that each material CC became closer to each other, However, they all have absorbed different amounts of water.

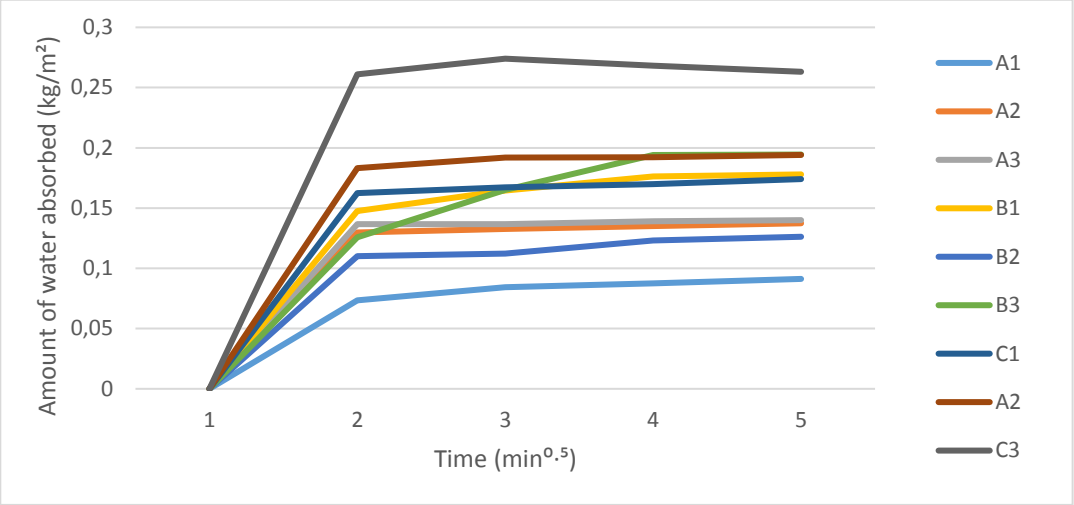

Figure 4-32. Earth with water Amount of water absorbed through time.

The amount of water absorbed through time can be related to the density of samples. where higher density means lower water capillary absorption. As can be seen from Figure 3.33. A1 (KeSdMo) has the highest density with the lowest capillary absorption, while C3 (KeSdFb-2) shows one of the lowest densities with the highest water absorption.

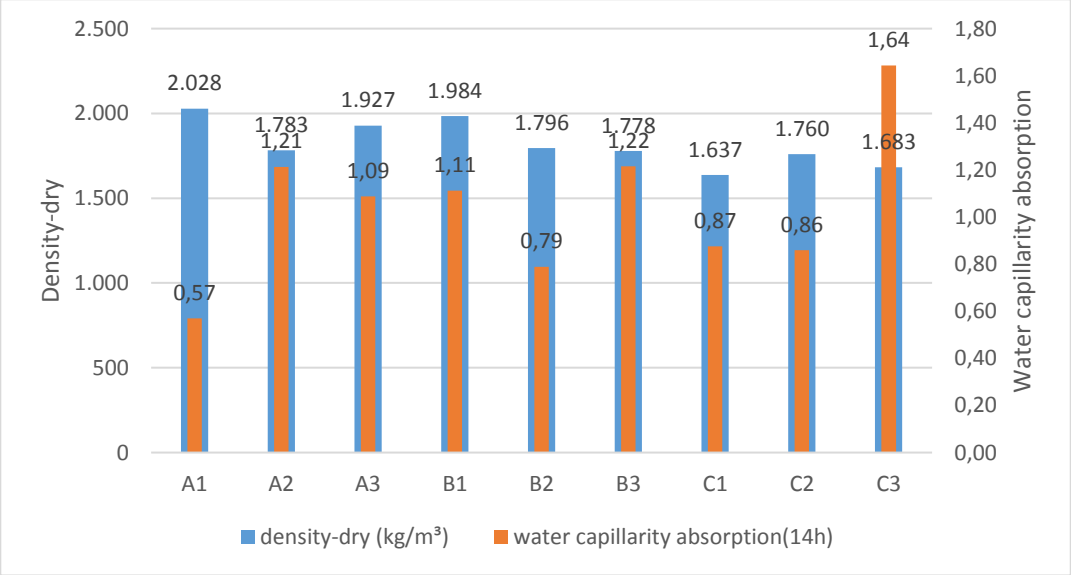

Figure 4-33. Water capillarity absorption with density

Additives also play a role in the CC of the samples. where although A1 (KeSdMo) and B1 (KeSd) have the same content except A1 (KeSdMo)'s additive content (molasses). shows a remarkable difference. where B1 (KeSd) has 1.11 CC A2 (KeSdFbEg) has 0.86 CC. Molasses did make A1 (KeSdMo) denser and water cannot go through easily. In addition to this. as it can be seen from Figure 3.34 all additives have an effect on the CC of samples. each additive increased the sample's density. therefore. they decreased the CC.

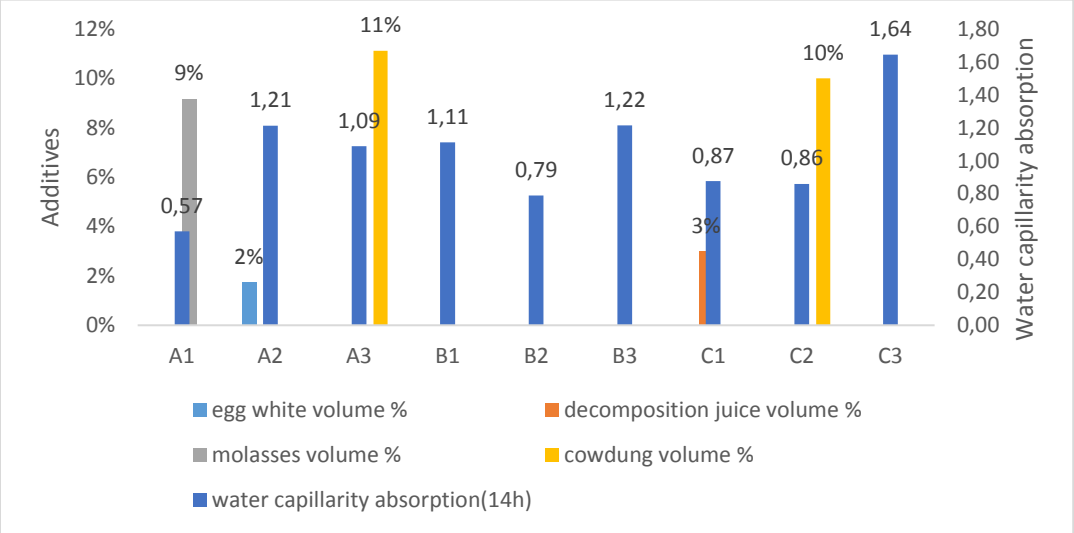

Figure 4-34. Water capillarity absorption with density with additives

4.5.2 Drying rate

Three distinct coefficients are used to describe the drying behavior of mortars: the primary drying rate (pDR). the secondary drying rate (sDR). and the drying index (DI). which indicates how difficult it is to accomplish complete drying.

Table 4.5 displays these data. while Figure 3.40 displays the drying curves. The mortar's main drying rates were determined in the first 24 hours of drying. while the secondary drying rates were determined after 4 days. The primary drying rate varies between 0.0016 kg/m²/h B1 (KeSd) and 0.0015 kg/m²/h C2 (KeFbCd). The second

phase of drying is varied between 0.0073 A1 (KeSdMo) kg/m²/h$^{0.5}$ and 0.0198 C3 (KeSdFb-2) kg/m²/h$^{0.5}$.

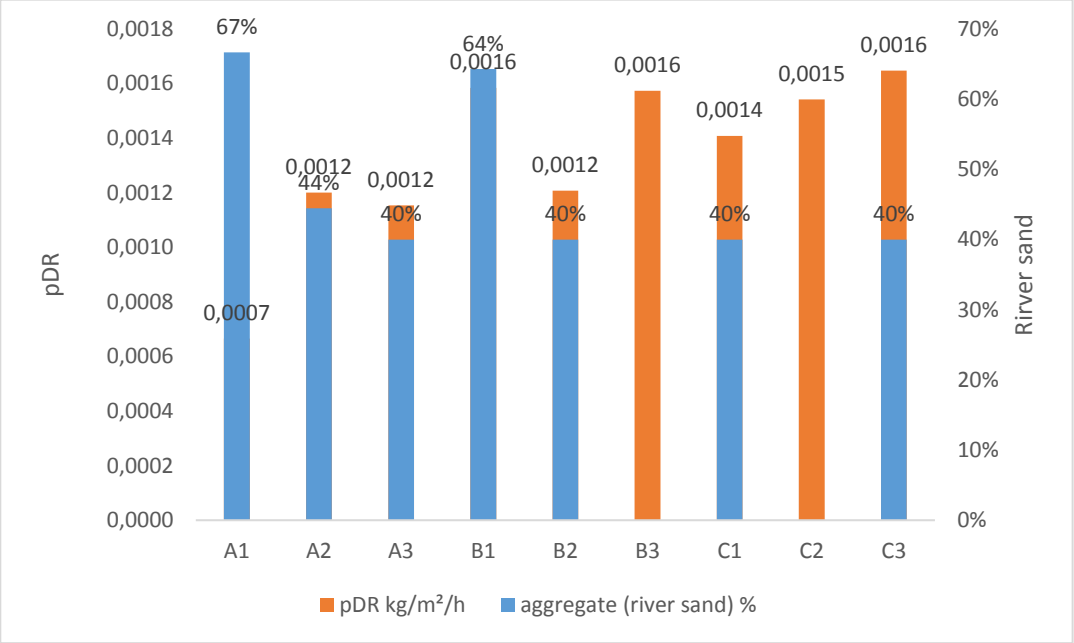

Figure 4-35. Drying rate (1st phase) with river sand.

It seems that the amount of sand has only a relative impact on the primary DR as shown by Lima & Faria (2017). B1 (KeSd) which contains %64 and has the highest drying rate. On the other hand, the secondary drying rate gets lower with the addition of sand as also underlined by the previous authors which shows that it is more difficult for the mortar to achieve a complete drying by evaporation. probably because of the difficulty of the water to migrate internally from the bottom of the sample to the top.

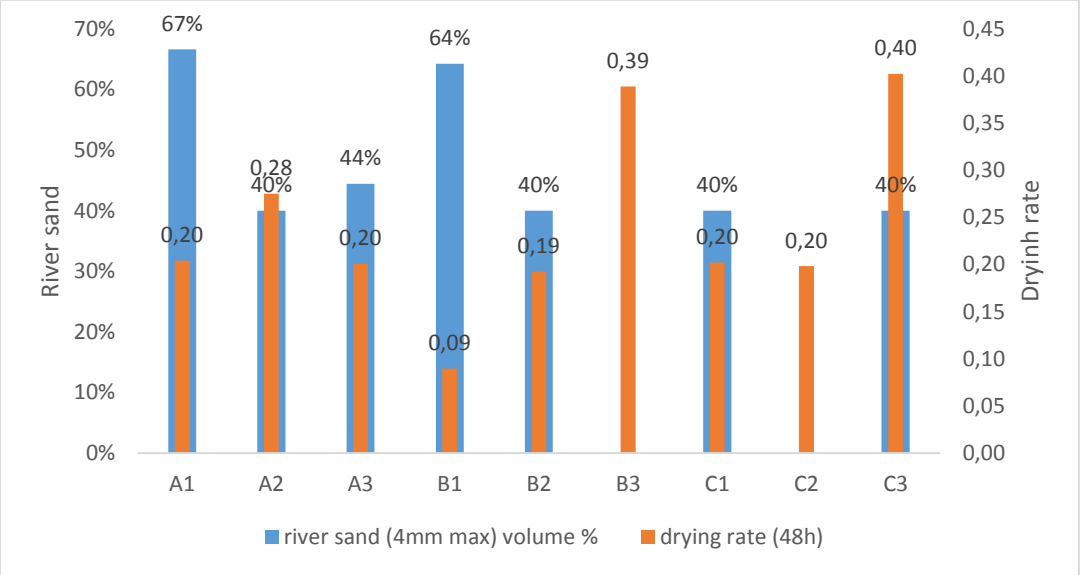

Figure 4-36. Drying rate (2nd phase) with river sand with river sand.

It can be said that the addition of sand reduces the drying rate during the first period but decreases the total drying time as the water molecules will not be trapped between the clay particles but free to migrate through the material.

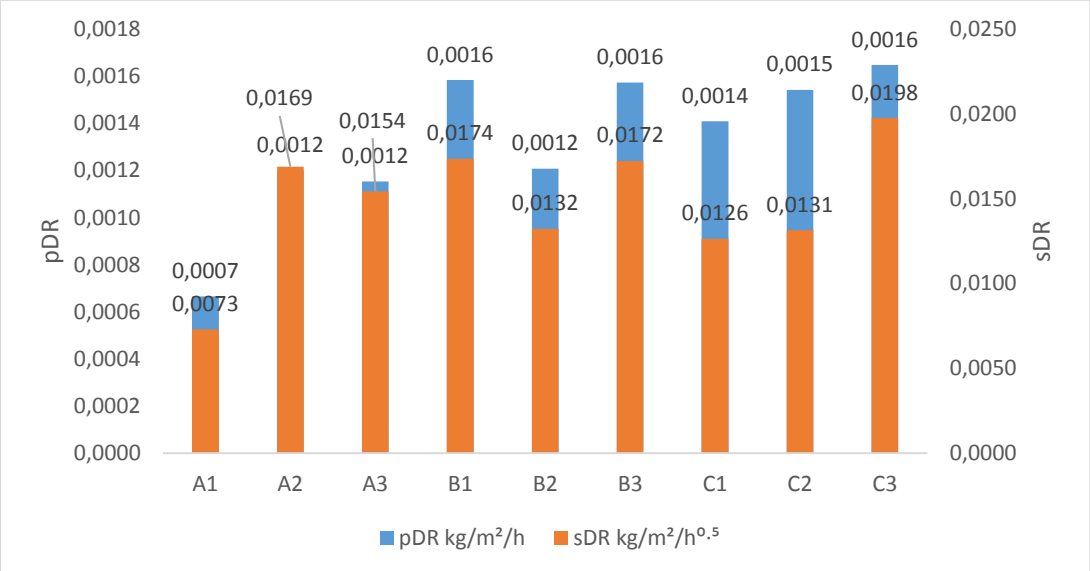

Figure 4-37. First and Second phase of Drying rates.

The Drying Index of samples varies from 0.89 B3 (KeFb) to 0.97 A1 (KeSdMo). A lower DI means an easier achievement of full drying of mortars; therefore, it seems that the addition of sand leads to an easier drying of the mortar. probably because the molecules of water are not trapped between the clay particles as the amount of clay is lower. It can be seen from Figure 3.37 that follows the drying rate. mortar B1 (KeSd) has a faster primary drying rate. but the secondary drying rate is smaller and therefore the total drying seems more difficult to achieve.

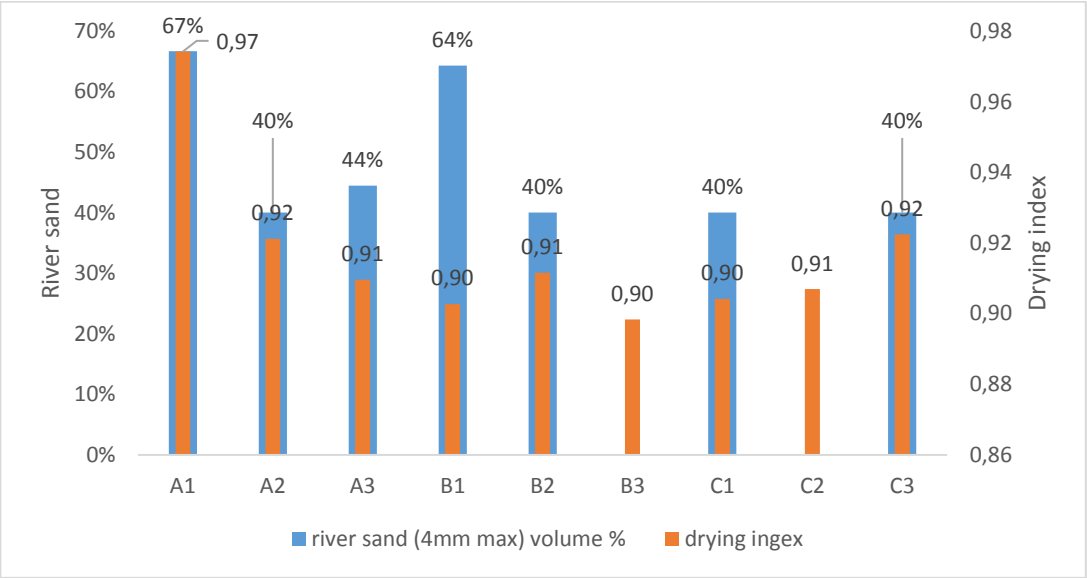

Figure 4-38. Drying index with river sand.

The amount of water desorbed (kg/m²) can be seen from Figure 3.39 that, all samples absorbed different amounts of water, while B1 (KeSd) absorbed the highest amount of water and loss the highest amount of water too. A1 (KeSdMo) has the lowest amount of water and it lost the lowest amount of water too.

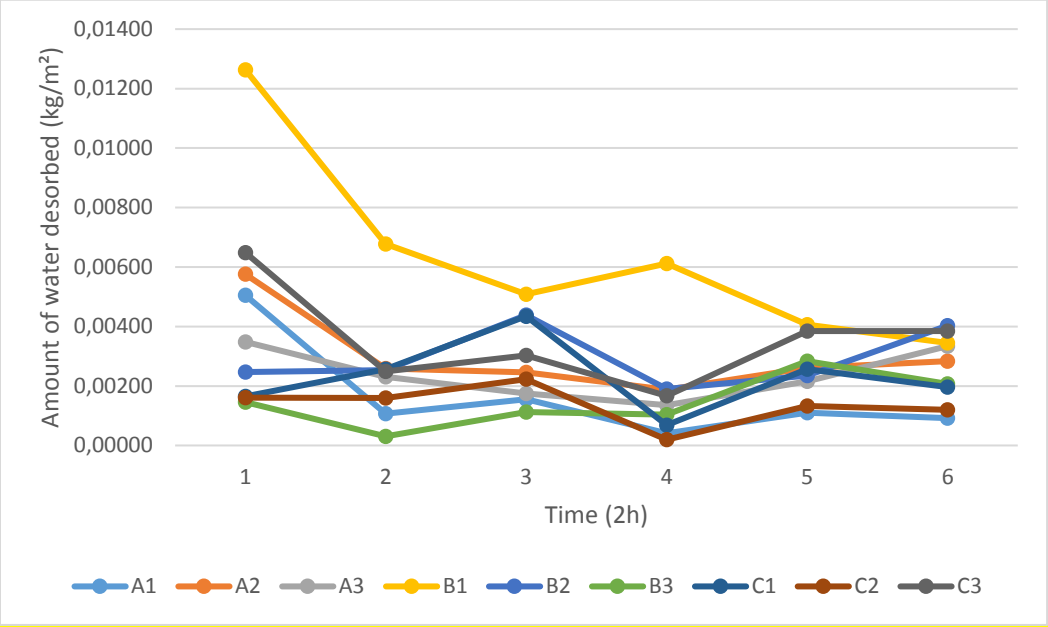

Figure 4-39. Amount of water desorbed (kg/m²) through Time (2h)

When both the "amount of water desorbed" graphs (2h and 144h) are analyzed, the higher the amount of water absorbed during the capillary absorption process, the higher the desorbed amount through the drying process.

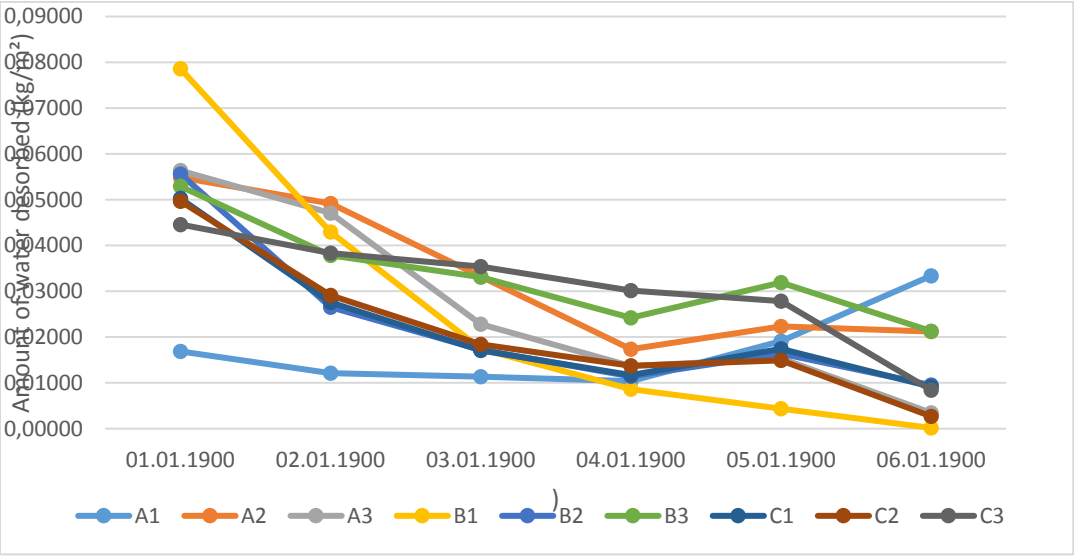

Figure 4-40. Amount of water desorbed (kg/m²) through Time (144h).

4.6 Hygric Properties

The water vapour permeability of mortars of samples is presented in Table 4.6.

Table 4.6 Hygric properties of mud plaster samples.

Name of samples	earth (Kerkenes with earth) volume %	river sand (4mm max) volume %	fiber (short straw) volume %	water volume %	egg white volume %	decomposition juice volume %	molasses volume %	cow dung volume %	water vapor permeability (48h)	Sd equivalent air layer (m)	μ water vapor diffusion resistance factor (-)
A1 (KeSdMo)	33%	67%		13%			9%		123.86	0.06	0.16
A2 (KeSdFbEg)	40%	40%	20%	24%	2%				253.54	0.03	0.08
A3 (KeSdFbCd)	44%	44%	11%	29%				11%	224.46	0.03	0.09
B1 (KeSd)	36%	64%		14%					282.17	0.03	0.07
B2 (KeSdFb-1)	40%	40%	20%	29%					206.44	0.04	0.09
B3 (KeFb)	80%		20%	39%					308.63	0.03	0.06
C1 (KeSdFbDj)	40%	40%	20%	24%		3%			273.73	0.03	0.07
C2 (KeFbCd)	80%		20%	25%				10%	269.16	0.03	0.07
C3 (KeSdFb-2)	40%	40%	20%	20%					253.20	0.03	0.08

4.6.1 Water vapour permeability

The water vapor permeability has been assessed on 3 different mixes (one sample per mix) and the water vapor diffusion resistance factor (μ) and the equivalent air layer (Sd) have been determined for comparison purposes with the literature.

The water vapour permeability of earth mortars is presented in Table 4.6 together with the density of the samples. The values for samples range from 308.63 B3 (KeFb) to 123.86 for A1 (KeSdMo).

All those samples have a very low vapor resistance. as expected for samples mortars containing earth. It seems that the amount of sand is increasing the diffusion resistance. Samples with the same volume of sand give a close result with each other. while samples B3 (KeFb) that contain %80 earth has the highest vapor permeability. in addition to this sample with the lowest earth content A1 (KeSdMo) %33 earth content has the lowest vapor permeability.

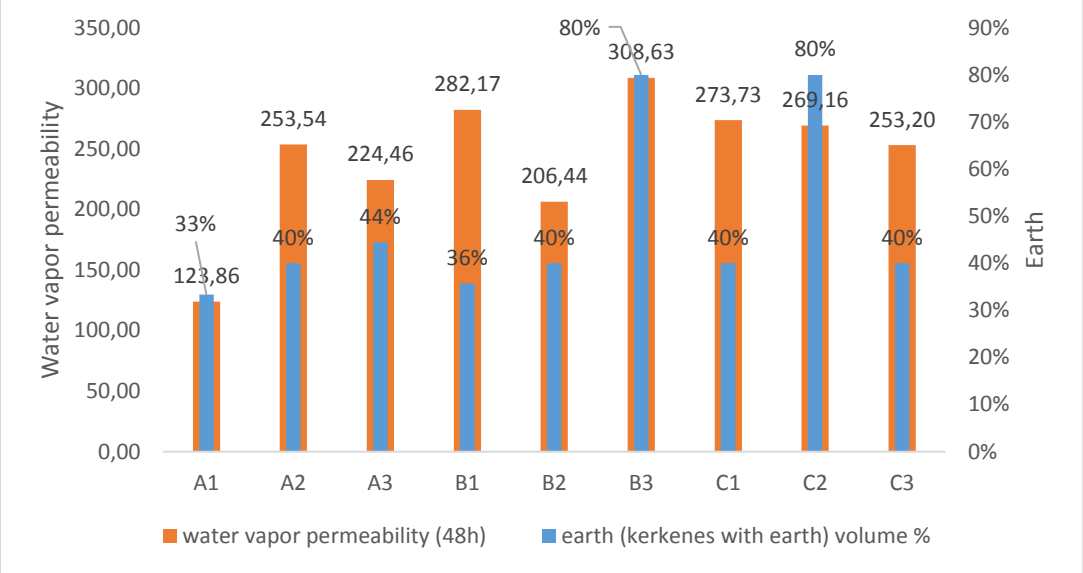

Figure 4-41. Water vapor permeability with earth volume.

In addition to the amount of earth the additive content also affects the vapor permeability. When A1 (KeSdMo) and B1 (KeSd) are compared A1 (KeSdMo) shows slightly lower vapor permeability than B1 (KeSd). that is the result thanks to the molasses in the A1 (KeSdMo).

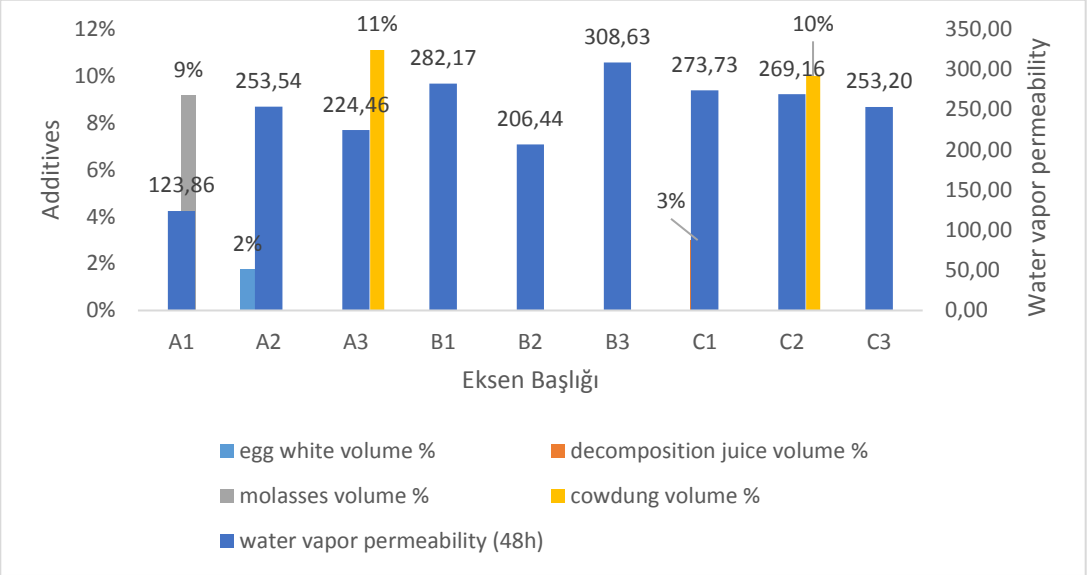

Figure 4-42. Water vapor permeability with additives

Density and vapor permeability are related in a way that, when density increases, it is expected that water permeability should decrease. A1 (KeSdMo) has the highest density. while having the lowest vapor permeability. in addition to this B3 (KeFb) has one of the lowest densities. and it has the highest vapor permeability.

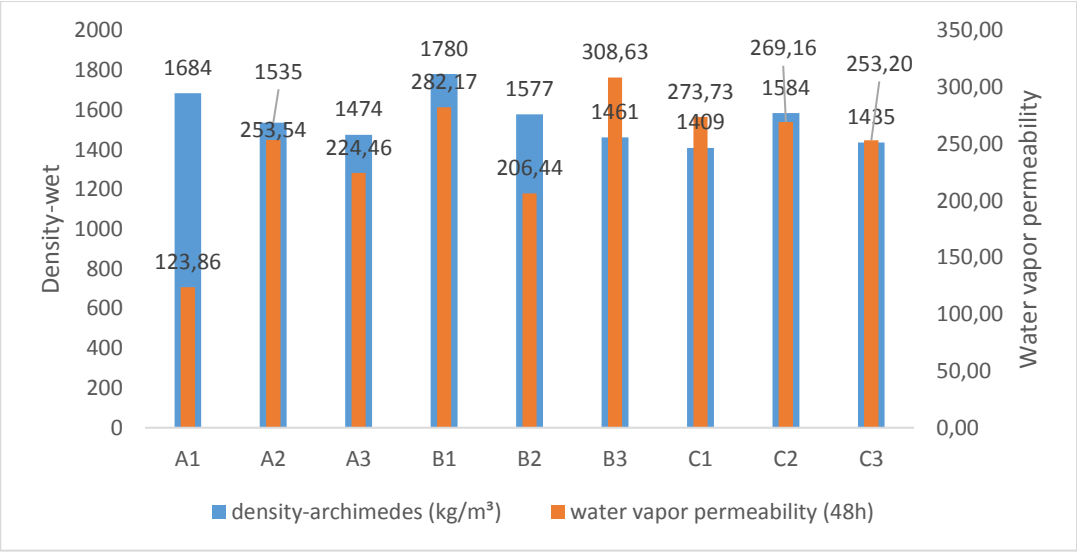

Figure 4-43. Water vapor permeability with density

CHAPTER 5

CONCLUSION

In this study the mud plaster samples from the experimental strawbale walls were examined for their physical, mechanical, hydric and hygric properties after being exposed to outside weather conditions for 5.5 years. In addition to the freeze and thaw cycles in Ankara's climate the samples were also stored in a small unventilated and unheated room in the Architecture annex building for another 2 years. The data obtained from this study are compared with the data gathered during the laboratory research on these mixes for the METU funded scientific research projects. The comparison of the nine samples with similar mixes are given individually in the following tables, starting from A1 (KeSdMo) to C3 (KeSdFb-2).

Table 5.1 Comparison of Ka610-21101 a, b, c with A1 (KeSdMo) (containing earth, sand, and molasses)

samples code Pedergnana (2022)		density-archimedes (kg/m³)	shrinkage (%)	vertical compressive strength (Mpa)	amount of material left on the tape (g/m²)	water resistance (min)	depth of the holde made by drops (cm)	frech rules -amount of trace (mm)	water vapor permability (48h)	μ water vapor diffusion resistance factor (-)	Sd equivalent air layer (m)	water capillarity absorption (14h)	drying rate (48h)	drying index (15days)
Ka610-21101	A1 (KeSdMo)	1.684	4.2%	3.6	0.59	180	0.7	0.5	170.14	0.12	0.05	0.57	0.20	0.97
Ka610-21101a	Lab	1742.8	1.4	5.0		2.880								
Ka610-21101b	Lab	1752.4	0.8	3.5		2.880			266.34			0.08	0.07	0.16
Ka610-21101c	Lab	1791.8	1.2	4.2		2.880	4.0							
Ka610-21101d	Lab	1761.7	0.8	3.5		2.880	3.5							

In comparison to the lab samples, A1 (KeSdMo) containing earth, sand, and molasses, which was subjected to outdoor conditions for 5 years with another 2 years in the unventilated mezzanine room, exhibits a much-decreased compressive strength of approximately 3.6 Mpa. This implies that A1 (KeSdMo)'s mechanical qualities were probably damaged by external factors like moisture and temperature fluctuations or application methods where mixes were prepared outside and applied

on a larger vertical surface manually. In addition to this, A1 (KeSdMo) also has a larger shrinkage than lab samples (4.2%) with surface cracking. With this huge difference in shrinkage. We can assume that the samples' size of A1 (KeSdMo)—outdoor conditions. And the application method affected its shrinkage. Comparing A1 (KeSdMo) with lab samples. The material's water vapor permeability is lower. The material dried faster after being exposed to outside conditions. as seen by A1 (KeSdMo)'s comparatively high drying rate and drying index. This could be the result of environmental stressors causing microcracking or increased porosity.

Table 5.2 Comparison of Ka011-2212a, b, c with A2 (KeSdFbEg) (containing earth, sand, short straw and egg white)

samples code Pedergnana (2022)		density-archimedes (kg/m³)	shrinkage (%)	vertical compressive strength (Mpa)	amount of material left on the tape (g/m²)	water resistance (min)	depth of the holde made by drops (cm)	frech rules -amount of trace (mm)	water vapor permability (48h)	μ water vapor diffusion resistance factor (-)	Sd equivalent air layer (m)	water capillarity absorption (14h)	drying rate (48h)	drying index (15days)
Ka011-2212	A2 (KeSdFbEg)	1.535	2.8%	0.7	0.36	25	1.0	3.0	314.47	0.06	0.02	1.21	0.28	0.92
Ka011-2212a	Lab	1730.0	1.4	0.6	0.18	2.00		14.00		5.1	0.2			
Ka011-2212b	Lab	1632.3	0.9	0.7	0.18	2.50						1.11	0.11	0.27
Ka011-2212c	Lab	1720.4	1.0	0.7	0.18	2.00	0.6		180.0					
Ka011-2212d	Lab	1714.0	1.4	-										

Comparing A2 (KeSdFbEg)'s density with the lab samples. It is possible that exposure to the outdoors reduced the material's compactness because of moisture or weathering, or it is also possible that, during the application phase due to the application method samples lost their compactness. A2 (KeSdFbEg) was subjected to outdoor conditions for 5 years with another 2 years in the unventilated mezzanine room, exhibits a small-decreased compressive strength which is approximately 0.7Mpa and A2 (KeSdFbEg) has higher shrinkage (2.8%) while lab samples have around (1%). This difference occurred because of the samples' size, outdoor conditions, and application method. A2 (KeSdFbEg)'s permeability is higher, suggesting that it is more porous or that it has formed microcracks that facilitate greater vapor flow. The much lower Sd value of the A2 (KeSdFbEg) sample indicates a significantly reduced resistance to vapor diffusion, perhaps due to

changes in porosity, A2 (KeSdFbEg) has a slightly reduced capillarity absorption. possibly because of a hardened coating growing on the surface that reduces capillary action, A2 (KeSdFbEg) dries down faster than other materials, which can be due to increased porosity brought on by weathering.

Table 5.3 Comparison of Ka211-221031a. b. c with A3 (KeSdFbCd) (containing earth, sand, short straw and cow dung)

samples code Pedergnana (2022)		density-archimedes (kg/m³)	shrinkage (%)	vertical compressive strength (Mpa)	amount of material left on the tape (g/m²)	water resistance (min)	depth of the holde made by drops (cm)	frech rules - amount of trace (mm)	water vapor permability (48h)	μ water vapor diffusion resistance factor (	Sd equivalent air layer (m)	water capillarity absorption (14h)	drying rate (48h)	drying index (15days)
Ka211-221031	A3 (KeSdFbCd)	1.474	2.3%	0.5	0.71	120	0.5	4.0	283.76	0.07	0.03	1.09	0.20	0.91
Ka211-221031a	Lab	1712.8	1.6	1.2	10.42	10		9.25						
Ka211-221031b	Lab	1700.5	1.6	1.2		10			408.4			1.21	0.11	0.35
Ka211-221031c	Lab	1650.1	1.3	1.2		10	0.45							

A3 (KeSdFbCd) has a lower density than lab samples. that could be the result of difference in application method where lab samples were prepared in the lab condition, while A3 (KeSdFbCd) is prepared on-site. Despite its lower density. A3 (KeSdFbCd) was subjected to outdoor conditions for 5 years with another 2 years in the unventilated mezzanine room, exhibits a much-decreased compressive strength which is approximately 0.7Mpa. Less material is left on the tape in A3 (KeSdFbCd) as compared to the lab samples, which could mean higher surface adherence or less surface degradation. A3 (KeSdFbCd) has a lower trace, indicating greater surface wear from exposure to the outside. When compared to certain lab samples, A3 (KeSdFbCd)'s permeability is lower, which could mean that it has a denser structure or less porosity. Because of structural alterations brought on by external factors, A3 (KeSdFbCd)'s reduced resistance factor indicates that it is more permeable to water vapor. When compared to the lab samples, A3 (KeSdFbCd) shows a reduced absorption of water capillarity. This might mean that because A3 (KeSdFbCd) has been exposed to the outside. its surface has become less porous or that it has formed a protective layer that prevents water absorption. A3 (KeSdFbCd) appears to lose moisture more quickly than the lab samples because of its faster drying rate. A3

(KeSdFbCd) dries faster than the lab samples over time, as indicated by its greater drying index. This can be an indication of how the weather has changed its structure and reduced its ability to hold moisture.

Table 5,4 Comparison of Ka010-2002a, b, c with B1 (KeSd) (containing earth, sand)

samples code Pedergnana (2022)		density-archimedes (kg/m³)	shrinkage (%)	vertical compressive strength (Mpa)	amount of material left on the tape (g/m²)	water resistance (min)	depth of the holde made by drops (cm)	frech rules -amount of trace (mm)	water vapor permability (48h)	μ water vapor diffusion resistance factor (-	Sd equivalent air layer (m)	water capillarity absorption (14h)	drying rate (48h)	drying index (15days)
Ka010-2002a,b,c	B1 (KeSd)	1.780	3.2%	0.6	0.45	10	-	5.0	341.36	0.06	0.02	1.11	0.09	0.90
Ka010-2002a	Lab	1707.9	2.4	0.7		7		16.50						
Ka010-2002b	Lab	1695.6	3.2	0.7		6			318.8			1.04	0.11	0.33
Ka010-2002c	Lab	1711.8	1.8	0.8		4	5.5							

The density of the B1 (KeSd) sample is marginally higher than that of the lab samples, indicating a possibility of material loss or application method. B1 (KeSd) shows a small-decreased compressive strength which is approximately 0.6Mpa. B1 (KeSd) and lab samples exhibit low water resistance. This finding raises the possibility that the sample did not pass this test, pointing to possible structural flaws. Similar performance is suggested by the B1 (KeSd) sample's trace depth, which is marginally lower than that of one of the lab samples. B1 (KeSd) has a marginally lower water vapor permeability than one of the lab samples, which could mean a decrease in porosity or moisture retention ability. The material's resistance to water vapor diffusion is shown by the μ-value, which can be used to infer resistance qualities without providing an exact comparison to lab samples. Without a direct comparison to lab data, Sd value indicates a moderate resistance to the flow of water vapor. After being exposed to the outdoors, the water capillarity absorption is marginally higher than in the lab samples suggesting increased porosity. The drying rate is much higher, indicating that moisture is being lost quickly, most likely because of increased porosity from the outside environment. The new sample has a greater drying index. which supports the idea that there is more moisture loss and less potential for retention.

Table 5.5 Comparison of Ka711-102211a, b, c with B2 (KeSdFb-1) (containing earth, sand and short straw)

samples code Pedergnana (2022)		density-archimedes (kg/m³)	shrinkage (%)	vertical compressive strength (Mpa)	amount of material left on the tape (g/m²)	water resistance (min)	depth of the holde made by drops (cm)	frech rules - amount of trace (mm)	water vapor permability (48h)	μ water vapor diffusion resistance factor (	Sd equivalent air layer (m)	water capillarity absorption (14h)	drying rate (48h)	drying index (15days)
Ka711-102211a,b,c ,	B2 (KeSdFb-1)	1.577	5.1%	0.8	0.16	25	0.8	5.0	244.64	0.08	0.03	0.79	0.19	0.91
Ka711-102211a	Lab	1463.6	2.8	0.8	0.92	7		10.50						
Ka711-102211b	Lab	1427.7	2.0	0.8		7			330.5			1.25	0.13	0.36
Ka711-102211c	Lab	1419.0	2.3	1.0		15								

The B2 (KeSdFb-1)'s somewhat greater density than that of the lab samples raises the possibility that the application method where the samples that are at the bottom of the wall get compressed by self-weight. B2 (KeSdFb-1) has also a larger shrinkage than lab samples (5.1%) with surface cracking. With this huge difference in shrinkage, we can assume that the samples' size of B2 (KeSdFb-1), outdoor conditions, and application method affected its shrinkage. The compressive strength of B2 (KeSdFb-1) (0.8 Mpa) is close to the lab samples. Strong adhesion or a surface layer produced as a result of environmental variables is indicated by minimal material remaining on the tape, also the site photos show a smooth surface. The B2 (KeSdFb-1) exhibits improved durability against moisture and a notably higher level of water resistance. Less depth from the water droplets in the fresh sample suggests improved resistance. Reduced permeability in the new B2 (KeSdFb-1) suggests reduced porosity, shows a modest level of vapor diffusion resistance, exhibits resistance to vapor transfer in line with laboratory specimens, shows reduced absorption, perhaps as a result of being outside, quicker rate of drying, indicating more surface porosity. Greater drying index (0.91). which denotes effective moisture removal.

Table 5.6 Comparison of Ka001-206 a, b, c with B3 (KeFb) (containing earth and short straw)

samples code Pedergnana (2022)		density-archimedes (kg/m³)	shrinkage (%)	vertical compressive strength (Mpa)	amount of material left on the tape (g/m²)	water resistance (min)	depth of the holde made by drops (cm)	frech rules - amount of trace (mm)	water vapor permability (48h)	µ water vapor diffusion resistance factor (	Sd equivalent air layer (m)	water capillarity absorption (14h)	drying rate (48h)	drying index (15days)
Ka001-206	B3 (KeFb)	1.461	8.0%	2.6	0.06	15	1.5	1.0	384.30	0.05	0.02	1.22	0.39	0.90
Ka001-206a	Lab	1531.6	4.0	2.9		10		2.25						
Ka001-206b	Lab	1530.6	4.2	2.7		10			447.8			1.12	0.15	0.38
Ka001-206c	Lab	1548.9	3.4	3.3		15	6							

The B3 (KeFb) sample has a lower density (1460 kg/m³) than the lab samples (1530kg/m³). This decline may have resulted from the sample being exposed to external circumstances or again application method. The B3 (KeFb) (2.6Mpa) sample has a lower compressive strength than the lab sample(2.9Mpa). B3 (KeFb) has good water resistance (Ka001-206c). This implies that even after being exposed to the outside, the material has maintained its resistance to water absorption. Comparable to or superior to certain lab samples. B3 (KeFb)'s relatively shallow depth indicates strong resistance to water penetration. The B3 (KeFb) sample's water vapor permeability is lower than that of the lab sample Ka001-206b's, indicating a potential decrease in porosity and moisture retention capacity following outdoor exposure. The B3 (KeFb) sample dries much more quickly than the other samples, which may indicate that the material is releasing moisture more quickly as a result of increased porosity from contact with the environment.

Table 5.7 Comparison of Ka111-32211, a, b, c, d with C1 (KeSdFbDj) (containing earth, sand. short straw and decomposition juice)

samples code Pedergnana (2022)		density-archimedes (kg/m³)	shrinkage (%)	vertical compressive strength (Mpa)	amount of material left on the tape (g/m²)	water resistance (min)	depth of the holde made by drops (cm)	frech rules -amount of trace (mm)	water vapor permability (48h)	µ water vapor diffusion resistance factor (	Sd equivalent air layer (m)	water capillarity absorption (14h)	drying rate (48h)	drying index (15days)
Ka111-32211	C1 (KeSdFbDj)	1.409	3.0%	0.9	0.67	110	0.7	16.0	322.71	0.06	0.02	0.87	0.20	0.90
Ka111-32211a	Lab	1603.2	1.4	1.2	0.97	37		9.50						
Ka111-32211b	Lab	1603.5	1.7	1.2		65			362.8			1.14	0.16	0.32
Ka111-32211c	Lab	1597.5	1.5	1.2		48								
Ka111-32211d	Lab	1611.3	1.9				1							

The C1 (KeSdFbDj)'s density (1409kg/m³) is much lower than that of the lab samples (1603 kg/m³), indicating that exposure to external circumstances may have reduced the material's mass or integrity. The C1 (KeSdFbDj)'s compressive strength (0.9Mpa) is lower than the lab samples (1.35 Mpa). In addition to this, C1 (KeSdFbDj) (3%) has also a larger shrinkage than lab samples (1.23%). With this huge difference in shrinkage, we can assume that the samples' size of C1 (KeSdFbDj). outdoor conditions, and application method affected its shrinkage. In comparison to the lab sample, the C1 (KeSdFbDj) shows nearly the same values as the lab sample about the amount of material remaining on the tape. The C1 (KeSdFbDj)'s water resistance is similar to that of the lab samples, indicating that the material has not lost its capacity to withstand water penetration even after being exposed to the outdoors. C1 (KeSdFbDj) has a similar water vapor permeability. C1 (KeSdFbDj) has retained or even enhanced its resistance to moisture absorption following outside exposure, as seen by the slightly lower water capillarity absorption than in the lab samples. The material may be releasing moisture more quickly in C1 (KeSdFbDj) because of its greater drying rate, which is most likely the result of increased porosity from exposure to the environment. C1 (KeSdFbDj) has a much greater drying index, which suggests that it has a lower capacity to retain moisture, which causes it to dry out more quickly after being exposed to the outdoors.

Table 5.8 Comparison of Ka701-10201a, b, c with C2 (KeFbCd) (containing earth. short straw and cow dung)

samples code Pedergnana (2022)		density-archimedes (kg/m³)	shrinkage (%)	vertical compressive strength (Mpa)	amount of material left on the tape (g/m²)	water resistance (min)	depth of the holde made by drops (cm)	frech rules - amount of trace (mm)	water vapor permability (48h)	µ water vapor diffusion resistance factor (	Sd equivalent air layer (m)	water capillarity absorption (14h)	drying rate (48h)	drying index (15days)
Ka701-10201	C2 (KeFbCd)	1.584	8.3%	0.8	0.56	35	1.0	15.0	320.80	0.06	0.02	0.86	0.20	0.91
Ka701-10201a	Lab	1632.7	2.7	1.6				5.00						
Ka701-10201b	Lab	1632.8	2.5	1.8					363.1			0.80	0.12	0.35
Ka701-10201c	Lab	1629.0	1.8	1.8			5							

C2 (KeFbCd) density (1584 kg/m³) is lower than that of the lab samples (1632 kg/m³), which may indicate that exposure to outdoor circumstances has reduced the material's mass. or the application method affected the integrity. C2 (KeFbCd)'s compressive strength (0.8Mpa) is lower than the lab samples(2.5Mpa). On the other hand, C2 (KeFbCd) has also a larger shrinkage than lab samples (8.3%). With this huge difference in shrinkage, we can assume that the samples' size of C2 (KeFbCd), outdoor conditions, and application method affected their shrinkage. In comparison to the lab samples, the C2 (KeFbCd) sample exhibits a modest depth, showing strong resistance to water penetration. The moderate range of the trace left in C2 (KeFbCd) suggests a reasonable resistance to mechanical wear from water impact, which may have been impacted by outside exposure. C2 (KeFbCd) has a lower water vapor permeability, which may indicate that exposure to the outside has reduced its porosity and ability to retain moisture. When comparing C2 (KeFbCd) to the earlier lab samples, the absorption of water vapor and water capillarity is also marginally higher. indicating that the material may have become less dense or more porous as a result of contact with the environment. The C2 (KeFbCd)'s drying rate is noticeably higher than that of the lab samples. This can be the effect of exposure to the outdoors increasing porosity or decreasing water retention capacity. C2 (KeFbCd) has a substantially greater drying index than the lab samples, indicating that it dries out more quickly. This could be because the material's composition alters structurally after being exposed to outdoor circumstances.

Table 5.9 Comparison of Ka011-2211a, b, c with C3 (KeSdFb-2)

samples code Pedergnana (2022)		density-archimedes (kg/m³)	shrinkage (%)	vertical compressive strength (Mpa)	amount of material left on the tape (g/m²)	water resistance (min)	depth of the holde made by drops (cm)	frech rules -amount of trace (mm)	water vapor permability (48h)	µ water vapor diffusion resistance factor (-)	Sd equivalent air layer (m)	water capillarity absorption (14h)	drying rate (48h)	drying index (15days)
Ka011-2211	C3 (KeSdFb-2)	1.435	4.7%	0.4	0.28	15	Fail	1.0	345.10	0.06	0.02	1.64	0.40	0.92
Ka011-2211a	Lab	1565.5	2.1	1.1	0.02	8		12.00		4.4	0.2			
Ka011-2211b	Lab	1550.2	2.0	1.3	0.01	10			232.5			1.18	0.16	0.32
Ka011-2211c	Lab	1526.2	2.0	1.2	0.02	9	6.5							

In comparison to the lab samples (0.022g/m²), C3 (KeSdFb-2) (0.27g/m²) has more material remaining on the tape, which may indicate lower adherence or increased surface roughness. C3 (KeSdFb-2)'s compressive strength (0.4 Mpa) is lower than the lab samples(1.1Mpa). In addition to this, C3 (KeSdFb-2) (4.7%) has also a larger shrinkage than lab samples (2%). With this huge difference in shrinkage, we can assume that the samples' size of C3 (KeSdFb-2), outdoor conditions, and application method affected its shrinkage. Compared to the lab samples, C3 (KeSdFb-2) exhibits greater water resistance, suggesting that it would be a better fit for applications where exposure to moisture is an issue. On the other hand, lab sample Ka011-2211a revealed a considerable depth, suggesting that it would be more vulnerable to erosion or water drop damage. Similar to the lab samples, particularly Ka011-2211b. C3 (KeSdFb-2) exhibits excellent water vapor permeability, indicating its breathability and possible usage in applications where vapor permeability is crucial. It appears that C3 (KeSdFb-2) permits water vapor to move through more readily than the lab samples because of its lower resistance factor. Compared to most lab samples. C3 (KeSdFb-2) exhibits a comparatively high-water capillarity absorption, indicating that it absorbs moisture more easily. In comparison to the lab samples, C3 (KeSdFb-2) dries more quickly, which is advantageous for a speedy recovery from moisture exposure, C3 (KeSdFb-2) performs better at drying out over an extended length of time, as seen by its higher drying index.

Overall comparison of mud- plaster samples

Higher mechanical strength and density are commonly seen in the A1 (KeSdMo) (Ka610-21101) and B3 (KeFb) (Ka001-206), especially in the case of A1 (KeSdMo) (Ka610-21101), which performs better than other samples in terms of compressive strength and water resistance. This implies that A1 (KeSdMo) (Ka610-21101) would be more appropriate for load-bearing applications in higher moisture-exposure situations. Better water vapor permeability and quicker drying rates are shown by B3 (KeFb) (Ka001-206) and C3 (KeSdFb-2) (Ka011-2211), suggesting that they would be more suited for applications where breathability and moisture management are essential. A1 (KeSdMo) (Ka610-21101) exhibits good mechanical characteristics and moisture resistance. The most breathable materials are B3 (KeFb) (Ka001-206) and C3 (KeSdFb-2) (Ka011-2211), which both exhibit superior vapor permeability and drying speeds. With their superior drying speeds and vapor permeability. C1 (KeSdFbDj), C2 (KeFbCd), and C3 (KeSdFb-2) may be more adaptable to changing weather conditions. On the other hand, the A1 (KeSdMo) (Ka610-21101) has superior mechanical stress and water resistance, indicating that it may be more durable under more adverse circumstances. In terms of additive impact on the samples, as discussed through the thesis that. A1 (KeSdMo) outperforms other samples thanks to its molasses content. Molasses outperforms other additives, while having negative impact on shrinkage on the other hand, each additive, improved material properties, some of them improved their durability, water resistance. and shrinkage like egg white for C1 (KeSdFbDj), and some of them slightly raised the general properties of samples. The use of water is crucial for mud-plaster samples, shrinkage, density, hygric and hydric properties. Using too little or too much makes the examples weak. The effect of river sand can be seen when comparing B2 (KeSdFb-1) and B3 (KeFb), with the lack of aggregate shrinkage. surface cohesion. surface water absorption. and surface durability against abrasion decreases. Plaster becomes stronger and less prone to catastrophic failure when fibers are added to distribute stress more evenly throughout the material as we can see from the B2

(KeSdFb-1) and C1 (KeSdFbDj). In the absence of it. the sample (B1 (KeSd)) (if it has no additives) easily can lose its integrity.

The mud-plaster samples' mechanical characteristics, particularly their compressive strength, differ greatly depending on their composition. In general, samples with higher densities have stronger compressive strengths. The A series (A1 (KeSdMo), A2 (KeSdFbEg), A3 (KeSdFbCd)), for example, displayed varied compressive strengths according to the mix and exposure conditions. In general, samples exposed to the outside had lower compressive strengths than samples stored in a laboratory. The external environment, which is defined by temperature swings, humidity, and precipitation, weakens the material's compressive strength because of factors like material expansion and contraction, drying cycles, and moisture infiltration.

The hygric qualities, which include drying rate, vapor permeability, and water absorption, are contingent upon the mud-plaster composition, specifically the organic additives employed. Samples containing additives, for instance, had different levels of water vapor permeability and water capillarity absorption. A1 (KeSdMo) exhibited reduced vapor permeability and capillarity absorption, suggesting a composition that is more resilient to moisture intrusion and maintains structural integrity in damp environments. On the other hand, samples with differing compositions and a higher proportion of sand, such as B1 (KeSd) and C1 (KeSdFbDj), showed higher rates of absorption and permeability, making them more vulnerable to degradation caused by moisture. Organic additions change the plaster's porosity and ability to bind water, which affects these characteristics.

Depending on the composition and exposure conditions, the samples' resilience to surface abrasion and cohesiveness varies. Samples like A1 (KeSdMo), which have lower water absorption and higher compressive strength, typically show better resistance to surface abrasion. As seen by the amount of material remaining on the tape, the cohesiveness qualities of samples exposed to outdoor conditions (e.g., A1 (KeSdMo), B1 (KeSd), C1 (KeSdFbDj)) are often poorer than those of lab samples. The breakdown of the plaster's binding agents, brought on by extended exposure to

moisture and fluctuating temperatures, causes this drop in cohesiveness, which also increases surface erosion and decreases surface strength.

Over time, the properties of mud-plaster samples are significantly influenced by external environmental variables. Variations in temperature, humidity, and precipitation cause a reduction in surface cohesiveness, an increase in water absorption, and a drop in compressive strength. The material expands and contracts as a result of frequent wetting and drying cycles, weakening the structure overall and resulting in the creation of microcracks. Furthermore, extended moisture exposure can lead to increased capillarity absorption and water vapor permeability, which increases the samples' susceptibility to deterioration. When compared to their lab counterparts, the mechanical and hydraulic performance of the outdoor-exposed samples, such as A1 (KeSdMo), B1 (KeSd), and C1 (KeSdFbDj), is clearly affected by these factors.

Conclusions Based on Aim and Objectives

Over the course of five years, the analysis of the nine distinct mud-plaster samples provides important new information about how well they function in outdoor environments. The main conclusion is that mechanical strength, surface cohesiveness, and resistance to water and erosion all generally deteriorate after being exposed to the outside. The study also emphasizes how composition plays a significant role in mud-plaster performance and longevity, with certain compositions being better able to withstand the negative impacts of exposure to the environment.

The impact of external conditions on critical material attributes, including compressive strength, surface strength, water resistance, and drying capacity, highlights the importance of selecting materials and additives carefully throughout construction. According to the relationships found between mechanical and hygric qualities, compositions that have reduced vapor permeability and water absorption tend to hold their mechanical integrity over time.

This study emphasizes how crucial it is to take the environment into account when designing and using mud plasters for environmentally friendly buildings. By

providing a better understanding of how external conditions affect the longevity and performance of mud-plaster samples, the findings contribute to the aim and objectives by offering insightful information that will help develop more resilient and long-lasting earth-based construction materials.

Mechanical strength, surface cohesiveness, and resistance to water and erosion all generally deteriorate after being exposed to the outside. The study also emphasizes how composition plays a significant role in mud-plaster performance and longevity, with certain compositions being better able to withstand the negative impacts of exposure to the environment.

The impact of external conditions on critical material attributes, including compressive strength, surface strength, water resistance, and drying capacity, highlights the importance of selecting materials and additives carefully throughout construction. According to the relationships found between mechanical and hygric qualities, compositions that have reduced vapor permeability and water absorption tend to hold their mechanical integrity over time.

This study emphasizes how crucial it is to take the environment into account when designing and using mud plasters for environmentally friendly buildings. By providing a better understanding of how external conditions affect the longevity and performance of mud-plaster samples, the findings contribute to the aim and objectives by offering insightful information that will help develop more resilient and long-lasting earth-based construction materials.

REFERENCES

Aguilar, R., Nakamatsu, J., Ramírez, E., Elgegren, M., Ayarza, J., Kim, S., Pando, M. A., & Ortega-San-Martin, L. (2016). The potential use of chitosan as a biopolymer additive for enhanced mechanical properties and water resistance of earthen construction. *Construction and Building Materials, 114*, 625–637. https://doi.org/10.1016/j.conbuildmat.2016.03.218

Araya-Letelier, G., Antico, F. C., Burbano-Garcia, C., Concha-Riedel, J., Norambuena-Contreras, J., Concha, J., & Saavedra Flores, E. I. (2021). Experimental evaluation of adobe mixtures reinforced with jute fibers. *Construction and Building Materials*, *276*, 122127. https://doi.org/10.1016/j.conbuildmat.2020.122127

Araya-Letelier, G., Concha-Riedel, J., Antico, F. C., & Sandoval, C. (2019). Experimental mechanical-damage assessment of earthen mixes reinforced with micro polypropylene fibers. *Construction and Building Materials*, *198*, 762–776. https://doi.org/10.1016/j.conbuildmat.2018.11.261

Ashour, T. A., Bahnasawy, A. B., & Ali, S. A. (2010). Absorption and desorption behavior of some clay-sandy plasters reinforced with natural fibers used for straw bale buildings. *Misr Journal of Agricultural Engineering*, *27*(2), 699–717. https://doi.org/10.21608/mjae.2010.105938

Aubert, J. E., Fabbri, A., Morel, J. C., & Maillard, P. (2013). An earth block with a compressive strength higher than 45 MPa! *Construction and Building Materials*, *47*, 366–369. https://doi.org/10.1016/j.conbuildmat.2013.05.068

Auld, H. (1999). Impacts of climate change on infrastructure in Canada. *Environment Canada*.

Aymerich, F., Fenu, L., & Meloni, P. (2012). Effect of reinforcing wool fibers on fracture and energy absorption properties of an earthen material. *Construction and Building Materials, 27*(1), 66–72. https://doi.org/10.1016/j.conbuildmat.2011.08.008

Azeredo, G. (2007). Compressive strength testing of earth mortars. *Journal of Urban and Environmental Engineering, 1*(1), 26–35. https://doi.org/10.4090/juee.2007.v1n1.026035

Babé, C., Kidmo, D. K., Tom, A., Mvondo, R. R. N., Boum, R. B. E., & Djongyang, N. (2020). Thermomechanical characterization and durability of adobes reinforced with millet waste fibers (*Sorghum bicolor*). *Case Studies in Construction Materials, 13*, e00422. https://doi.org/10.1016/j.cscm.2020.e00422

Bamogo, H., Ouedraogo, M., Sanou, I., Ouedraogo, K. A., Dao, K., Aubert, J.-E., & Millogo, Y. (2020). Improvement of water resistance and thermal comfort of earth renders by cow dung: An ancestral practice of Burkina Faso. *Journal of Cultural Heritage, 46*, 42–51. https://doi.org/10.1016/j.culher.2020.04.009

Caron, P., & Lynch, M. F. (1988). Making mud plaster. *APT Bulletin, 20*(4), 7. https://doi.org/10.2307/1504233

Clausell, J. R., Signes, C. H., Solà, G. B., & Lanzarote, B. S. (2020). Improvement in the rheological and mechanical properties of clay mortar after adding *Ceratonia siliqua* L. extracts. *Construction and Building Materials, 237*, 117747. https://doi.org/10.1016/j.conbuildmat.2019.117747

Coffman, C. V., Duffin, R. J., & Knowles, G. P. (1980). Are adobe walls optimal phase-shift filters? *Advances in Applied Mathematics, 1*(1), 50–66. https://doi.org/10.1016/0196-8858(80)90006-8

Colas, E., & Bourgès, A. (2013). Mises au point de protocoles pour mesurer les performances, la durabilité et la compatibilité d'enduits de protection en terre et biopolymères.

Concha-Riedel, J., Araya-Letelier, G., Antico, F. C., Reidel, U., & Glade, A. (2019). Influence of jute fibers to improve flexural toughness, impact resistance, and drying shrinkage cracking in adobe mixes. *Springer Transactions in Civil and Environmental Engineering*, 269–278. https://doi.org/10.1007/978-981-13-5883-8_24

Costi de Castrillo, M., Ioannou, I., & Philokyprou, M. (2021). Reproduction of traditional adobes using varying percentage contents of straw and sawdust. *Construction and Building Materials*, *294*, 123516. https://doi.org/10.1016/j.conbuildmat.2021.123516

Day, C. (1990). Evaluating embodied energy impacts in buildings: Some research outcomes and issues.

DIN18947. (2013). Pub. L. No. DIN 18947.

Ding, G. K. C. (2014). Life cycle assessment (LCA) of sustainable building materials: An overview. *Eco-Efficient Construction and Building Materials*, 38–62. https://doi.org/10.1533/9780857097729.1.38

Du Plessis, C. (2007). A strategic framework for sustainable construction in developing countries. *Construction Management and Economics*, *25*(1), 67–76. https://doi.org/10.1080/01446190600601313

Duggal, S. K. (2017). *Building materials*. Routledge.

Emery, V. L. (2011). Mud-brick. In W. Wendrich (Ed.), *UCLA Encyclopedia of Egyptology*. Los Angeles. http://digital2.library.ucla.edu/viewItem.do?ark=21198/zz0026vj53

Emiroğlu, M., Yalama, A., & Erdoğdu, Y. (2015). Performance of ready-mixed clay plasters produced with different clay/sand ratios. *Applied Clay Science, 115*, 221–229. https://doi.org/10.1016/j.clay.2015.08.005

Faria, P., dos Santos, T., & Silva, V. (2014). Earth-based mortars for masonry plastering. *9th International Masonry Conference*, 1–12.

Faria, P., Santos, T., & Aubert, J.-E. (2016). Experimental characterization of an earth eco-efficient plastering mortar. *Journal of Materials in Civil Engineering, 28*(1). https://doi.org/10.1061/(ASCE)MT.1943-5533.0001363

Franzoni, E. (2011). Materials selection for green buildings: Which tools for engineers and architects? *Procedia Engineering, 21*, 883–890. https://doi.org/10.1016/j.proeng.2011.11.2090

Giada, G., Caponetto, R., & Nocera, F. (2019). Hygrothermal properties of raw earth materials: A literature review. *Sustainability, 11*(19), 5342. https://doi.org/10.3390/su11195342

Goodland, R. (1992). The case that the world has reached limits: More precisely that current throughput growth in the global economy cannot be sustained. *Population and Environment, 13*(3), 167–182. https://doi.org/10.1007/bf01256413

Green, M., Jones, D., & Smith, R. (2003). Aging infrastructure: Challenges and solutions. *Journal of Structural Engineering, 129*(4), 398–405.

Guihéneuf, S., Rangeard, D., Perrot, A., Cusin, T., Collet, F., & Prétot, S. (2020). Effect of bio-stabilizers on capillary absorption and water vapour transfer into raw earth. *Materials and Structures*, 53(6), 138. https://doi.org/10.1617/s11527-020-01571-z

Hamard, E., Morel, J.-C., Salgado, F., Marcom, A., & Meunier, N. (2013). A procedure to assess the suitability of plaster to protect vernacular earthen architecture. *Journal of Cultural Heritage*, 14(2), 109–115. https://doi.org/10.1016/j.culher.2012.04.005

Hastak, M. (1995). A decision support system for construction materials selection using sustainability as a criterion. *Academia*.

Intergovernmental Panel on Climate Change (IPCC). (2001). *Climate change 2001: Impacts, adaptation, and vulnerability. Contribution of Working Group II to the Third Assessment Report of the Intergovernmental Panel on Climate Change*. Cambridge University Press.

Jayasinghe, C., & Kamaladasa, N. (2007). Compressive strength characteristics of cement stabilized rammed earth walls. *Construction and Building Materials*, 21(11), 1971–1976. https://doi.org/10.1016/j.conbuildmat.2006.05.049

Jiménez Delgado, M. C., & Guerrero, I. C. (2007). The selection of soils for unstabilised earth building: A normative review. *Construction and Building Materials*, 21(2), 237–251. https://doi.org/10.1016/j.conbuildmat.2005.08.006

Kilian, R., Borgatta, L., & Wendler, E. (2023). Investigation of the deterioration mechanisms induced by moisture and soluble salts in the necropolis of Porta Nocera, Pompeii (Italy). *Heritage Science*, 11, Article 10. https://doi.org/10.1186/s40494-023-00900-z

Laborel-Préneron, A., Giroudon, M., Aubert, J. E., Magniont, C., & Faria, P. (2019). Experimental assessment of bio-based earth bricks durability. *IOP Conference Series: Materials Science and Engineering*, 660(1), 012069. https://doi.org/10.1088/1757-899x/660/1/012069

Laborel-Préneron, A., Magniont, C., & Aubert, J.-E. (2018). Hygrothermal properties of unfired earth bricks: Effect of barley straw, hemp shiv, and corn cob addition. *Energy and Buildings*, 178, 265–278. https://doi.org/10.1016/j.enbuild.2018.08.021

Lacasse, M. A. (2003). Environmental impacts on concrete and masonry structures. *Construction and Building Materials*, 17(4), 265-277.

Lagouin, M., Aubert, J. E., Laborel-Préneron, A., & Magniont, C. (2021). Influence of chemical, mineralogical, and geotechnical characteristics of soil on earthen plaster properties. *Construction and Building Materials*, 304, 124339. https://doi.org/10.1016/j.conbuildmat.2021.124339

Lstiburek, J. (2002). Moisture control in buildings. *Journal of Building Physics*, 25(4), 323-331.

Li, X., Zhu, Y., & Zhang, Z. (2010). An LCA-based environmental impact assessment model for construction processes. *Building and Environment*, 45(3), 766–775. https://doi.org/10.1016/j.buildenv.2009.08.010

Lima, J., Correia, D., & Faria, P. (2016, June). Rebocos de terra: Influência da adição de gesso e da granulometria da areia. *Argamassas 2016 – II Simpósio de Argamassas e Soluções Térmicas de Revestimento*.

Lima, J., Faria, P., & Santos Silva, A. (2020). Earth plasters: The influence of clay mineralogy in the plasters' properties. *International Journal of Architectural Heritage*, 14(7), 948–963. https://doi.org/10.1080/15583058.2020.1727064

Lima, J., & Faria, P. (2016). Eco-efficient earthen plasters: The influence of the addition of natural fibers. *RILEM Bookseries*, 12, 315–327. https://doi.org/10.1007/978-94-017-7515-1_24

Lima, J., Faria, P., & Santos Silva, A. (2020). Earth plasters: The influence of clay mineralogy in the plasters' properties. *International Journal of Architectural Heritage*, 14(7), 948–963. https://doi.org/10.1080/15583058.2020.1727064

Lima, J., Silva, S., & Faria, P. (2016). Rebocos de terra: Influência da adição de óleo de linhaça e comparação com rebocos convencionais. *Teste 2016 - 1º Congresso de Ensaios e Experimentação Em Engenharia Civil*, 1–8.

Maheri, M. R., Maheri, A., Pourfallah, S., Azarm, R., & Hadjipour, A. (2011). Improving the durability of straw-reinforced clay plaster cladding for earthen buildings. *International Journal of Architectural Heritage*, 5(3), 349–366. https://doi.org/10.1080/15583051003663859

Marques, F. M., & Salgado, M. S. (2007). The building material selection importance at the building design process for its sustainability. In R. Milford (Ed.), *Proceedings of the CIB World Building Congress "Construction for Development"* (pp. 2384–2396). Cape Town, South Africa.

Magnuson, S., Nelson, T., & Gray, L. (2000). Freeze-thaw durability of clay bricks. *Materials and Structures*, 33(5), 332-340.

Melià, P., Ruggieri, G., Sabbadini, S., & Dotelli, G. (2014). Environmental impacts of natural and conventional building materials: A case study on earth plasters. *Journal of Cleaner Production*, 80, 179–186. https://doi.org/10.1016/j.jclepro.2014.05.073

Mesbah, A., Morel, J. C., & Olivier, M. (1999). Comportement des sols fins argileux pendant un essai de compactage statique: Détermination des paramètres pertinents. *Materials and Structures*, 32(9), 687–694. https://doi.org/10.1007/bf02481707

Minke, G. (2009). *Building with earth: Design and technology of a sustainable architecture*. Birkhauser Basel.

Minke, G. (2012). *Building with earth*. https://doi.org/10.1515/9783034612623

Muñoz, P., Letelier, V., Muñoz, L., & Bustamante, M. A. (2020). Adobe bricks reinforced with paper & pulp wastes improving thermal and mechanical properties. *Construction and Building Materials*, 254, 119314. https://doi.org/10.1016/j.conbuildmat.2020.119314

Navarro, A., Palumbo, M., Gonzalez, B., & Lacasta, A. M. (2015). Performance of clay-straw plasters containing natural additives. In *First International Conference on Bio-based Building Materials* (pp. 275–280). Clermont-Ferrand, France.

Pacheco-Torgal, F., & Jalali, S. (2011). Cementitious building materials reinforced with vegetable fibres: A review. *Construction and Building Materials*, 25(2), 575–581. https://doi.org/10.1016/j.conbuildmat.2010.07.024

Palumbo, M., McGregor, F., Heath, A., & Walker, P. (2016). The influence of two crop by-products on the hygrothermal properties of earth plasters. *Building and Environment*, 105, 245–252. https://doi.org/10.1016/j.buildenv.2016.06.004

Pedergnana, M., & Ozkan, S. T. (2021). Hygro-thermal, hydric, and mechanical properties of fibre and aggregate-reinforced earth plasters. *International*

Journal of Digital Innovation in the Built Environment, 10(2), 29–45. https://doi.org/10.4018/ijdibe.2021070103

Pedergnana, M. J. (2022). *Impacts of natural additives on the properties of earth plasters* (Doctoral dissertation, Middle East Technical University, Graduate School of Natural and Applied Sciences).

Piattoni, Q., Quagliarini, E., & Lenci, S. (2011). Experimental analysis and modelling of the mechanical behaviour of earthen bricks. *Construction and Building Materials*, 25, 2067–2075. https://doi.org/10.1016/j.conbuildmat.2010.11.039

Qasab, R. A., Mir, R., Dar, A., Ashraf, A., Ali, U., Parray, F., & Manzoor, B. (2018). An experimental study to address the issues of low durability and low compressive strength of mud plaster. *Journal of Emerging Technologies and Innovative Research*, 141–165.

Ouédraogo, M., Dao, K., Millogo, Y., Aubert, J.-E., Messan, A., Seynou, M., Zerbo, L., & Gomina, M. (2019). Physical, thermal, and mechanical properties of adobes stabilized with fonio (Digitaria exilis) straw. *Journal of Building Engineering*, 23, 250–258. https://doi.org/10.1016/j.jobe.2019.02.005

Rajapaksha, U., et al. (2016). *Building the future – resilient environments: Proceedings of the 9th International Conference of Faculty of Architecture Research Unit (FARU)*, University of Moratuwa, Sri Lanka, September 09-10, Colombo, 250–261.

Ramesh, T., Prakash, R., & Shukla, K. K. (2010). Life cycle energy analysis of buildings: An overview. *Energy and Buildings*, 42(10), 1592–1600. https://doi.org/10.1016/j.enbuild.2010.05.007

Rescic, S., Mattone, M., Fratini, F., & Luvidi, L. (2021). Earthen plasters stabilized through sustainable additives: An experimental campaign. *Sustainability*, 13(3), 1090. https://doi.org/10.3390/su13031090

Rojat, F., Olivier, M., Mesbah, A., & Millon, D. (2014). Caractérisation mécanique des enduits en terre crue fibrée. *ECOBAT Sciences & Techniques*, 93–108.

Sasui, J. W., & Hengrasmee, S. (2018). The effects of raw rice husk and rice husk ash on the strength and durability of adobe bricks. *Civil Engineering Journal*, 4(4), 732. https://doi.org/10.28991/cej-0309128

Wibaut, T., Aubert, J.-E., Ros, J., Kotarba, J., & Verdin, P. (2016). Les enduits de terre crue de deux fosses antiques. *Archeopages*, 42, 88–93. https://doi.org/10.4000/archeopages.1248

Zak, P., Ashour, T., Korjenic, A., Korjenic, S., & Wu, W. (2016). The influence of natural reinforcement fibers, gypsum, and cement on compressive strength of earth bricks materials. *Construction and Building Materials*, 106, 179–188. https://doi.org/10.1016/j.conbuildmat.2015.12.031

Zabalza Bribián, I., Valero Capilla, A., & Aranda Usón, A. (2011). Life cycle assessment of building materials: Comparative analysis of energy and environmental impacts and evaluation of the eco-efficiency improvement potential. *Building and Environment*, 46(5), 1133–1140. https://doi.org/10.1016/j.buildenv.2010.12.002

APPENDICES

A. Appendix Sampling

B. Appendix Density Experiments

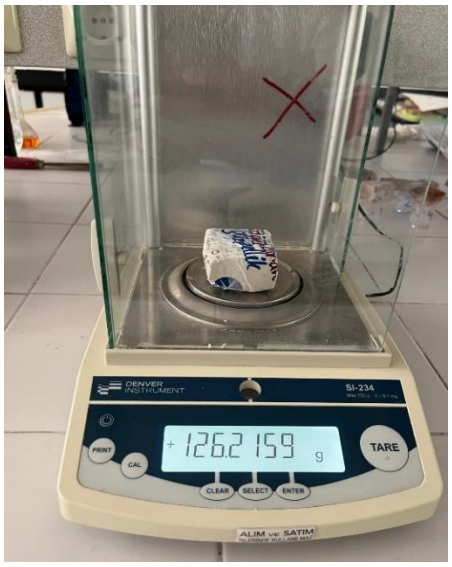

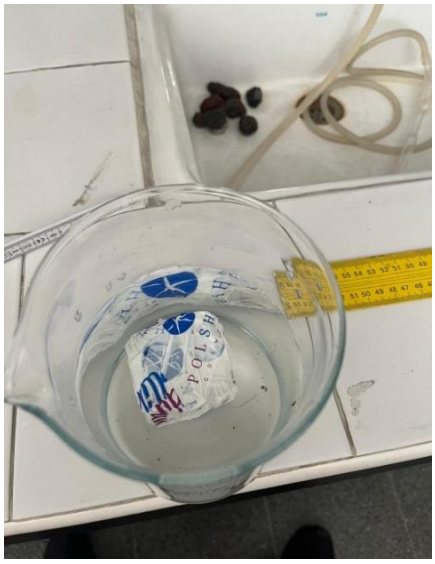

C. Appendix Shrinkage Experiments

D. Appendix Compressive Strength Experiments

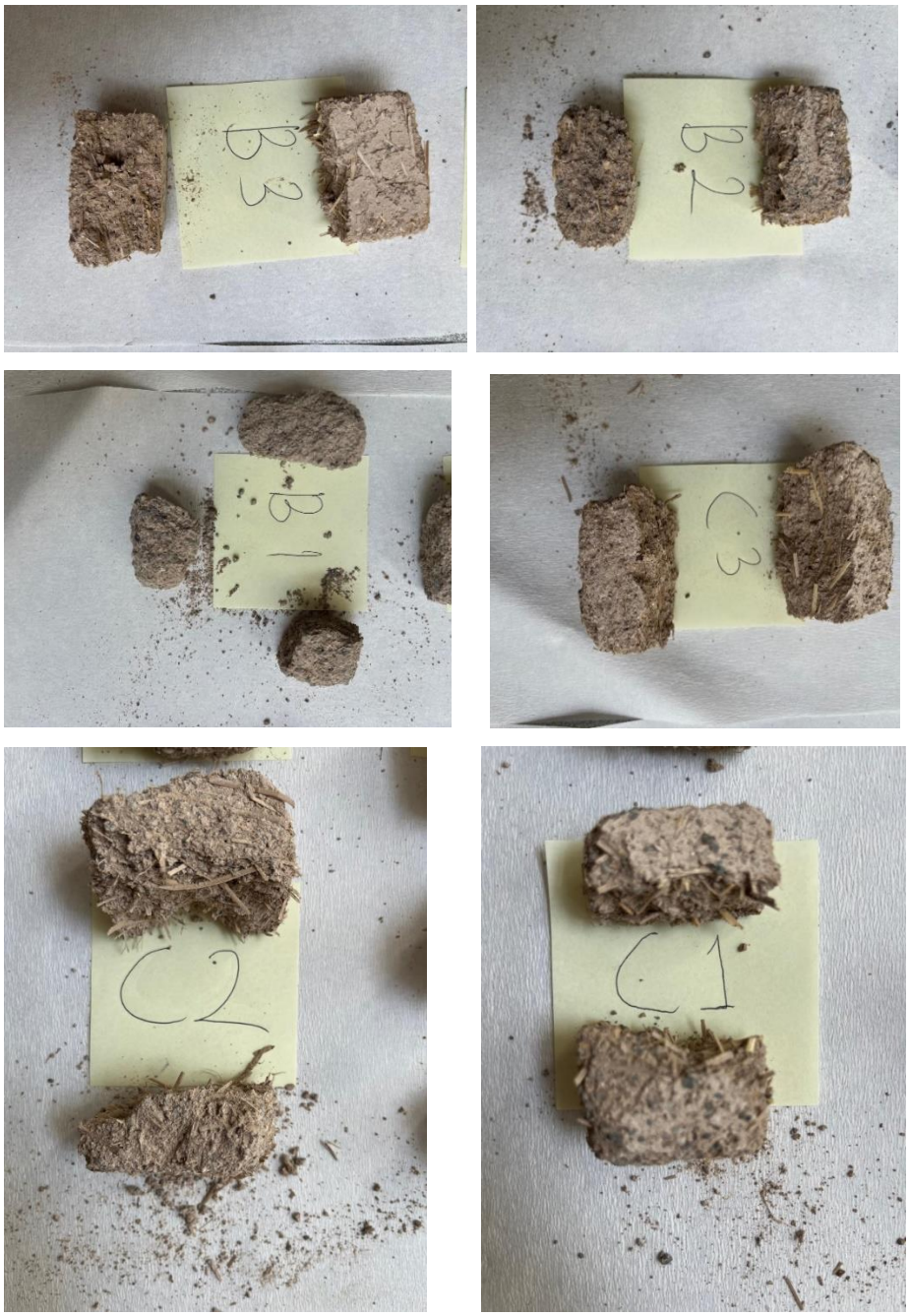




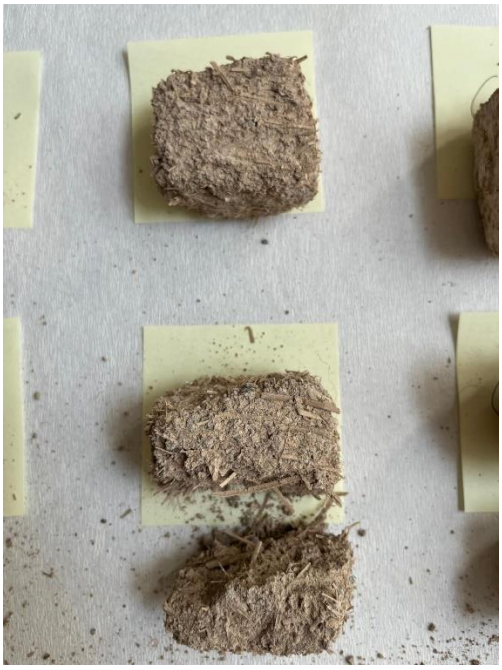





1
2
3
A
B
C


1
2
3
A
B
C

E. Appendix Peeling Experiments

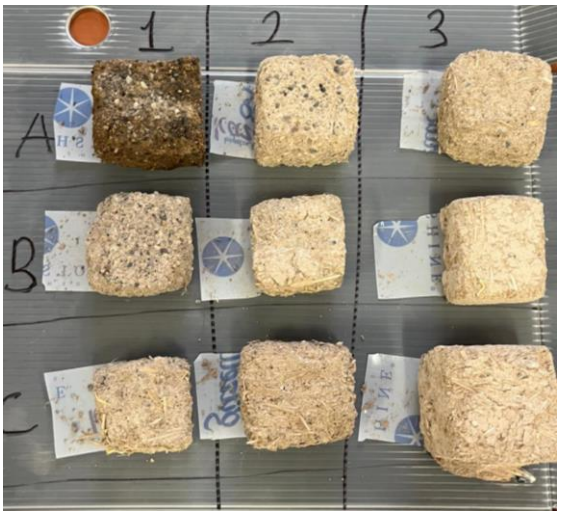

F. Appendix Surface water absorption Experiments

G. Appendix Erosion Resistance Experiments

H. Appendix Resistance to abrasion Experiments

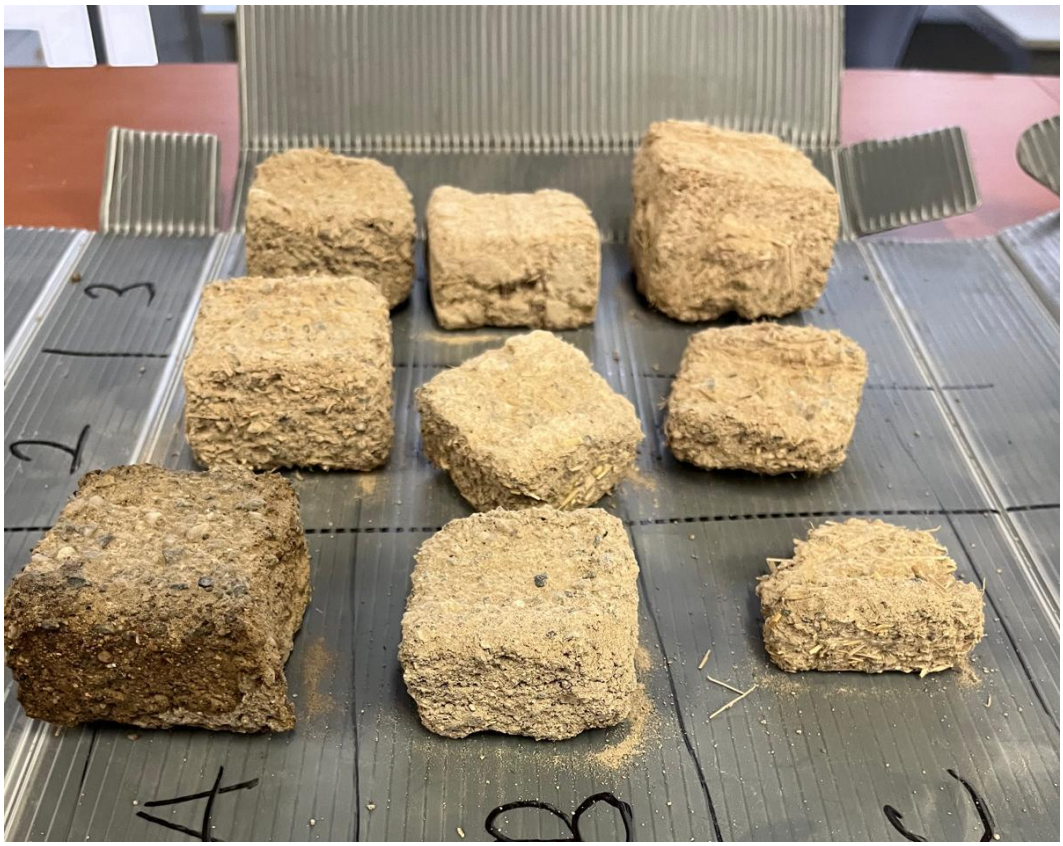


A

İ. Appendix Water capillarity absorption Experiments

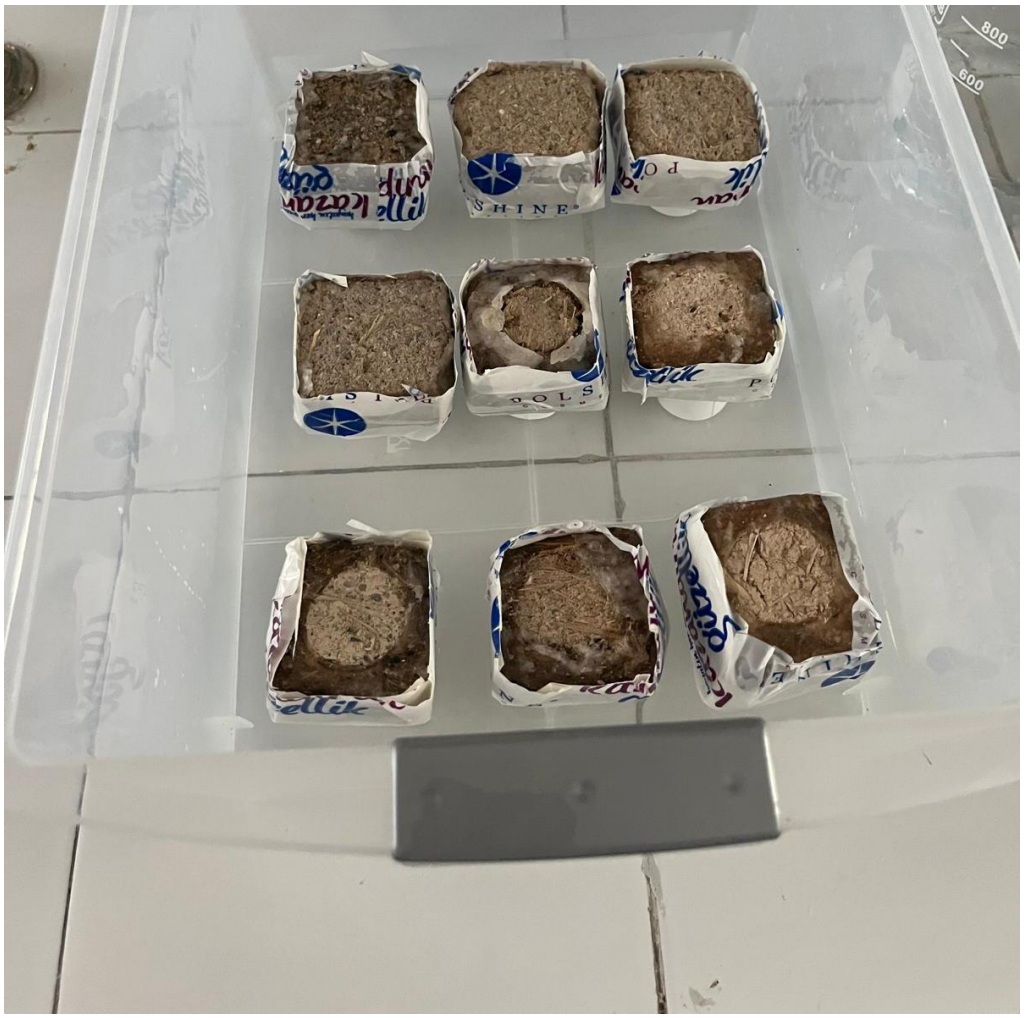

J. Appendix Drying capacity Experiments

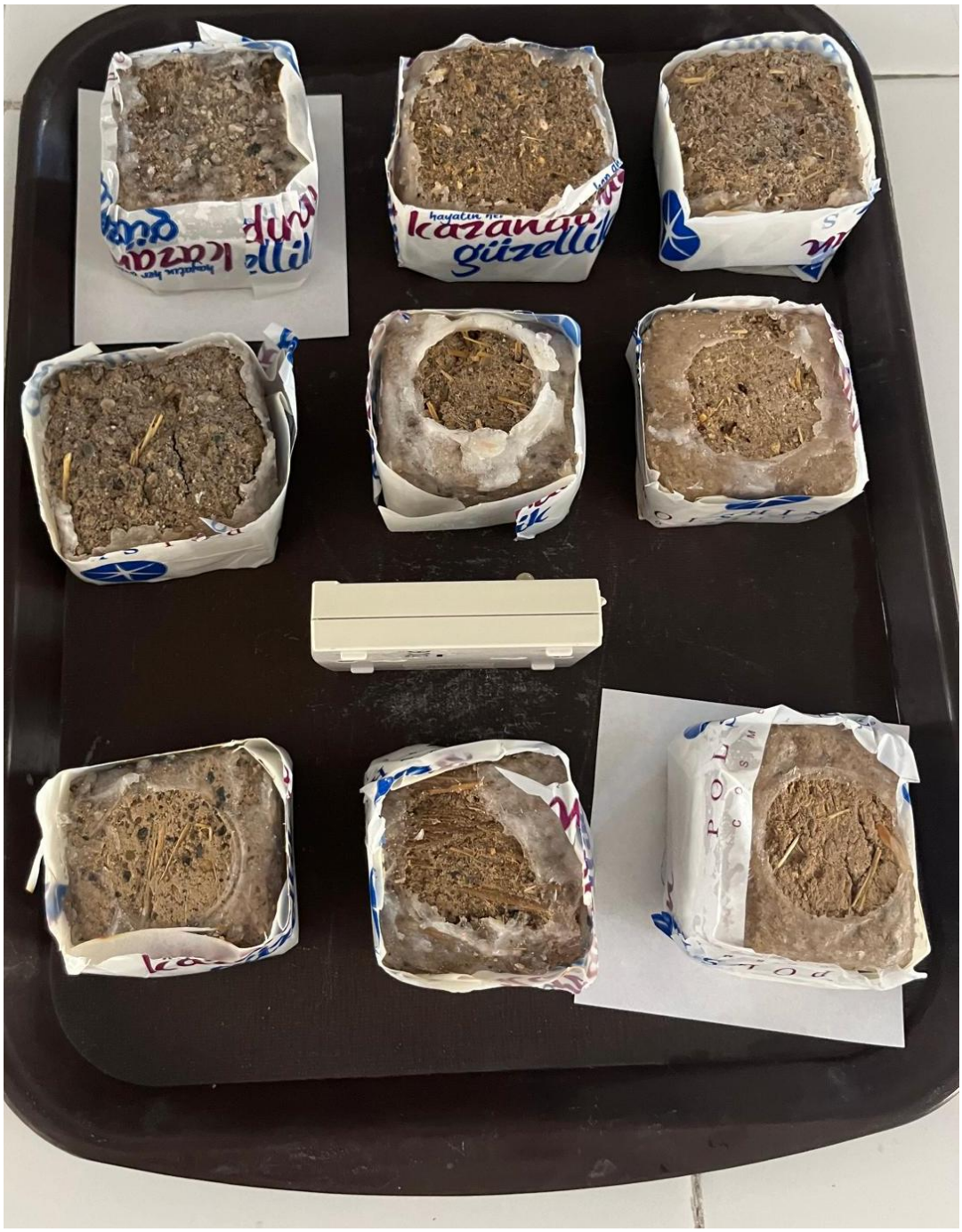

K. Appendix Water vapor permeability Experiments